Experimental Characterization of Powder Metallurgy Processed Ti-6Al-4V Based CeO_2/Cr/Gr Metal Matrix Composite

Yonaf Wakuma Nemomsa

A Thesis Submitted to Department of Mechanical Engineering School of Mechanical, Chemical and Materials Engineering

Presented in Partial Fulfillment of the Requirement for the Degree of Masters in Manufacturing Engineering

Office of Graduate Studies

Adama Science and Technology University

January, 2024

Adama, Ethiopia

Experimental Characterization of Powder Metallurgy Processed Ti-6Al-4V Based CeO_2/Cr/Gr Metal Matrix Composite

Yonaf Wakuma Nemomsa

Advisor: Dr. Devendra Kumar Sinha

A Thesis Submitted to Department of Mechanical Engineering

School of Mechanical, Chemical and Materials Engineering

Presented in Partial Fulfillment of the Requirement for the Degree of Master's in Manufacturing Engineering

Office of Graduate Studies

Adama Science and Technology University

January, 2024

Adama, Ethiopia

CANDIDATE'S DECLARATION

This Master Thesis, titled "**Experimental Characterization of Powder Metallurgy Processed Ti-6Al-4V Based CeO_2/Cr/Gr Metal Matrix Composite**", is the result of my own independent research and analysis. I confirm that this thesis has not been previously submitted, in whole or in part, for the award of any academic degree, diploma or certificate in any other institution of higher education. I also certify that I have properly cited and referenced all the sources of information that I have used for this thesis, following the academic standards and ethical principles of research.

Yonaf Wakuma Nemomsa	__________	__________
Name of student	Signature	Date

RECOMMEDATION OF ADVISORS

As the advisor of this thesis, I have carefully reviewed the revised version of the thesis with the title "**Experimental Characterization of Powder Metallurgy Processed Ti-6Al-4V Based CeO_2/Cr/Gr Metal Matrix Composite**". This thesis was prepared by Mr. Yonaf Wakuma under my supervision and guidance. The thesis meets the academic standards and requirements for the degree of Masters of Science in Manufacturing Engineering. I hereby endorse the thesis and recommend its submission to the department for further evaluation and approval.

Dr. Devendra Kumar Sinha	__________	__________
Main advisor	Signature	Date

APPROVAL SHEET

As the advisor of the thesis titled "**Experimental Characterization of Powder Metallurgy Processed Ti-6Al-4V Based CeO_2/Cr/Gr Metal Matrix Composite**", which was written by Mr. Yonaf Wakuma, I confirm that the final version of the thesis has considered the feedback and advice given by the board of examiners.

Dr. Devendra Kumar Sinha	___________	___________
Main advisor	Signature	Date

APPROVAL OF BOARD OF REVIEWERS

As members of the Board of Examiners, we have carefully reviewed and assessed the thesis of **Mr. Yonaf Wakuma**, which is titled "**Experimental Characterization of Powder Metallurgy Processed Ti-6Al-4V Based CeO_2/Cr/Gr Metal Matrix Composite**". We have also witnessed and evaluated the candidate's performance during the open defense session. Based on our judgment, we hereby declare that the thesis meets the standards and criteria for partial fulfillment of the requirement of the degree of Master of Science Manufacturing Engineering.

______________________________	__________	__________
Chairperson	Signature	Date
______________________________	__________	__________
Internal Examiner	Signature	Date
______________________________	__________	__________
External Examiner	Signature	Date

Final approval and acceptance of the thesis is contingent upon submission of its final copy to the Office of Postgraduate Studies (OPGS) through the Department Graduate Council (DGC) and School Graduate Committee (SGC).

______________________________	__________	__________
Department Head	Signature	Date
______________________________	__________	__________
School Dean	Signature	Date
______________________________	__________	__________
Office of postgraduate Studies, dean	Signature	Date

ACKNOWLEDGEMENT

First and foremost, I want to acknowledge the grace and mercy of the Almighty God, who gave me the strength and health to complete my study with His guidance and to achieve my highest potential. I also want to express my profound appreciation to my advisor, Dr. Devendra Kumar Sinha. Dr. Sinha is an outstanding advisor to work with, and I am honored to be part of his research group. He has been a role model for me in his professional ethics, as well as his genuine commitment and patience to mentor the students to excel in their research and future endeavors. He is truly an exceptional advisor to work with. I also want to thank my friends, my teachers and other benevolent people who supported me with their time and valuable feedback during my work. I have a deep respect and admiration for my teachers Dr. Devendra, Dr. Moera Gutu, Dr. P.J. Ramulu, Dr. Guteta.K, and Dr. Habtamu Beri from the Mechanical Design and Manufacturing Engineering program. They have provided me with excellent education and shared their wisdom and insights from their academic and personal experiences. They have inspired me to pursue my passion and to strive for excellence in my field.

TABLE OF CONTENTS

CHAPTER THREE

CHAPTER FOUR

TABLES OF TABLES

CHAPTER THREE

CHAPTER FOUR

TABLES OF FIGURES

CHAPTER TWO

CHAPTER THREE

CHAPTER FOUR

LIST OF ACRONYMS

ASTM	American Society for Testing Materials
CeO_2	Cerium oxide (CeO_2)
CMC	Ceramics Metal Composite
CR	Corrosion Rate
Cr	Chromium (Cr)
DD	Dislocation Density
Ecorr	Corrosion Potential
EDS	Energy Dispersive Spectroscopy
EIS	Electrochemical Impedance Spectroscopy
FMMC	Ferrous Metal Matric Composites
FTIR	Fourier Transform Infrared Spectroscopy
FWHM	Full Width Half Maximum
Gr	Graphite Powder
HV	Vickers Hardness
Icorr	Corrosion Current
JCPDS	Joint Committee on Powder Diffraction Standards
LS	Lattice Strain
MMC	Metal Matrix Composites
MPa	Mega Pascal
NFMMC	Non-Ferrous Metal Matrix Composite
NI-TI	Nickel Titanium
NITINOL	Nickel Titanium -Naval Ordnance Laboratory
NMC	Nickel Metal Matrix Composite
OCP	Open Circuit Potential
OM	Optical Microscopy

PM	Powder Metallurgy
PMC	Polymer Metal Composite
Rp	Polarization Resistance
SCE	Standard Calomel Electrode
SEM	Scanning Electron Microscopy
TI-MMC	Titanium Metal Matrix Composite
UCS	Ultimate Compressive Strength
UTM	Universal Testing Machine
VHN	Vickers Hardness Number
wt%	Weight Percentage
XRD	X-Ray Diffractometer
ρsint.	Sintered Density
μ**(%)**	Protection Efficiency

ABSTRACT

Composite materials, composed of two or more different materials with distinct physical or chemical properties, exhibit high resistance to deformation, damage, and corrosion even at elevated temperatures. Among the most promising composite materials are titanium metal matrix composites (Ti-MMCs). This study investigates the impact of varying reinforcement particle amounts on the mechanical and metallurgical properties of titanium composites. The matrix material consists of titanium grade 5 powder particles, while cerium oxide (CeO2), chromium (Cr), and graphite (Gr) powder particles serve as reinforcement materials. The composites are synthesized using powder metallurgy techniques, involving mixing matrix and reinforcement particles, compacting milled powders via hydraulic presses, and sintering in high-temperature furnaces. Microstructure and phase composition analysis is performed using Optical Microscopy (OM) and X-Ray Diffraction (X-RD). Vickers hardness testing reveals that the Ti-MMC with the composition (Ti-6Al-4v)-5%CeO2-10%Cr-4%Graphite exhibits the highest hardness (682 HV) and compressive strength (914 MPa) among all fabricated samples. Notably, this composite also demonstrates superior corrosion resistance, achieving a protection efficiency of 76% and a low corrosion current (19.27 mA cm-2) compared to pure Ti-6Al-4v alloy. The FT-IR spectrum confirms the material's ability to resist corrosion. These features position Ti-MMCs as ideal candidates for high-performance applications, including artificial bones and joints in medicine.

Keyword: Titanium metal matrix composites, Phase composition, Vickers hardness, Compressive strength, Corrosion resistance, Protection efficiency, FT-IR spectrum, Artificial bones and joints

CHAPTER ONE

INTRODUCTION

1.1 Background of the Study

A composite material is a combination of two or more materials that have different properties, such as metals, ceramics, or organics. Among the various types of composite materials, metal matrix composites (MMCs) are gaining popularity in many industries, such as automotive and aerospace, because they offer better performance than traditional engineering materials. MMCs have at least one metal component, which acts as the matrix, and another component, which acts as the reinforcement (**Campbell, J. 2015**); (**Rajasekar et al., 2018**); (**Raturi, 2019**). The reinforcement can be a ceramic or organic material, such as silicon carbide, alumina, or Graphite, that is embedded into the metal matrix as hard particles.

The metal matrix can be aluminum, magnesium, titanium, or other metals, depending on the desired application. The combination of the matrix and the reinforcement creates a new material with enhanced properties, such as high specific strength, which is the ratio of strength to weight, high stiffness, which is the resistance to deformation, better wear resistance, which is the ability to withstand friction and abrasion, and improved thermal resistance, which is the ability to withstand high temperatures (**Singh et al., 2022**), (**Aydogmus, 2015**); MMCs have superior tribological properties, which are related to the friction, wear, and lubrication of materials, and can perform well under various operating conditions, such as high speed, high load, or high temperature.

One of the challenges of modern medicine is to find ways to repair, restore, or enhance tissues, organs, and esthetics that are damaged or degenerated due to aging or other factors. This is especially important as people live longer and face more health issues. Among the various tissues that need replacement, bone tissue is one of the most common ones. Bone tissue is essential for supporting the structure and function of the body. Therefore, it is crucial to find materials that can interact with bone tissue and replace or augment its function. These materials should have certain properties that make them suitable for bone implants. For example, they should be hard, ductile, and wear-resistant, so that they can endure the mechanical forces and friction that bone tissue experiences. They should also be biocompatible, which means that they do not trigger any negative responses from the body, such as inflammation, infection, or rejection.

The most popular material for bone implants is titanium, which has many benefits over other materials. Titanium has a high degree of integration with bone tissue, which means that it creates a stable and secure connection with the bone surface. Titanium is also resistant to corrosion, which means that it does not deteriorate or release any toxic substances in the body. Titanium has a modulus of elasticity that is close to that of bone, which means that it can cope with similar levels of stress and strain without cracking or bending. Titanium is also compatible with soft tissues, which means that it reduces the risk of irritation and infection around the implant site. Titanium's exceptional properties are due to the oxide layer that forms on its surface when it comes in contact with oxygen. This layer acts as a barrier that protects the material from corrosion and improves its attachment to bone tissue.

Titanium alloys are rare and special materials that have different types of structural alloys. They have various applications in different fields, such as aerospace, where they can resist high temperatures and pressures, machines, where they can prevent corrosion and fatigue, energy, where they can enhance the performance and safety of nuclear reactors and gas turbines, and medicine, where they can heal wounds and replace damaged tissues. Titanium alloys can also be used to create metal matrix composites (MMCs), which are materials that combine a metal matrix with another material as a reinforcement, such as a ceramic or a polymer. These composites have high stiffness and strength, which depend on the type and amount of reinforcement. Titanium is biocompatible, which means that it does not cause harmful reactions in the body. This makes titanium an ideal biomaterial for bone implants, especially those that have a low Young's modulus, which is a measure of how elastic a material is. Titanium alloys with a low Young's modulus can match the mechanical properties of bone and avoid stress shielding, which is a phenomenon that occurs when an implant takes over the load from the bone and causes it to weaken.

1.2 Problem Statement

The medical field is always in search of new materials that can provide better performance, durability and biocompatibility for various applications. One type of material that has shown great potential is composite materials, which are made of two or more different materials that have different physical or chemical properties. In particular, metal matrix composites, which consist of a metal matrix and a reinforcing material, have gained a lot of interest due to their superior properties such as high specific strength, high stiffness, better wear resistance and improved thermal resistance (**Kumar et al., 2021**). These properties make them suitable for applications that require high mechanical performance and resistance to harsh environments.

Titanium alloy-based composites are one of the most promising types of metal matrix composites for medical applications, such as bone implants and stents. These composites combine the advantages of titanium alloys, such as excellent biocompatibility, corrosion resistance, low density and high fatigue strength, with the benefits of various reinforcements, such as improved strength, wear resistance, hardness, yield strength, tensile strength and machinability. However, the development of titanium alloy-based composites faces many challenges, such as the selection of suitable reinforcements, the optimization of processing methods, the control of microstructure and properties, and the evaluation of biocompatibility and bioactivity. Therefore, this dissertation aims to develop new titanium alloy-based composites reinforced with CeO2, Cr and Gr, and to investigate their microstructure, mechanical properties and corrosion behavior. The dissertation also explores the effects of different reinforcement types, contents and distributions on the properties of the composites, and compares them with the conventional titanium alloys. The dissertation hopes to provide some insights and guidance for the design and fabrication of titanium alloy-based composites for medical applications.

1.3 Objective of the Study

The general and the specific objectives of the study described as follows:

1.3.1 General Objectives

The General objective of this study is to produce, examine and explore the Mechanical and Metallurgical Properties of (Ti-6Al-4V) - $Ce0_2$ – Cr - Gr, reinforced Metal Matrix Composites synthesized through powder metallurgy technique.

1.3.2 Specific Objectives

1. Fabricate of (Ti-6Al-4V) - $Ce0_2$ - Cr - Gr, reinforced Metal Matrix composite through powder metallurgy route at different weight percentages of reinforcement particles.
2. Analyze the phase, microstructure, and grain distribution uniformity of the composite matrix using X-RD, SEM, and OM methods.

3. Evaluate the characteristics of porosity, density and hardness of the composite synthesized composite material.
4. Investigate the compression strength of the developed composite material.
5. Investigate the corrosion behavior of the developed composited materials

1.4 Significance of the Study

The proposed study work is to produce Titanium Metal Matrix composite (Ti-MMC) by using powder metallurgy technique with different levels of reinforcement particles ($Ce0_2$ and Cr). This study is significant for my academic and practical development, as well as for other researchers and various industries that demand this composite material. Through this study, I will acquire both theoretical and practical skills in the research area and add to the existing body of knowledge on Ti-MMC. Additionally, this study will assist students who want to pursue this research area and offer them useful insights. Moreover, this study will have implications for medical, aerospace, and automobile sectors that use Ti-MMC for their products. By mastering how to reduce porosity in the samples and how to improve the mechanical and metallurgical characteristics of the materials, It will enhance the quality and durability of Ti-MMC.

1.5 Scope of the Study

The scope of this study is to the development of Cerium oxide and Chromium- reinforced Titanium-metal matrix composites to improve corrosion resistance and wear was the primary focus of research. Powder metallurgy techniques were used in the fabrication process, which was characterized by XRD for phase transformation, SEM for microstructure, and OM for grain size refinement and other specific activities involved in this study are:

- Fabricating Ti-MMCs with Ti-6AL-4V as the matrix and varying weight fractions of Cerium oxide and Cr as the reinforcements using powder metallurgy technique.
- Identifying the distribution and phase of the reinforcement particles in the Ti-MMCs using scanning electron microscopy (SEM), X-ray diffraction (XRD) and other technique analysis.
- Investigating the porosity, density, hardness of the Ti-MMCs using standard test methods and equipment.
- Investigating the corrosion behavior of the developed composited materials.

1.6 Research Motivation

Reinforced Titanium based metal matrix composites (MMCs) have been discontinued for research purposes due to their low wear resistance, high cost and poor machinability. New composites with improved mechanical and metallurgical properties have been developed, but they only show a slight improvement in hardness, wear resistance, and thermal stability compared to the base metal. These composites are still inadequate for the medical field, which requires a higher strength to weight ratio, higher wear resistance, higher hardness, higher yield strength, higher tensile strength, better corrosion resistance and better machinability. Therefore, this study focuses on enhancing the mechanical and tribological performance of the new composites by adding smart reinforcing particles of Cerium oxide and Chromium, which can increase the corrosion and wear resistance of the matrix.

1.7 Limitation of the work

The challenges which faced on work were:

- One of the difficulties in creating metal matrix composites is ensuring that the reinforcing phase, which is the material that strengthens the composite, is evenly distributed throughout the metal matrix, which is the material that holds the composite together. If the reinforcing phase consists of very small particles, they may tend to clump together or scatter unevenly in the metal matrix. This can affect the overall properties of the composite, such as its strength, stiffness, or wear resistance.
- High melting point: The metal matrix composite consists of titanium as the base material and cerium oxide and chromium as the reinforcements. These elements have high melting points, which means they require a lot of heat to melt. This makes it challenging to melt
- The more challenging work was lack of vacuum furnace, (to minimize or prevent formation of reaction) during sintering of the compacted Ti-6Al-4v/CeO2/Cr samples.
- Budget scarcity for all process and to conduct a greater number of experiments.

1.8 Expected Outcome of the Study

The main objective of this research is to produce a lightweight, hard, wear-resistant, and corrosion-resistant (Ti-6Al-4V) - $Ce0_2$ - Cr, reinforced Metal Matrix Composites for enhancing its mechanical and metallurgical properties. The expected outcomes of this research are manifold, such as:

- The research will develop a method of synthesizing (Ti-6Al-4V) - $Ce0_2$ - Cr, reinforced Metal Matrix Composites using powder metallurgy and hot isostatic pressing techniques.
- The research will investigate the effects of $Ce0_2$ and Cr additions on the microstructure, phase composition, hardness, wear resistance, and corrosion resistance of the composites.
- The research will compare the performance of the composites with conventional (Ti-6Al-4V) alloys and other metal matrix composites in terms of mechanical and metallurgical properties.
- The research will demonstrate the potential applications of the composites in aerospace, biomedical, automotive, and industrial sectors, where high strength, low weight, and good resistance to wear and corrosion are required.

1.9 Thesis organization

This thesis has five chapters and each chapter's main points are summarized below.

CHAPTER 1 provides an overview of the research topic, which is the development and evaluation of a novel metal matrix composite (MMC) based on Ti-6Al-4V alloy with CeO_2 and Cr particles as reinforcements. It explains the motivation and the aim of the study, the research questions and hypotheses, the significance and scope of the research, the limitations and assumptions, the expected output and contribution, and the organization of the thesis.

CHAPTER 2 presents a comprehensive literature review on the relevant aspects of the research, such as the MMCs and their applications, the Ti-6Al-4V alloy and its properties, the CeO_2 and Cr particles and their effects, the mechanical and wear testing methods and standards, and the microstructure characterization techniques and tools. It also identifies the literature gap and the research opportunities that this work addresses.

CHAPTER 3 details the materials and methods used in this work, such as the selection and preparation of the Ti-6Al-4V matrix and the CeO_2 and Cr reinforcements with different weight fractions (0, 5, 7.5, and 10 wt.%), the fabrication process of the (Ti-6Al-4V)- CeO_2- Cr reinforcement metal matrix composite using powder metallurgy and hot isostatic pressing, the mechanical and wear testing procedures and equipment, and the optical microscopy (OM) and scanning electron microscopy (SEM) analysis methods and instruments.

CHAPTER 4 reports and discusses the experimental results of the mechanical and wear properties, such as the hardness, Compression strength, and as well as the OM and SEM images of the (Ti-6Al-4V)- CeO_2- Cr reinforcement metal matrix composite. It also compares the results with the literature and the theoretical predictions, and explains the underlying mechanisms and factors that influence the properties and the microstructure of the composite.

CHAPTER 5 summarizes the main findings and conclusions of the work, and provides suggestions and directions for future research. It also discusses the implications and limitations of the work, and the potential applications and benefits of the (Ti-6Al-4V)- CeO_2- Cr reinforcement metal matrix composite.

CHAPTER TWO

LITERATURE REVIEW

This chapter presents a comprehensive overview of the existing research on composite materials, focusing on their fabrication methods, mechanical and tribological properties and microstructural features. The chapter also introduces the research problem and its significance in the context of composite materials engineering. Based on the summary of the literature review, the chapter identifies and discusses the research gaps that need to be addressed in future studies.

2.1 Introduction to composite materials

A composite material is a material system composed of a suitably mixture or combination of two or more macro, Micro or Nano constituents with an interface separating them that differ in form and chemical composition. Composite is a multiphase material that exhibits a significant proportion of the properties of both the reinforcement (with discrete constituent) and matrix (continuous phase) constituent phases such that a better combination of properties is realized (**Bodunrin et al., 2015**); (**Mavhungu et al., 2017**). The composite materials have high strength to weight ratio and modulus to weight ratio, excellent fatigue properties, good wear and corrosion resistance behaviors.

The development of new materials for biomedical applications is driven by the need to improve the performance, safety, and biocompatibility of existing materials, as well as to create novel materials that can meet the emerging challenges in the field of medicine. The basic aim of developing new materials for biomedical applications is to design materials that can interact with biological systems in a controlled and beneficial way, either by mimicking the natural properties of tissues and organs, or by providing new functionalities that can enhance the diagnosis, treatment, or prevention of diseases. Some of the criteria that guide the development of new materials for biomedical applications are biodegradability, bioactivity, mechanical strength, chemical stability, electrical conductivity, optical transparency, and magnetic responsiveness (**Vivek Sheel Rajput** and **Jasdeep Bhinder 2024**).

The performance of composites depends largely on the characteristics of the materials that make up the composite, how they are arranged and how they interact with each other. The composites may have properties that are simply the weighted average of the properties of the individual materials, or the materials may work together in a synergistic way to produce enhanced or superior properties.

The nature of the constituent materials is not the only factor that affects the properties of the composites. The shape, size and distribution of the particles that reinforce the composite also play a significant role in determining its properties. The amount and direction of the reinforcement influence how much each material contributes to the overall properties of the composites. The reinforcement is not only the most critical parameter that affects the properties of the composites, but also a variable that can be easily manipulated during the manufacturing process to modify its properties (**Chandramohan, Marimuthu 2011** and **Banga 2015**).

2.2 Classification of composite materials

Composite materials are made of two or more different materials that have distinct physical and chemical properties. When these materials are combined, they create a new material that has specific characteristics for a certain purpose, such as being stronger, lighter, or more resistant to electricity. The new material also has different properties than any of the original materials. Composite materials can be classified into various types depending on the kind of matrix material, the type and shape of reinforcement material, the size and amount of reinforcement material, and other factors (**Chandra Kandpal et al. 2018**).

The main types of composite materials are: Metal Matrix Composites, Ceramic Matrix Composites, and Polymer Matrix Composites. These types are based on the nature of the matrix material and the shape of the reinforcement material. The main categories of composite materials can be classified;

- Based on chemical nature of the matrix phase (matrix material).
- Based on dispersed phase (geometry of reinforcements).

Based on the chemical nature of the matrix phase measurement, composite materials are classified as metal matrix (MMC), polymer matrix (PMC) and ceramic matrix composites (CMC), composite materials are also classified as particle reinforced composite, fiber reinforced composite and structural composites, based on geometry of the reinforcements (dispersed phase) **Kalaa et al. (2014)**.

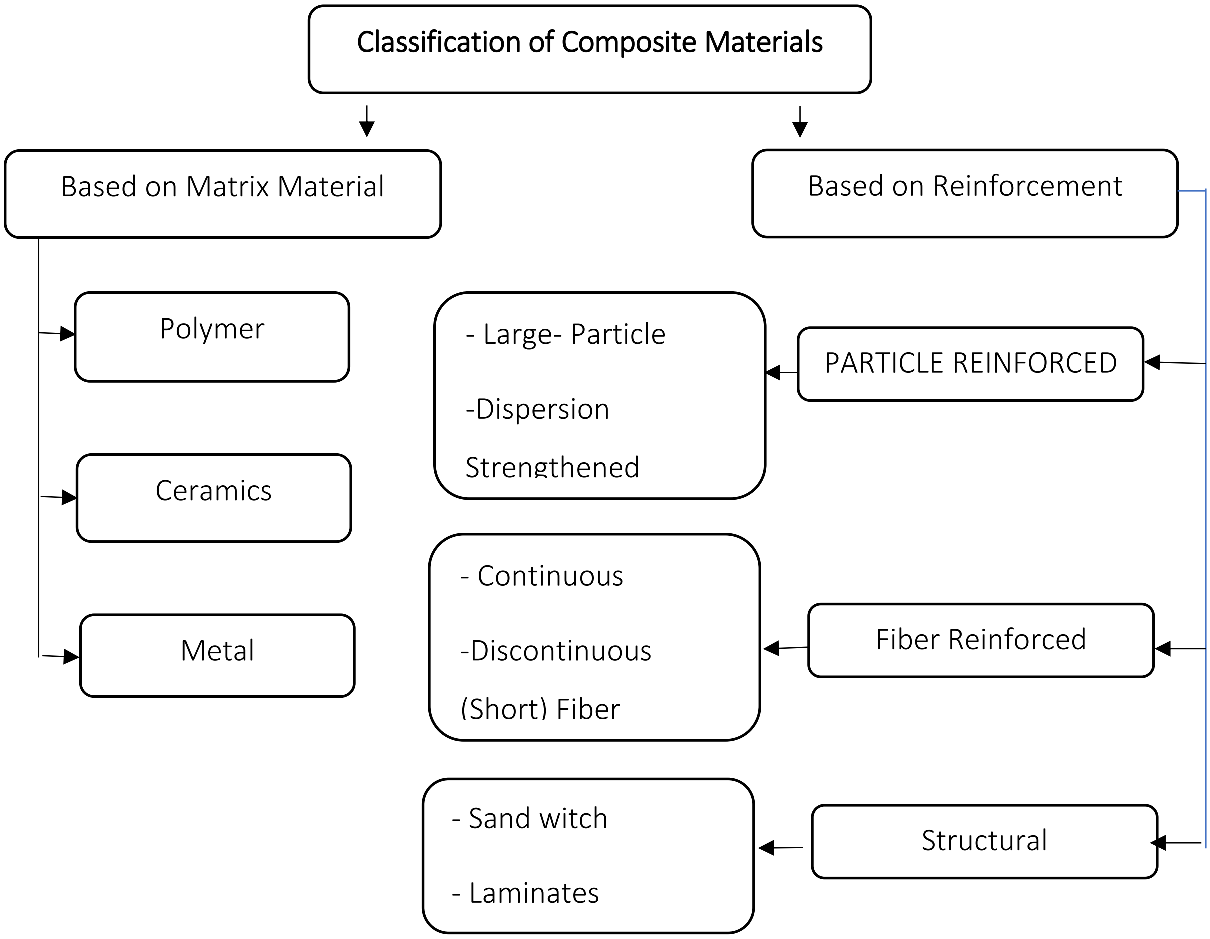

Figure 2.1 Classification of Composite Materials (**Rajak et al., 2019**); (**Ashebir, 2022**).

2.2.1 Metal matrix composites

Metal matrix composites (MMCs) are a type of composite material that consists of two or more different materials, usually a metal and a ceramic, that are fused together to create a new material with enhanced properties. MMCs are designed to achieve a combination of high strength and stiffness with low density, which are difficult to obtain from a single material. MMCs are often used as engineering materials for various applications that require high performance and durability.

One of the main features of MMCs is that they have a metal matrix that provides ductility and toughness, and a ceramic reinforcement that provides high strength and high modulus. This results in a material that has higher resistance to shear and compression forces, and can withstand higher temperatures than the metal matrix alone, as reported by (**Kok 2005**). MMCs also have some advantageous physical characteristics, such as low moisture absorption, non-flammability, high electrical and thermal conductivities, and resistance to most types of radiation, according to (**Russo 2006**).

(**Toptan et al. 2010**) have developed MMCs to meet the demand for materials with superior mechanical properties, such as high stiffness, wear resistance, greater shear and compressive strengths, and better high temperature capabilities. Some of the most common metal matrix alloys used to produce MMCs are aluminum and magnesium, which are light weight and have good corrosion resistance. These alloys are reinforced with ceramic particles or fibers, such as silicon carbide, alumina, or carbon, that improve the properties of the MMCs.

MMCs based on aluminum and Titanium matrix alloys are widely used in various industrial sectors, such as aerospace, automotive, biomedical, and electronics, due to their desirable properties, such as high strength-to-weight ratio, high modulus, and low ductility, high wear resistance, high thermal conductivity, and low thermal expansion, as stated by (**Chawla et al. 2006**) and (**Hussain et al. 2017**).

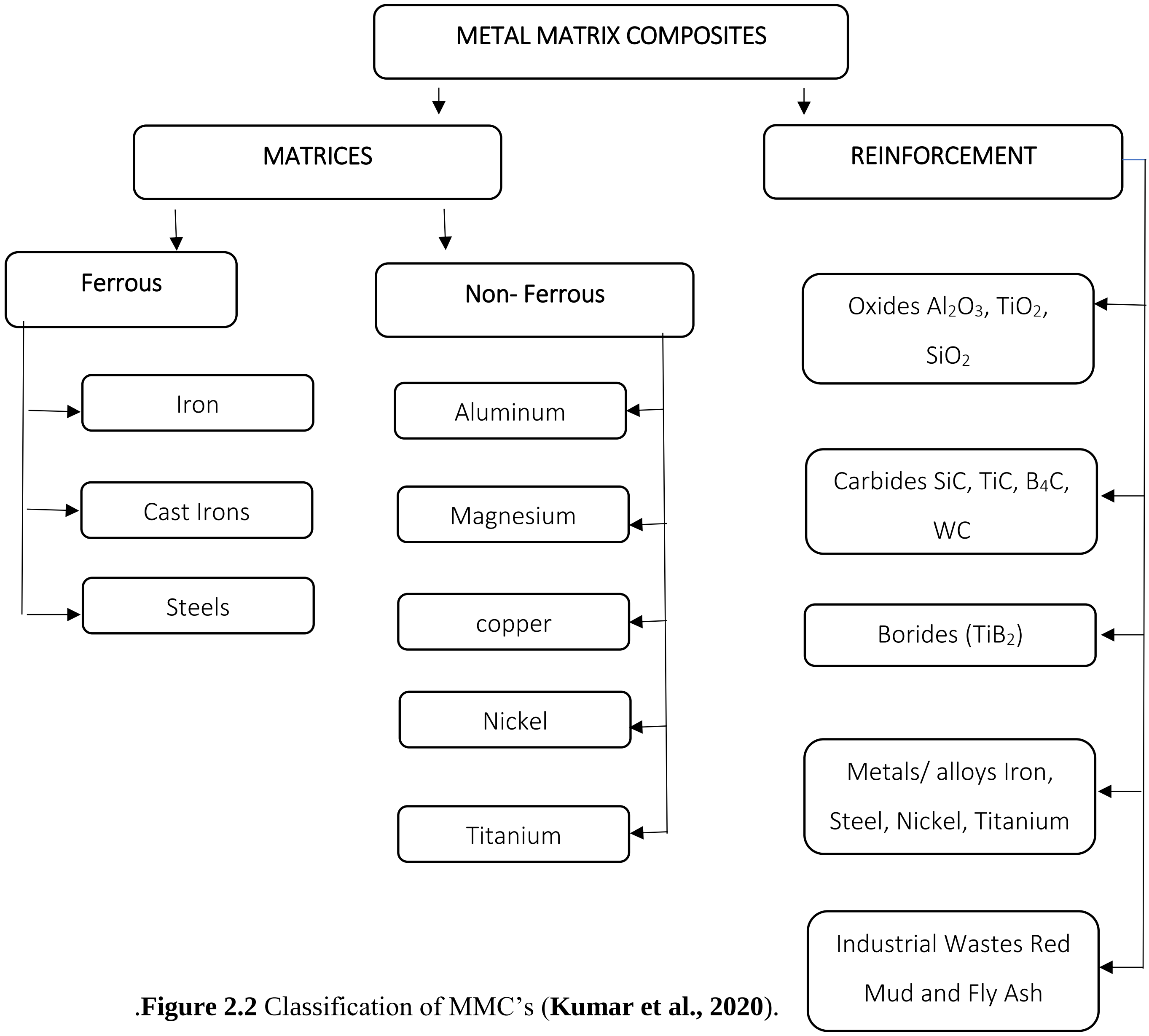

.**Figure 2.2** Classification of MMC's (**Kumar et al., 2020**).

2.2.1.1 Titanium based matrix composite

Titanium based matrix composites (TMCs) are a type of composite material that consists of a titanium alloy matrix and a ceramic reinforcement, usually in the form of fibers or particles. TMCs have superior properties compared to pure titanium alloys, such as higher strength, stiffness, wear resistance, and thermal conductivity. TMCs are widely used in aerospace, automotive, biomedical, and other industries that require high-performance and lightweight materials.

The properties of TMCs depend on various factors, such as the composition and microstructure of the matrix and the reinforcement, the volume fraction and distribution of the reinforcement, the fabrication method and heat treatment, and the interface characteristics between the matrix and the reinforcement. (**Naghmeh Abavi Torghabeh** and **Rasoul Pouriamanesh 2022**)

2.3 Introduction of Effectible Variables on The Metal Matrix Composite Properties

Metal matrix composites (MMCs) are materials that consist of a metal matrix and a ceramic reinforcement. The metal matrix provides ductility and toughness, while the ceramic reinforcement provides high strength and stiffness. MMCs have many advantages over pure metals, such as higher strength-to-weight ratio, higher thermal conductivity, lower thermal expansion, and better wear resistance.

However, the properties of MMCs depend on various factors, such as the type and composition of the matrix and reinforcement, the volume fraction and morphology of the reinforcement, the fabrication method and heat treatment, and the orientation and distribution of the reinforcement. These factors affect the microstructure and the interface between the matrix and the reinforcement, which in turn affect the mechanical and physical behavior of the MMCs **(Singh.et al. 2015**). Therefore, it is important to understand the effect of these variables on the MMCs and optimize them for specific applications.

2.4 Manufacturing Methods and Processing of Metal Matrix Composites

Metal matrix composites (MMCs) are composite materials that consist of a metal matrix and a reinforcement phase, such as ceramic particles or fibers. The manufacturing process of MMCs has a significant influence on their final properties, such as strength, stiffness, wear resistance, and thermal conductivity. Therefore, choosing an appropriate manufacturing method requires considering several factors, such as the desired properties of the MMC, the scale of production, the cost-effectiveness, the type of metal matrix, the shape and size of the reinforcement phase, and the intended application of the product. There are various manufacturing methods for MMCs, but they can be broadly categorized based on the state of the metal matrix during processing:

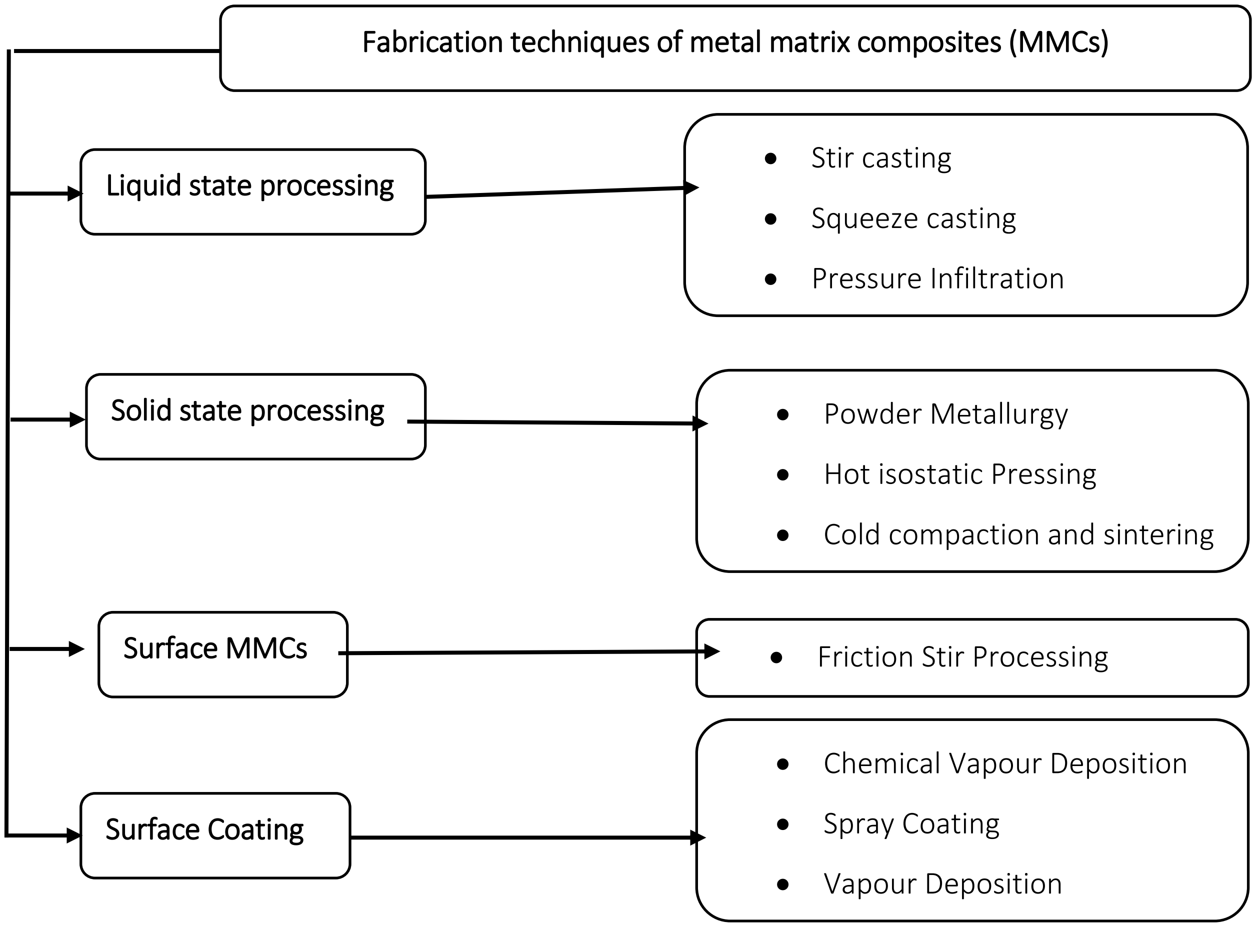

Figure 2.3 Fabrication Technique of MMC's (**Singh et al., 2022**); (**Chandel et al., (2021**).

Liquid state process includes; stir casting, squeeze casting, liquid infiltration, spray disposition. Solid metallurgical process includes; the powder blending and consolidation, diffusion bonding and physical vapor deposition.

2.4.1 Solid state processing technique

Solid state fabrication of metal matrix composites (MMCs) is a technique that involves the formation of MMCs by the bonding of a metal matrix and a dispersed phase through mutual diffusion in solid states at high temperature and pressure. This technique avoids undesirable reactions between the matrix and the dispersed phase that may occur in liquid state fabrication of MMCs.

There are various methods to produce particulate reinforced MMCs, such as diffusion bonding, sintering, hot pressing, hot isostatic pressing, and hot powder extrusion. Among these methods, powder metallurgy (PM) is one of the most cost-effective processes for fabricating near net shape particulate reinforced MMCs. Powder metallurgy is a process that involves mixing different metal powders and forming them into finished or semi-finished components by compression. The compressed components are then heated at high temperature in a furnace under a controlled atmosphere to achieve sufficient strength and density (**Kumar et al. 2016** and **Kanthavel et al. 2016**).

Powder metallurgy is one of the best methods to obtain the desired properties of MMCs, such as low porosity, uniform distribution of the reinforcement, and enhanced mechanical properties. It also allows for the adjustment of various process parameters, such as compaction pressure, holding time, sintering temperature, sintering time, heating rate, etc.By using powder metallurgy, the uniformity of the reinforcement material in the matrix is improved, which reduces the problems of clustering and porosity and increases the hardness, tensile and compressive properties of the composite. Moreover, the low processing temperatures of powder metallurgy prevent the interaction between the matrix and the reinforcement phases, which may affect the properties of the composite (**Wang et al. 2011**, **Ghasali et al. 2015** and **Mendoza et al. 2015**).

- Powder metallurgy (PM) is a manufacturing technique that uses metal or alloy powders as the main raw materials to produce high-quality and precise parts at a lower cost than other methods.
- One of the benefits of PM is that it reduces the waste of raw material, since the powder metal components have a close-to-final shape and need minimal or no machining after forming.
- Another advantage of PM is that it allows for the creation of complex and intricate shapes that are difficult or impossible to achieve by other techniques, such as casting or forging. PM can also produce parts with a wide variety of properties, such as strength, hardness, wear resistance, corrosion resistance, etc., depending on the powder characteristics and the processing parameters.
- Moreover, PM offers the possibility of designing the material composition and microstructure of the powder metal components to suit the specific requirements of the application. For example, PM can create composite materials, gradient materials,

porous materials, and nanostructured materials, among others, by manipulating the powder size, shape, distribution, and alloying elements.

Ceramic particles can enhance the properties of metal matrix composites (MMCs), but they are hard to incorporate by casting methods due to their high melting points. However, powder metallurgy (PM) techniques can overcome this challenge by mixing and sintering the metal and ceramic powders at lower temperatures (**Groover 2007**). This is why PM is a popular method for making aluminum MMCs with various ceramic reinforcements.

2.4.1.1 Powder Metallurgy

Powder metallurgy (PM) is a manufacturing technique that involves blending fine powders of different materials, such as metals and ceramics, shaping them into the required configuration, and sintering them in a controlled environment to form a solid bond. PM can create complex shapes with high precision and quality, as well as enhanced properties such as higher density, strength, and durability. PM is especially useful for producing metal matrix composites (MMCs), which are materials that combine a metal matrix with a reinforcing phase to improve the performance of the base metal (**Meignanamoorthy and Ravichandran, 2018**). By using PM, MMCs can achieve a better distribution of the reinforcement phase, a lower level of porosity, and a higher degree of compaction of the powder mixture (**Kumar, Bharti, and Dixit, 2021**). One of the advantages of PM is that it can produce parts with minimal waste and energy consumption, as well as lower costs, compared to conventional methods. PM also allows for the sintering of the parts in air, which means that the temperature of the process is kept below the melting point of the materials, preventing oxidation and contamination (**Khazaal et al., 2022**). It consists of the following steps:

2.4.1.1.1 Powder Preparation and Mixing

The quality and consistency of the final product depend on the proper mixing of the powder components. Before the powders are mixed, binders and/or lubricants are added to the mixture to improve the flowability and compatibility of the powder. Lubricants also help to prevent wear and tear of the equipment and reduce the friction between the powder particles. The powders are then mixed using wet or ball milling methods, which ensure a uniform distribution of the different powders in the desired ratios. The mixing process and the quality of the prepared powder are carefully monitored and controlled to achieve the optimal results (**Sankhla et al., 2022**; **Panda, 2016**).

2.4.1.1.2 Compaction

Die compaction is a technique that involves putting powder into a mold and applying a hard punch to form it into a desired shape. The powder is then ejected from the mold and ready for further processing. The powder can be a mixture of different materials that form a composite. The mold is usually rigid and can withstand high pressures ranging from 150 to 900 MPa (**Sinka, 2007**). Figure 2.6 shows a schematic diagram of the general die compaction process. The density of the compacted powder depends on the pressure applied by the punch. Higher pressures result in higher densities and stronger compacts. Die compaction is one of the steps in the powder metallurgy process.

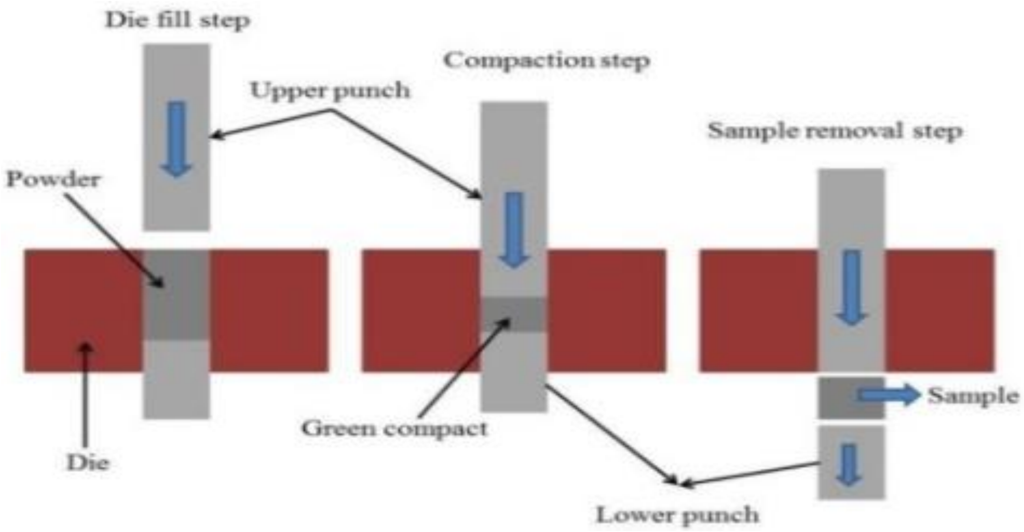

Figure 2.4 Compaction Process (**Panda, 2016**).

To facilitate the compression of the powder in the die, a lubricant is necessary to reduce the friction between the powder and the die wall. Graphite and molybdenum sulphide are examples of such lubricants. Friction causes the powder to have a non-uniform density distribution, which leads to residual stresses in the green body. These stresses can adversely affect the quality of the PM pieces when they undergo high temperature consolidation, as they can create defects such as pores and cracks. This can compromise the mechanical properties and performance of the PM pieces, according to (**Honnaiah et al. 2023**).

To achieve the desired density and strength of the final product, some lubricant elements are needed to help the powder particles stick together during the compaction process. These elements include molybdenum disulfide (MoS_2), magnesium (Mg), and paraffin waxes. They also act as friction reducers between the powder and the die, which is the metal mold that shapes the powder into a solid form.

2.4.1.1.3 Sintering

Sintering is a heat treatment process that enhances the strength of powder composites or compacts by creating bonds between the particles. The process involves heating the green compact, which is a loosely or physically connected assembly of powder particles, in a controlled environment of inert or reducing gases such as argon, hydrogen or nitrogen. The heating temperature is lower than the melting point of the powder material, typically ranging from 60% to 75% of the melting point of the constituent components (**Wang et al., 2021**). The sintering process causes the powder particles to fuse together and form a solid structural part with the desired properties, such as density, porosity, hardness, and electrical conductivity (**Fisika et al., 2008**). Depending on the sintering conditions, such as temperature, time, pressure, and atmosphere, the process can achieve different degrees of densification and shrinkage. In some cases, sintering can result in no net dimensional change, which is desirable for applications that require high dimensional accuracy (**Manohar et al., 2020**). Sintering is a widely used technique for producing various materials, such as ceramics, metals, alloys, and composites, with strong inter-particle bonds.

The sintering process is a technique that can enhance the physical and mechanical properties of the materials by heating and compacting the powder under controlled conditions (**Adnan Khan et al., 2020**). The sintering temperature is a key factor that influences the rate and magnitude of the changes that occur during the process, such as densification, grain growth, and phase transformation (**Panda, 2016**). The sintering duration, on the other hand, has a negligible effect compared to the sintering temperature. The sintering process can produce various PM materials with desirable characteristics, such as sintered self-lubricating bearings, sintered magnets, and sintered automotive parts and gears (**Meignanamoorthy and Ravichandran, 2018**); (**Yong et al., 2021**); (**Khazaal et al., 2022**).

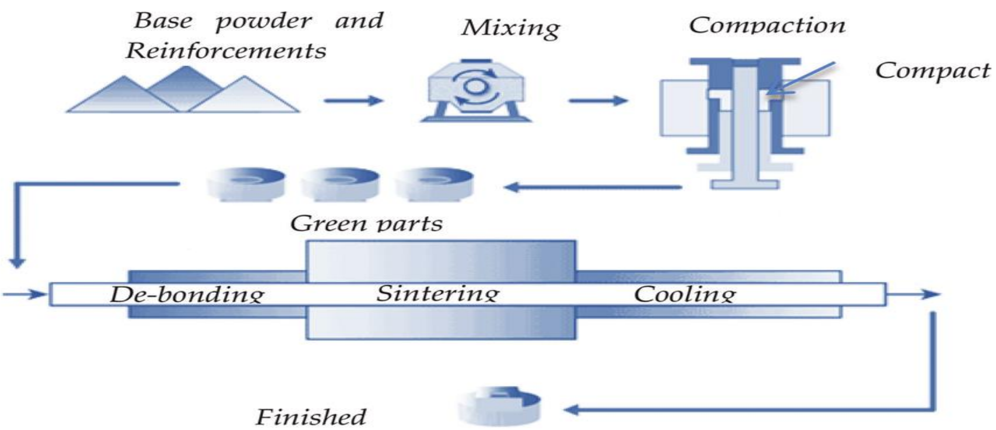

Figure 2.5 Schematic Diagram Powder Metallurgy Fabrication Process (**Bharat and Bose, 2021**).

2.5 Effects of Powder Metallurgy Process Parameters on Composites

Powder metallurgy (PM) is a process that involves the production of metal or composite materials from powders. The process parameters of PM, such as powder characteristics, compaction pressure, sintering temperature and time, can affect the properties and performance of the composites. For example, the powder size and shape can influence the packing density, porosity, and surface area of the composites. The compaction pressure can affect the green density, strength, and dimensional accuracy of the composites. The sintering temperature and time can determine the degree of densification, diffusion, and bonding of the composites. Therefore, optimizing the process parameters of PM is essential for obtaining high-quality composites with desired features.

2.5.1 Milling Time

Milling time is the length of time required to finish a milling operation, which is a method of reducing the size of particles by grinding them with a rotating device called a mill. The milling time is not fixed, but it depends on various factors such as how complicated the shape of the product is, how hard or soft the material to be milled is, and what kind of milling technique is applied. As the milling time increases, the crystalline size of the particles decreases, which causes more distortion in the crystal structure (**Singh et al., 2019**). This leads to a reduction in the amount of powder produced by the milling process (**Parveen et al., 2021**).

(**Singh et al. 2019**) reported that the porosity of the powder and its characteristics at different stages of milling affected the mechanical properties of the sintered products, such as yield strength and modulus. They observed that as the milling time increased, the porous steel sintered at 1200 °C showed higher compressive strength and ductility. This was attributed to the improved densification and microstructure of the sintered material. Ball milling is a crucial process for achieving a uniform distribution of the reinforcement particles in the metal matrix. The duration of ball milling depends on the type and composition of the materials to be blended and the desired characteristics of the final product. (**Skotnicova et al. 2015**) suggested that the optimal ball milling time can vary from a few minutes to several days, depending on the application.

2.5.2 Compaction Pressure

Compaction pressure is the amount of force that is used to shape the composite powder into a specific form before it is heated and fused together in a process called sintering. Powder compaction is the most important stage in powder metallurgy, as it allows for the control and manipulation of various material attributes, such as shape, size, density, porosity, hardness, and other mechanical properties, during this stage (**Manohar et al. 2020**). Compaction pressure also affects the composite's mechanical performance, density, compressive strength, microstructure, and the quality of the bonds between the reinforcement and matrix materials (**Manohar et al., 2020**); (**Kumar et al., 2021**). The main objectives of this cold compaction process are to achieve the following outcomes: (**Ankur & Singh., 2021**).

- To create the desired form and appearance of the product,
- To control the size and measurements of the product and its components,
- To adjust the amount and distribution of air spaces within the product and
- To ensure the product has sufficient durability and resistance to withstand manipulation

2.5.3 Sintering Temperature and time

Powder metallurgy (PM) is a process that involves compacting and heating metal powders to form solid products. The heating step, called sintering, causes the metal particles to bond together and create a denser and stronger material. The sintering temperature is chosen to be below the melting point of the main metal in the powder, to avoid melting and deformation. The sintering temperature can vary depending on the type and composition of the powder, but it typically ranges from 1000 to over 1300 °C.

The sintering time can also affect the final properties of the PM product. For example, some studies have shown that Titanium-based PM composites can improve their mechanical and physical properties, such as hardness, strength, and porosity, by sintering at high temperatures for longer durations (**Fisika et al. 2008**); (**Delavari et al., 2011**); (**Jabur, 2013**). One recent study reported that a wet-milled composite powder of Titanium, iron, copper, and Graphite achieved a maximum hardness of 450 VHN and a compressive strength of 525 MPa when sintered at 1300 °C for two hours (**Meher et al., 2021**).

2.6 Reinforcements Used for Developing the Metal Matrix Composites

Reinforcement is a process that enhances the properties of metal matrix composites (MMCs) by adding particles of another material. Reinforcement improves the strength, stiffness, and thermal stability of MMCs, while reducing their density. Particle-reinforced composites are a type of MMCs that use ceramic particles as the reinforcing material. These particles can be derived from various ceramics, such as silicon carbide (SiC), alumina (Al_2O_3), boron carbide (B_4C), and others. Particle-reinforced composites have a wide range of applications in different industries, such as automotive, aerospace, electronics, marine, medical, and construction. This is because they offer high strength and stiffness at both ambient and high temperatures, as well as low ductility and high wear resistance. These advantages are supported by research studies published by (**Bozic et al. 2010** and **Hossain et al. 2018**).

2.6.1 Cerium (IV) oxide (CeO_2)

Cerium (IV) oxide for reinforcement for titanium metal matrix composite is a topic that relates to the development and application of titanium matrix composites (TMCs), which are materials that combine titanium metal with ceramic or carbon reinforcements to improve their properties. TMCs offer high specific strength and stiffness compared with steel and nickel-base materials, and can reduce weight and increase temperature capability for jet engine propulsion systems. Some common reinforcements for TMCs are carbon nanotubes, Graphite Nano flakes, and cerium (IV) oxide (**klaus Reinhardt** and **Herwig Winkler 2000**).

Cerium (IV) oxide is a rare-earth metal oxide with the chemical formula CeO_2. It is a pale yellow-white powder that is used as an intermediate in the purification of cerium from its ores. It is also an important commercial product for various applications, such as catalysts, polishing agents, oxygen sensors, and fuel cells. Cerium (IV) oxide has a fluorite structure and can release oxygen at high temperatures to form a non-stoichiometric oxide with both ionic and electronic conduction that can enhance the wear resistance, hardness, and thermal conductivity of titanium metal. Different fabrication methods such as powder metallurgy, spark plasma sintering, and direct metal laser sintering can be used to produce TMCs with cerium (IV) oxide reinforcement. The mechanical properties of TMCs depend on the type, size, shape, and distribution of the reinforcement, as well as the processing parameters and conditions (**Samira Bagheri** and **Ibrahim Khalil 2019).**

2.6.2 Chromium (Cr)

Chromium is a metal that has a high melting point, high hardness, high thermal conductivity, and good oxidation resistance. Chromium can be used as a secondary reinforcement for TMCs to enhance their mechanical and tribological properties. Chromium particles can be introduced into the titanium matrix by different methods, such as powder metallurgy, spark plasma sintering, direct metal laser sintering, or hot extrusion. Chromium particles can form intermetallic compounds or solid solutions with titanium, which can increase the strength and hardness of the composite. Chromium particles can also form protective oxide layers or coatings on the surface of the composite, which can improve the wear resistance and corrosion resistance of the composite (**Raviraj Shetty** and **Aditihya Hegde 2022**).

The mechanical properties of TMCs with chromium as secondary reinforcement depend on the type, size, shape, and distribution of the chromium particles, as well as the processing parameters and conditions. Some studies have reported that TMCs with chromium particles have higher tensile strength, compressive strength, fracture toughness, hardness, wear resistance, and corrosion resistance than pure titanium or TMCs with other reinforcements. However, some studies have also reported that TMCs with chromium particles have lower ductility, impact toughness, fatigue resistance, and thermal stability than pure titanium or TMCs with other reinforcements. Therefore, the optimal amount and composition of chromium particles for TMCs need to be carefully designed and controlled according to the specific application and operating environment of the composite (**Dhanunjay Kumar Ammisetti** and **S S Harish Kruthiventi 2020**).

2.6.3 Graphite Powder (Gr)

Graphite powder (Gr) is a carbon-based material that has a layered structure with hexagonal rings of carbon atoms. It has remarkable properties, such as high thermal and electrical conductivity, low thermal expansion, good lubrication, and resistance to oxidation and corrosion. Graphite powder can be used to enhance the performance of metal matrix composites (MMCs) by adding it as a reinforcing phase (**Mohammad Fallah Barzoki** and **Shohreh Faremi 2022**).

Graphite powder can be combined with different metal powders, such as copper, nickel, bronze, aluminum, etc., to form MMCs using powder metallurgy methods, such as mixing, compacting, and sintering. The characteristics and behavior of the MMCs depend on the amount, size, shape, and distribution of Graphite powder in the metal matrix. For instance, increasing the Graphite content can improve the hardness, wear resistance, and electrical conductivity of the MMCs, but reduce the density, ductility, and strength. To achieve a good adhesion between the Graphite and the metal matrix, some techniques, such as coating the Graphite powder with metal or alloy, or using an in-situ reaction method, can be applied (**Fatemeh Nemati** and **Maryam Rezaie 2021**).

2.7 Researchers Developed on Reinforced Ti-6Al-4v Matrix Composite

Ti-6Al-4V is a widely used titanium alloy that has high strength, corrosion resistance, and biocompatibility. However, it also has some drawbacks, such as low wear resistance, high density, and poor machinability. To overcome these limitations, researchers have developed various methods to reinforce Ti-6Al-4V matrix with ceramic particles, such as TiB, TiC, and TiB2. These particles can improve the hardness, wear resistance, and specific strength of the composite, as well as modify the microstructure and phase transformation of the matrix.

One of the common techniques to fabricate Ti-6Al-4V matrix composites is powder metallurgy, which involves mixing, compacting, and sintering of metal and ceramic powders. This method can produce near-net-shape components with uniform distribution of reinforcement and low porosity. However, the sintering temperature and time, as well as the amount and type of reinforcement, can affect the properties and performance of the composite. Therefore, researchers have investigated the optimal conditions and parameters to achieve the desired characteristics of Ti-6Al-4V matrix composites. Some of the recent studies on this topic are summarized below.

- (**Zhai et al. 2022**) fabricated Ti-6Al-4V/TiB composites by hot pressing of recycled Ti-6Al-4V chips and boron powder. They found that the addition of 3 vol.% boron resulted in the highest tensile strength and ductility of the composite, due to the formation of fine and discontinuous TiB whiskers. The heat treatment did not significantly improve the mechanical properties of the composite.
- (**Al-Hamdani et al. 2023**) produced Ti-6Al-4V/TiB2-TiC composites by spark plasma sintering of Ti-6Al-4V, TiB2, and Ti powders. They observed that the increase of TiB2 and TiC content enhanced the hardness and wear resistance of the composite, but reduced the fracture toughness and strain. The TiB2 and TiC particles also acted as nucleation sites for the alpha phase of Ti-6Al-4V, leading to a refined microstructure.
- (**Sivakumar et al. 2017**) prepared Ti-6Al-4V/WCp composites by squeeze casting of Ti-6Al-4V and WC powders. They reported that the addition of 10 wt.% WCp increased the hardness and wear resistance of the composite, due to the presence of hard and dense WC particles. The coefficient of friction of the composite decreased with the increase of load and sliding distance, due to the formation of a protective layer on the worn surface.

These studies demonstrate the potential of Ti-6Al-4V matrix composites for various applications that require high strength, hardness, and wear resistance. However, further research is needed to optimize the fabrication process, understand the interfacial reactions, and evaluate the long-term performance and reliability of the composites.

2.8 Effects of Reinforcement on Improvement of Mechanical Properties of MMCs

Cerium dioxide (CeO2), chromium (Cr) and Graphite (Gr) are nanomaterials that can be used as reinforcements to enhance the performance of titanium metal matrix composites (TMCs).

(**Lingyue HU 2020**) reported that CeO2 can improve the corrosion resistance, thermal stability and electrochemical properties of NiCoCrAlY coating by forming a protective oxide layer on the surface and enhancing the hydrophobicity of the coating.

(**Di Wang 2022**). reported that CrN/CrAlN multilayer coatings can increase the hardness, wear resistance and high-temperature strength of titanium alloy by forming intermetallic compounds with titanium and enhancing the oxidation resistance of the coatings.

(**Hanieh Ghodrati 2019**) reviewed the recent advances and challenges in the fabrication and characterization of graphene-reinforced metal matrix composites (MMCs). They discussed how Graphite can improve the dispersion, interfacial bonding and mechanical properties of MMCs by synergizing with other reinforcements such as CNTs, CeO_2, or TiC. They also highlighted the potential applications and future prospects of graphene-based MMCs. These nanomaterials can be incorporated into the titanium matrix by ex situ or in situ methods, such as powder metallurgy, spark plasma sintering, laser sintering, and vacuum induction melting. The optimal content and distribution of these reinforcements depend on the processing parameters, matrix material, and application requirements of TMCs.

(**Jiang Et Al 2020**) investigated the microstructure and properties of CeO_2-modified FeCoCrAlNiTi high-entropy alloy coatings by laser surface alloying. They found that CeO_2 resulted in the refined microstructure of the alloyed coating and improved its hardness and wear resistance.

(**Jiang et al 2021**) investigated the effects of Cr on the microstructures and mechanical properties of AlCoCr x FeNi 2.1 eutectic high entropy alloys (EHEAs) by laser surface alloying. They found that Cr enhanced the hardenability and refined the final microstructure of the alloyed coating, shifting the ferrite start curve to lower cooling rates. They also reported that the AlCoCr 0.5 FeNi 2.1 alloy showed the best comprehensive mechanical properties with a yield strength of 536.5 MPa, a fracture strength of 1062 MPa, and an elongation of 13.8%.

(**Chen et al 2021**) studied the effects of CeO_2 addition on the microstructure and properties of ceramics reinforced Fe-based coatings by laser cladding. They reported that CeO2 reduced the cracks and porosities in the coatings and enhanced their bonding performance with the substrate. They also observed that CeO_2 promoted the melting of large-size ceramic particles and increased the nucleation sites, leading to a finer microstructure and better mechanical properties.

(**Mohammed Ali et al 2020**) studied the influence of Cr content on the microstructure and mechanical properties of thermomechanical hot-rolled low-carbon bainitic steels containing Nb. They showed that Cr increased the hardenability and reduced the fraction of polygonal ferrite in the microstructure, leading to higher yield strength but lower ductility and toughness. They also observed that pre-deformation of austenite promoted the formation of polygonal ferrite at lower cooling rates, which decreased the hardness.

(**Li et al 2020**) Examined the microstructure and thermophysical properties of CeO2-doped SmTaO4 ceramics for thermal barrier coatings (TBCs). They showed that CeO2 doping induced defects in the SmTaO4 lattice, which significantly reduced its thermal conductivity. They also measured the hardness, fracture toughness, and thermal expansion coefficient of the CeO2-doped SmTaO4 ceramics.

(**Zhang et al 2020**) Examined the effects of Cr content on the microstructure and room temperature mechanical properties of WMoNbTiCr high entropy alloys (HEAs) by mechanical alloying and spark plasma sintering. They reported that there were three body-centered cubic (BCC) solid solution phases in the sintered alloys, including W-rich, Nb-rich, and Cr-rich phases. They also measured the hardness and compressive strength of the alloys and found that they increased with increasing Cr content.

2.9 Corrosion and Tribological Behavior of Reinforced Ti-MMC’s

Ti-MMCs are materials that consist of a titanium metal matrix and various reinforcements, such as ceramic particles, fibers, or nanomaterials. Ti-MMCs have many advantages, such as high strength, low density, good biocompatibility, and excellent corrosion resistance. However, they also face some challenges, such as high cost, poor machinability, and complex fabrication processes. Therefore, researchers have been exploring different ways to improve the properties and performance of Ti-MMCs, especially in terms of tribology and corrosion.

Tribology is the study of friction, wear, and lubrication of interacting surfaces. Tribological behavior of Ti-MMCs is important for many applications, such as aerospace, automotive, biomedical, and industrial. Some of the factors that affect the tribological behavior of Ti-MMCs are the type, size, shape, and distribution of the reinforcements, the applied load, speed, and temperature, the surface roughness, and the environment. Researchers have investigated the effects of these factors on the coefficient of friction, wear rate, wear mechanism, and wear debris of Ti-MMCs. For example, one study found that adding Si3N4 nanoparticles to Al2219 alloy improved its wear resistance, hardness, and tensile strength (**Wang, T. et al 2022**). Another study reported that the tribological performance of Ti-MMCs was influenced by the formation of tribofilms, which are thin layers of material that form on the sliding surfaces during friction (**Manjunatha, D. et al 2022**).

Corrosion is the deterioration of a material due to chemical or electrochemical reactions with the environment. Corrosion behavior of Ti-MMCs is important for applications that involve exposure to corrosive media, such as seawater, body fluids, or acids. Some of the factors that affect the corrosion behavior of Ti-MMCs are the composition, microstructure, and surface condition of the material, the type and concentration of the corrosive agent, the temperature, and the presence of mechanical stress. Researchers have investigated the effects of these factors on the corrosion rate, corrosion potential, corrosion current, and corrosion morphology of Ti-MMCs. For example, one study found that adding Cu and Ti to a Cu-Ti alloy reduced its corrosion rate and increased its corrosion resistance in 3.5% NaCl solution (**Ghasemi, F. 2021**). Another study reported that the corrosion behavior of Ti-MMCs was influenced by the formation of passive films, which are protective layers of oxide or hydroxide that form on the metal surface during corrosion (**Ramesh, S 2020**).

2.10 Summary of Literature Review

The literature review provides the foundation for this research by presenting the state of the art in the field of composites. It shows that previous researchers have explored various types of composites and their properties. Among the composites, metal matrix composites (MMCs) offer superior mechanical properties, such as strength, hardness, stiffness and corrosion resistance, compared to conventional metals. This research focuses on a specific type of MMC, namely titanium alloy reinforced with cerium oxide (CeO_2) and chromium (Cr) particles, which has unique characteristics and potential applications. The literature review also outlines the optimal strategy for enhancing the corrosion resistance of this composite, which is one of the main objectives of this research.

Furthermore, the literature review emphasizes the importance of selecting the appropriate processing parameters, testing factors, type, size and quantity of reinforcement to improve the mechanical properties and performance of the composite. These factors influence the microstructure and properties of the composite, and the literature review identifies the gaps and challenges in this area. The literature review also reviews the various experimental methods and techniques that have been used by previous researchers to study different types of reinforcement, particle sizes, fabrication methods and testing conditions. The literature review concludes by highlighting the need for further research on the titanium alloy-CeO_2-Cr composite and its properties.

2.11 Literature Gaps

Titanium metal matrix composites (Ti-MMCs) are materials that combine a titanium alloy matrix with different reinforcements, such as fibers, particles, or whiskers. These reinforcements improve the mechanical, corrosion, and wear properties of titanium. Ti-MMCs are widely used in various industries, such as aerospace, automotive, and biomedical, because they have high strength, stiffness, and oxidation resistance. However, Ti-MMCs also have some challenges, such as the difficulty of machining and heat treating them, because of the high hardness and brittleness of the reinforcements. Moreover, the wear and corrosion behavior of Ti-MMCs with different types of reinforcements and compositions are not well studied and understood. In particular, there is a lack of research on how adding smart materials, such as cerium oxide and chromium, and Graphite to a Ti-6Al-4V matrix affects the friction, wear, and corrosion performance of the composite. This study aims to fill this gap by examining how different amounts of cerium oxide and chromium, as well as graphene, influence the microstructure, physical and mechanical properties, corrosion resistance, and compressive strength of the Ti-6Al-4V-based composite.

CHAPTER THREE

MATERIALS AND METHODOLOGY

This chapter consists the materials used for the fabrication of Titanium based (Ti-6Al-4V) matrix composite, fabrication approach and methods for samples preparation, experimental procedure and set ups for testing activities, the instruments and equipment used and methodology of data analysis.

3.1 Materials

The objective of this study is to investigate the mechanical and metallurgical characteristics of titanium-based composites with various reinforcements. The study will use both numerical and experimental methods to analyze the effects of different weight fractions of CeO2, Cr, and Graphite on the properties of titanium matrix composites. The composites will be produced by a powder metallurgy technique, which involves mixing, compacting, and sintering the powders. The microstructure of the composites will be characterized by X-ray diffraction (X-RD) and optical microscopy to examine the distribution and bonding of the reinforcements in the titanium matrix. The hardness of the samples will be evaluated by a Vickers hardness tester, which applies a known force to the surface of the material and measures the indentation size. The wear resistance of the samples will be assessed by a Pin-on-Disc device, which simulates the sliding contact between two materials under different conditions of load, speed, and distance. The corrosion morphology of the corroded samples will be studied by scanning electron microscopy (SEM). The compressive strength of the samples at different strain rates will be measured by a universal testing machine, which applies a gradually increasing load to the material until it fails. The selection of the reinforcements and their weight fractions will be based on the cost, availability, and desired properties of the composites.

3.1.1 Titanium Ti-6AL-4V Matrix Selection

One of the most widely used titanium alloys in the world is Ti-6AL-4V, also known as Ti 6-4. This alloy accounts for almost 50% of the global titanium consumption. Ti 6-4 is composed of nearly 90% titanium, 6% aluminum, 4% vanadium, and trace amounts of iron and oxygen (less than 0.25% and 0.2%, respectively). Ti 6-4 has outstanding properties such as high strength, low elastic modulus, great resistance to corrosion, and easy weldability. It can also be heat treated to enhance its performance. The presence of aluminum and vanadium in the alloy makes the material harder and stronger by modifying its microstructure and mechanical behavior.

Figure 3.1 Titanium Ti-6AL- 4V powder

Table 3.1 Mechanical properties of Titanium Ti-6Al-4V from MiT Database

MECHANICAL PROPERTIES	VALUE	UNIT
Compressive strength	848 - 1080	MPa
Elastic modulus	110 - 119	GPa
Hardness	6.5	Mohs
Density	4.43 - 4.51	g/cm3
Thermal conductivity	0.8	W/mK
Melting point	2400	°C
Poisson's Ratio	0.31-0.37	

3.1.2 Cerium (IV) oxide (CeO_2) Reinforcement

Cerium (IV) oxide, or ceria, is a pale yellow-white powder that consists of oxygen and cerium, which is a rare-earth metal. Its chemical formula is CeO2 and it is widely used in industry and research. It is also a key intermediate in the extraction of pure cerium from its mineral sources. Cerium (IV) oxide has a cubic crystal structure that resembles the mineral fluorite, where each cerium atom is coordinated by eight oxygen atoms in a cubic arrangement, and each oxygen atom is coordinated by four cerium atoms in a tetrahedral arrangement. When the temperature is high, cerium (IV) oxide can lose some of its oxygen atoms and form a non-stoichiometric compound with a lower oxygen content,

CeO_{2-x} where - x, can range from 0 to 0.28 depending on the temperature and the amount of oxygen in the surrounding environment.

This property makes cerium (IV) oxide a valuable material for storing and releasing oxygen and for catalyzing various chemical reactions. Cerium (IV) oxide can be synthesized by heating cerium oxalate or cerium hydroxide, or by oxidizing cerium (III) oxide. It can also be prepared by adding an oxidizing agent to a solution of cerium ions in water and a base, which causes cerium (IV) oxide to precipitate as a solid that does not dissolve in water. Cerium (IV) oxide has a density of 7.13 g/mL, a melting point of 2400 °C, and a boiling point of 3500 °C.

It is very hard, with a hardness of 6.5 on the Mohs scale. Cerium (IV) oxide has many applications in various fields, such as polishing glass, making ceramics, sensing gases, generating electricity in fuel cells, converting sunlight into electricity in solar cells, reducing harmful emissions in catalytic converters, and engineering biomedical devices. Cerium (IV) oxide can also improve the performance of other catalysts by increasing their surface area and preventing them from aggregating and losing their porosity at high temperatures.

Figure 3.2 Cerium oxide (CeO_2)

Table 3.2 Mechanical properties of Cerium Oxide (CeO2) from MiT Database

Mechanical Properties	**Value**	**Unit**
Compressive strength	590	MPa
Elastic modulus	180	GPa
Hardness	6.5	Mohs
Density	7.13	g/cm^3
Thermal conductivity	0.8	W/mK
Melting point	2400	°C
Poisson's Ratio	0.28	

3.1.3 Chromium (Cr) Reinforcement

Chromium is a metal that has a white color, a hard texture, an excellent quality, and a brittle nature. It can resist corrosion very well, which means it does not rust easily. Chromium is used to coat some parts of cars, such as bumpers, wheels, and exhaust pipes, to make them last longer and look shiny. Chromium is also very important for many industries, because it has properties that make it suitable for harsh conditions, such as high hardness, high temperature, and high tensile strength. Hardness is the ability to resist scratches or dents, temperature is the measure of how hot or cold something is, and tensile strength is the measure of how much force something can withstand before breaking.

When chromium is mixed with Titanium, it forms a new material called a composite, which is harder than Titanium alone. This is useful for making tools, machines, and structures that need to be strong and durable. A study by (**Bairwa et al. 2021**) showed that adding chromium to Titanium increased the hardness of the composite. Another study by (**Konishi et al. 2005**) showed that adding different amounts of chromium to Titanium (5%, 7.5%, and 10% by weight) reduced the amount of corrosion that occurred on the Titanium. Corrosion is the process of metal breaking down due to chemical reactions with water, air, or other substances. Corrosion can damage metal and make it weaker or less functional. Therefore, adding chromium to Titanium can make it more resistant to corrosion and extend its lifespan.

Figure 3.1 Chromium (Cr) powder

The microstructure of the composite material shows that the Titanium matrix is uniformly reinforced with chromium particles, and no flaws or cracks are present in the sample (**Varadaraj et al, 2023**). The metal matrix has a martensitic structure, which can improve its strength and toughness. By adding sufficient chromium to the metal matrix, the composite material can also resist corrosion and abrasion better (**Hill et al, 2011**). Chromium powder was selected as the reinforcement material because of its outstanding properties of hardness, wear resistance and corrosion resistance.

Table 3.3 properties of Chromium (Cr) from MiT Database

Mechanical Properties	Value	Unit
Compressive strength	282	MPa
Elastic modulus	140	GPa
Hardness	8.5	Mohs
Density	7.15	g/cm^3
Thermal conductivity	69.1	W/mK
Melting point	1907	°C
Poisson’s Ratio	0.21	

3.1.4 Graphite Powder

Natural Graphite powder is a type of Graphite that has a high purity and crystallinity, and it can be used as a lubricant for MMC, which are metal matrix composites that consist of a metal matrix and a reinforcement material. Natural Graphite powder can improve the lubrication of MMC by reducing the friction and wear between the metal matrix and the reinforcement material, as well as between the MMC and other surfaces. Natural Graphite powder can also enhance the mechanical, thermal, and corrosion resistance of MMC by forming in situ carbides or borides with the metal matrix or the reinforcement material.

Figure 3.4 Graphite powder: Material Used in The Research Work (Purchased from Parshwamani Metal Manufacturer, Mumbai, India).

For example, natural Graphite powder can be used as a carbon source to produce composites that have titanium carbide and titanium boride as reinforcements and titanium alloy Ti-6Al-4V as the matrix by a process that involves heating and pressing the powders together **Wang, Hd. (2013)**. These composites have improved densification, hardness, wear resistance, and corrosion resistance compared to pure Ti-6Al-4V. Therefore, natural Graphite powder is a useful lubricant for MMC that can improve their performance and quality.

Table 3.4 properties of Graphite powder from MiT Database

Mechanical Properties	Value	Unit
Compressive strength	14	MPa
Elastic modulus	11.5	GPa
Density	2.26	g/cm^3
Thermal conductivity	200	W/mK
Melting point	3600	°C
Hear Capacity	720	J/gk

Flow Chart of This Research Work Methodology

The research work methodology can be expressed as follow by using flow chart.

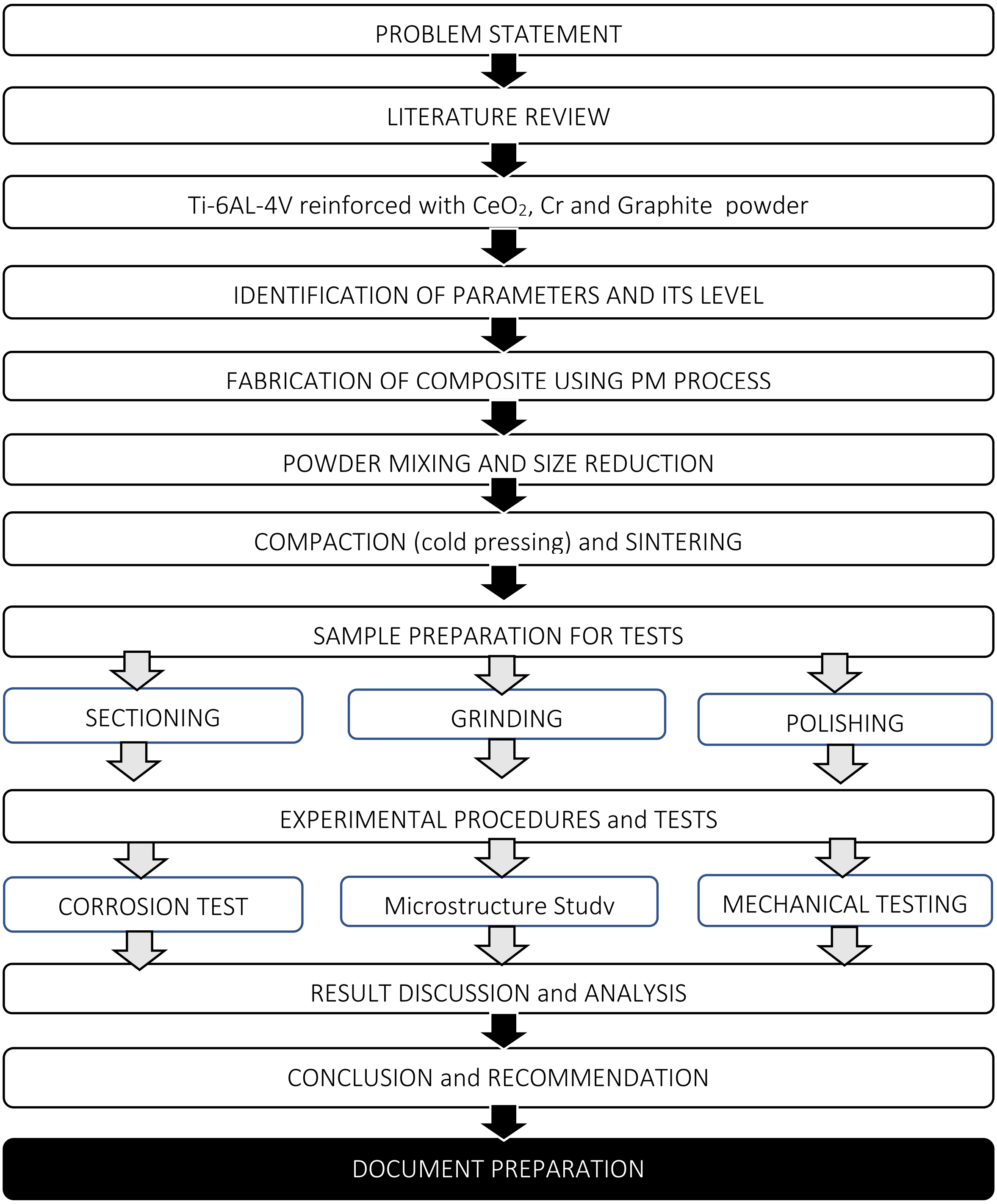

Figure 3.5 Flow chart of the methodology of the thesis

3.2 Methodology

3.2.1 Matrix and Reinforcement Material Selection

The matrix alloy in a metal matrix composite (MMC) is not merely a binder for the reinforcement, but a vital component that influences its attributes and performance. Hence, it should be chosen with caution based on its chemical interaction with the reinforcement, as well as its own properties and processing behavior. A general guideline for adding alloying elements is to steer clear of those that create intermetallic compounds with the matrix elements or highly stable compounds with the reinforcements. The best properties of a composite system can be attained when the reinforcement particulates and matrix have the highest physical and chemical compatibility (**Ashwath, P 2016**).

As discussed in the literature review (chapter two), automobile designers and manufacturers have been striving to reduce the weight of their products in order to save energy and preserve natural resources in the current situation. Metal matrix composites (MMCs) are a class of materials that offer several advantages for this purpose, as they combine a metal matrix with ceramic or metallic reinforcements, such as fibers, whiskers, or particles. MMCs have superior mechanical properties, such as high strength, hardness, stiffness, and wear resistance, compared to conventional metals (Russo 2006).

They also have desirable physical properties, such as high electrical and thermal conductivities and resistance to most types of radiation. Among the various MMCs, titanium matrix composites (TMCs) have gained popularity due to their low density and outstanding mechanical performance, as well as their good corrosion resistance. In particular, Ti-CeO2/Cr-matrix alloy is a promising candidate for achieving significant weight reduction, as it has a higher elastic modulus than pure titanium, owing to the addition of CeO_2 and Cr reinforcements, which have elastic moduli of 180 and 140 GPa respectively.

Cerium oxide and chromium are two ceramic materials that have been widely studied for their outstanding properties of oxidation and corrosion resistance, even under high-temperature conditions without failing, according to (**Li et al 2020**). When these materials are applied to metal surfaces, they create protective oxide layers that inhibit further deterioration by oxygen or other corrosive agents. However, they have different mechanisms of action: cerium oxide blocks the cathodic sites, where reduction reactions occur, while chromium blocks the anodic sites, where oxidation reactions occur. By combining cerium oxide and chromium, the corrosion resistance can be improved, as cerium oxide helps to form a thinner and more durable layer of chromium oxide, as reported by (**Mendez, J.A. 2022**). Therefore, a mixture of cerium oxide and chromium could be a better option than using either of them separately for corrosion protection.

One of the promising materials for engineering applications are the Titanium matrix composites (Ti MMC) reinforced with cerium oxide (CeO_2) and chromium (Cr) particles. These composites exhibit improved hardness, compressive strength and wear resistance, which are important properties for high-performance materials.

According to the literature reviews, cerium oxide has a greater effect than chromium on enhancing the strength, hardness and wear resistance of Ti MMC. This is because cerium oxide is a rare-earth metal oxide that has a high melting point of 2400°C and a low solubility of 0.001 g/L in water at 25°C.

When cerium oxide is coated on the surface of Ti MMC, it forms a thin film that improves the lithium ion transport and reduces the polarization, which are beneficial for the electrochemical performance of the composites. Moreover, cerium oxide has more oxygen vacancies than chromium, which means it can provide more active sites for the deep oxidation of volatile organic compounds (VOCs), as reported by (**Yu, Y., Guo, Y 2019**).

Another advantage of cerium oxide is that it is chemically compatible with Titanium alloy and does not form any inter-metallic phase that could degrade the mechanical properties of the composites. Cerium oxide also has good thermal conductivity and workability, as stated by (**Venkatesan. et al. 2014**). Therefore, CeO_2/ Cr-particulate-reinforced Ti MMC are superior materials that have a combination of excellent properties.

3.2.2 Design the Experiment for Ti-MMC Fabrication

Four samples of Ti-based metal matrix composites (MMCs) were fabricated using powder metallurgy technique, following a literature review. Powder metallurgy is a method of producing metal-based materials by compacting and sintering metal powders. Ti-based MMCs are lightweight materials that have high specific strength, excellent chemical resistance, and good biocompatibility.

The fabrication process consisted of four steps:

- First, Ti powder was mixed with reinforcement particles of CeO_2 and Cr in different weight fractions. CeO_2 and Cr are used to improve the wear resistance, heat resistance, and oxidation stability of Ti-based MMCs.
- Second, the powder mixture was milled for 2 hours to achieve a homogeneous distribution of the reinforcement particles and to reduce the particle size.
- Third, the milled powder was compacted at 60 MPa to form a green compact with a high density and a desired shape.
- Fourth, the green compact was sintered at 1100°C for 2 hours to consolidate the powder particles and to form a strong bond between the matrix and the reinforcement.

The process parameters, such as milling time, compaction pressure, sintering temperature, sintering time, and weight fraction of reinforcement, were kept constant for all samples to ensure a fair comparison. The fabricated samples were then subjected to various characterization and testing methods to evaluate their mechanical and physical properties, such as hardness, tensile strength, fracture toughness, density, porosity, and microstructure.

The properties of Ti-based metal matrix composites (MMCs) depend on the type and amount of reinforcement particles, as well as the fabrication process. To investigate how these factors, influence the Ti-based MMCs, various characterization and testing methods were employed, such as:

- Scanning electron microscopy (SEM): This technique uses a focused beam of electrons to scan the surface of a sample and generate a high-resolution image of its microstructure and morphology. SEM can reveal the distribution, shape, and size of the reinforcement particles, as well as the presence of defects, cracks, or pores in the matrix.
- X-ray diffraction (XRD): This technique uses a beam of X-rays to diffract from the crystal lattice of a sample and produce a pattern of peaks that corresponds to the interplanar spacing and orientation of the atoms. XRD can identify the phases and crystallinity of the matrix and the reinforcement particles, as well as the residual stresses and lattice strain in the composite.

- Density measurement: This technique uses the mass and volume of a sample to calculate its density, which is an important indicator of the quality and performance of the composite. Density measurement can also estimate the porosity and relative density of the composite, which affect its mechanical and physical properties.
- Hardness test: This technique uses a hard indenter to apply a load on the surface of a sample and measure the depth or area of the resulting indentation. Hardness test can evaluate the resistance to indentation, deformation, and wear of the composite, as well as the effect of reinforcement particles on the hardness of the matrix.
- Compression test: This technique uses to measures how a material or a product resists a compressive load. It can evaluate properties like compressive strength, yield strength, elastic modulus, and more. It uses a machine to apply a force and measure the deformation or strain. The data can be plotted as a stress-strain curve. A compression test can help select the best materials or products for different applications.

The data obtained from these methods were compared and analyzed to understand the relationship between the microstructure, composition, and properties of the Ti-based MMCs. The results were also discussed in the context of the existing literature and the potential applications of the composites.

Table 3.5 Reinforced Ti-MMC made by powder metallurgy.

SAMPLES	COMPOSITION	WEIGH PERCENTAGE (%)
S1- Samples	Titanium (Ti-6Al-4V)	81%
	Cerium oxide (CeO_2)	5%
	Chromium (Cr)	10%
	Graphite	4%
S2- Samples	Titanium (Ti-6Al-4V)	81%
	Cerium oxide (CeO_2)	10%
	Chromium (Cr)	5%
	Graphite	4%

S3- Samples	Titanium (Ti-6Al-4V)	81%
	Cerium oxide (CeO_2)	7.5%
	Chromium (Cr)	7.5%
	Graphite	4%
S4- Samples	Titanium (Ti-6Al-4V)	100%
	Cerium oxide (CeO_2)	0%
	Chromium (Cr)	0%
	Graphite	0%

3.2.3 Specification of Weight Percentage Composition

The weight percentage (wt.%) of the reinforcements affects the mechanical and wear properties of the developed composite materials significantly. In this research work, the weight percentage composition of CeO_2 and Cr was chosen based on the literature review and the previous studies of the following researchers. Each sample had a different wt% composition of reinforcement according to the experimental design.

Yu, Y., Guo, Y (2019) review focuses on the use of CeO_2 as a reinforcement in aluminum matrix composites (AMCs) for improving the mechanical and tribological properties. The authors prepared different AMCs with varying CeO_2 content from 0 to 10 wt% by stir casting method. They found that the addition of CeO_2 improved the hardness, tensile strength, wear resistance, and friction coefficient of the AMCs. They attributed this to the uniform dispersion of CeO_2 particles, the formation of intermetallic compounds, and the enhanced load-bearing capacity of the matrix. The optimal CeO_2 content was found to be 6 wt%, which showed the highest performance among the AMCs.

Gupta et al (2022) studied the synergetic effect of CeO_2 doping on structural and tribological behavior of Fe-Al_2O_3 metal matrix nanocomposites. They prepared the nanocomposites with 0.5 and 1.0 wt% of CeO_2 by ball milling and microwave sintering process. They observed that increasing the amount of CeO_2 in the material resulted in an increase in both density and hardness, as well as a decrease in wear rate.

Himyan Mohammed et al (2018) examined the structural and mechanical properties of CeO_2 reinforced Al matrix nanocomposites. They fabricated the nanocomposites with various concentrations of CeO_2 (0, 1, 3, and 5 wt%) by ball milling and microwave sintering process. They reported that a significant increase in microhardness and compressive strength was noticed with increasing concentration of CeO_2 nanoparticles due to a dispersion hardening effect of the reinforcement.

Zhang et al (2019) synthesized titanium-based matrix composites reinforced with particulate chromium carbide (Cr3C2) by spark plasma sintering. They used different amounts of Cr_3C_2 (0, 5, 10, and 15 wt%) as the reinforcement phase. They found that the addition of Cr_3C_2 increased the hardness, elastic modulus, and wear resistance of the composites, as well as reduced the coefficient of friction. They also observed that the optimal amount of Cr_3C_2 was 10 wt%, which resulted in the highest relative density and mechanical properties.

Monowar Wadud Hridoy et al (2019) fabricated aluminum-based matrix composites reinforced with chromium oxide (Cr_2O_3) nanoparticles by stir casting method. They used four different weight fractions of Cr_2O_3 (0, 1, 2, and 3 wt%) as the reinforcement phase. They reported that the addition of Cr2O3 improved the microstructure, hardness, tensile strength, and wear resistance of the composites. They also noted that the best performance was achieved with 2 wt% of Cr_2O_3, which showed a significant increase in hardness and tensile strength compared to the pure aluminum matrix.

Rohatgi et. al (2020) prepared magnesium-based matrix composites reinforced with chromium nitride (CrN) nanoparticles by powder metallurgy and hot extrusion. They used three different weight percentages of CrN (0, 0.5, and 1 wt%) as the reinforcement phase. They demonstrated that the addition of CrN enhanced the grain refinement, hardness, yield strength, and corrosion resistance of the composites. They also revealed that the optimal amount of CrN was 0.5 wt%, which exhibited the highest hardness and yield strength among the samples. However, in Titanium metal matrix composites reinforced with CeO_2 and Cr fabricated through powder metallurgy process, not much work has been reported so far. From the available literature, it can be seen that the optimization and modeling of mechanical and wear performance of the Ti-6Al-4V composites has not been investigated in detailed way yet.

3.2.4 Weight (In Mass) Estimation for Matrix and Reinforcement Inquires

The amount of matrix and reinforcement materials needed to produce Ti-6Al-4V/ CeO_2 and Cr composite samples was calculated from the number and size of specimens required for hardness, microstructure, compression and wear tests. The specimens were prepared using a die and a punch with pre-designed dimensions. The die had an inner diameter of 20 mm and a height of 50 mm, while the punch had a diameter of 20 mm with a small clearance to fit into the die. The powder mixture was compacted by a hydraulic pressing machine inside the die using the punch. Cylindrical specimens of Ti-6Al-4V-matrix and Ti-6Al-4V/ CeO_2 and Cr composite were fabricated with the same diameter (d) as the die and punch, and a variable length (L) depending on the amount of powder and the applied pressure. The length of the specimens was constrained by the capacity of the hydraulic pressing machine. The dimensions of the specimens are shown in Figure 3.2.

Figure 3.6 Dimension for all samples

The specimens for the tests were manufactured using a pre-designed die and punch. The dimensions and types of the specimens are as follows:

- For the hardness and microstructural tests, cylindrical specimens with a length of 6 mm and a diameter of 20 mm were prepared.
- For the compression test, cylindrical specimens with a length of 20 mm and a diameter of 6 mm were prepared.
- For the wear test, cylindrical specimens with a length of 12 mm and a diameter of 6 mm were prepared.

The specimens were cut from the composite material using a hand saw and a file. A grinding allowance of 10 mm was considered to account for the material removal during the finishing process. The total length and diameter of the composite material were calculated by adding the lengths and diameters of all the specimens, respectively.

L= hardness and microstructure (15mm) + compression (20mm) + corrosion (12mm) + Wear (12mm) + allowance (10mm)

L= 69mm

D = 12mm

The volume of cylindrical specimen is calculated using Eq (3.1);

$$V = (\pi \times D^2 \times L)/4 = \pi \times L \times r^2 \quad (3.1)$$

Where V= volume of sample in mm^3, L=length of sample in mm, and D=diameter sample in mm, VT= the total volume of material required for each sample in mm^3

$$V = (\pi\ (12mm)^2 \times 69mm)/4 = 7799.76\ mm^3 = \mathbf{7.79\ cm^3}$$

For four samples, $V_T = 7.79\ cm^3 * 4 = 31.16\ cm^3$ the total volume of material required for sample fabrication includes both matrix and reinforcement materials and for four (4) sample fabrications $V_T = 31.16\ cm^3$

Table 3.6 The Total mass of Ti and CeO_2/ Cr powder required for samples production.

Sample No	**Ti-6Al-4V**		**CeO_2**		**Cr**		**Graphite**	
	V(cm^3)	Mass	V(cm^3)	Mass	V(cm^3)	Mass	V(cm^3)	Mass
Sample 1	6.3	28.4g	0.39	2.97g	0.78	5.53g	0.31	0.71g
Sample 2	6.3	28.4g	0.78	5.95g	0.39	2.77g	0.31	0.71g
Sample 3	6.3	28.4g	0.58	4.47g	0.58	4.15g	0.31	0.71g
Sample 4	7.79	35.1g	-	-	-	-	-	-
Total Volume required	26.69 cm^3		1.75 cm^3		1.75 cm^3		0.93 cm^3	

Density of Titanium (Ti-6Al-4V) = 4.507g/cm^3, Density of Cerium oxide (CeO_2) = 7.65g/cm^3, Density of Chromium (Cr)= 7.1 g/cm^3, Density of Graphite = 2.266g/cm^3.

The weights of matrix material (Ti-6Al-4V) and reinforcement materials (CeO_2, Cr, Graphite) for each sample of given composition are estimated as follows: The mass of a material is the product of the volume of the material and the density of the material (m=V*ρ). Therefore,

Total weight of (Ti-6Al-4V) = Total volume of (Ti-6Al-4V) * Density of (Ti-6Al-4V)

= 26.69 cm^3 * 4.507g/cm^3 = 120.29 g

Total mass of Cerium oxide (CeO_2) = Total volume of (CeO_2) * Density of (CeO_2)

= 1.75 cm^3 * 7.65g/cm^3 = 13.39 g

Total mass of Chromium (Cr) = Total volume of (Cr) * Density of (Cr)

= 1.75 cm^3 * 7.1 g/cm^3 = 12.43 g

Total mass of Graphite = Total volume of Graphite * Density of Graphite

= 0.93 cm^3 * 2.266g/cm^3 = 2.11 g

Total weight (mass) required for the work is approximately 150 g

3.3 Equipment's and Tools Used to Fabricate and Prepare the Samples

The basic tools and equipment used in this thesis work are mentioned in table 3.7 and in table 3.8 respectively with their functions. The usage of each tools and equipment used in this thesis are described in detail in the fabrication and specimen preparation methods.

Table 3.7. Tools used to prepare the specimens for different tests

No	Tools	Function/ task
1	Hack Saw	Used for sectioning the fabricated small size samples
2	File/ rasp	For filing/rasping the sectioned sample for further grinding and polishing processes
3	Caliper	To measure the test specimen's dimensions

Table 3.8. Equipment's required for the thesis work

No	Equipment's	Function/ usage
1	High energy ball milling	For mixing and powder size reduction of the Ti-6Al-4v alloy and SiC reinforcement
2	Hydraulic pressing machine	To compact the mixed Ti-6Al-4v/ Sic powder
3	Furnace	For sintering the green- compacted samples at a given temperature for further samples strength increment
4	Argon gas with cylinder	An argon gas was inserted through copper tube into the furnace during sintering process for atmospheric air control to prevent reaction of the Ti-6Al-4v samples.
5	Grinder/ polisher	To obtain a flat mirror like surface free from excessive deformation
6	Chemical (killer's etchant) solution	To avoid any particles, dust, debris.... etc. from the prepared specimen for micro structural characterization
7	Optical microscope (OM)	For examining the structural characteristics of the Ti-6Al-4v matrix and Ti-6Al-4v/SiC composite specimens
8	Scanning electron microscope (SEM)	For morphological characterization of the wear surfaces the Ti-6Al-4v matrix and Ti-6Al-4v/SiC composite.
9	Vickers hardness machine	To test hardness of the matrix and composite
10	Universal testing machine (UTN)	To test the compressive strength or capacity of the Ti-6Al-4v matrix and Ti-6Al-4v/SiCp composite material to withstand loads tending to reduce size.
11	Electronic weighting machine	To measure the weight loss of the specimens during the wear test.

3.4 Fabrication of The Ti-6Al-4v / (Ceo2, Cr) Composite Samples

This study investigated the fabrication of Ti-6Al-4V / (CeO_2, Cr) composites by using the powder metallurgy method. The composites consisted of a Ti-6Al-4V alloy matrix and CeO_2 and Cr particles as reinforcements. The powder metallurgy method involved mixing, compacting, and sintering the powders under controlled conditions.

3.4.1 Powder Metallurgy Process

Particulate reinforced metal matrix composites (MMCs) are materials that consist of a metal matrix (such as aluminum or magnesium) and ceramic particles (such as silicon carbide or Graphite) that enhance the physical and mechanical properties of the metal. Among the various techniques for producing these composites, powder metallurgy (PM) is one of the most economical and flexible methods. PM allows fabricating near-net-shape particulate reinforced MMCs with reduced manufacturing costs, minimized machining processes, and minimized scrap losses. Moreover, PM offers more uniformity in the distribution of the reinforcement material and reduces the clustering problem, which results in improved mechanical properties. This has been demonstrated by several studies, such as (**Kumar et al. 2016**), (**Kanthavel et al. 2016**), and (**Nassar et al. 2017).**

3.4.1.1 Powder Mixing

Mixing is the process of blending powders of different types in a uniform manner. This is essential for achieving the desired performance of the composite materials made from the selected powders. To ensure a homogeneous distribution of the powders in the matrix, a high energy ball milling machine is used. This machine grinds the metal alloy powders in a high-speed chamber using tungsten balls, creating a mechanically alloyed intermetallic compound. High energy ball milling also produces fine particles from the alloy powders, which enhance the physical and structural homogeneity of the final product.

The pre-alloyed Ti-6Al-4v matrix powder is mixed with a measured weight percentage of CeO2 and Cr, which are also reduced in size by the ball milling process. One weight percentage of n-butanol is added to the composite powder mixture to prevent any disturbance in the distribution, to avoid the spilling of the matrix powders from the Graphite molds, and to reduce the friction between the mold and the powder. After the mixing process is completed, the mixture is stored in a vacuum tube to prevent oxidation by exposure to air.

This study investigated the effects of different proportions of pre-alloyed Cerium oxide (CeO2) and chromium (Cr) reinforcements on the properties of titanium (Ti) matrix composites. Three samples were prepared with varying weight percentages of CeO2 and Cr as follows: sample one had 5% CeO2 and 10% Cr, sample two had 7.5% CeO2 and 7.5% Cr, and sample three had 10% CeO2 and 5% Cr. The rest of the composition (81%) was Ti for all samples. The powder mixture was milled using a high-energy planetary ball mill with zirconia balls as the grinding media, following the method of (**Jha et al. 2022**). The milling parameters were set as:

- Milling speed: 200 rpm
- Ball diameter: 10 mm
- Milling Temperature: room temperature
- Milling time: 2hours
- Ball-to-powder weight ratio: 10:1

Figure 3.7 High energy ball milling machine for powder mixing process and

3.4.1.2 Powder Compaction

Powder compaction is a powder metallurgy technique that involves applying high pressure to a mixture of metal and ceramic powders in a die to form a solid compact or sheet. In this study, the powder mixture consists of titanium alloy (Ti-6Al-4V), cerium oxide (CeO_2), chromium (Cr), and Graphite. The powder compaction can be performed using different methods, such as uniaxial, multiaxial, or isostatic pressing. Uniaxial pressing is the most common method, where the pressure is applied from one or both sides of the die. In this case, the tools are usually arranged vertically, with the punch tool at the bottom of the die cavity and the upper tool at the top, as illustrated in figure 3.7. The density and uniformity of the powder compact depend on several factors, such as the properties of the original powder, the type and magnitude of the pressure, and the design of the die structure.

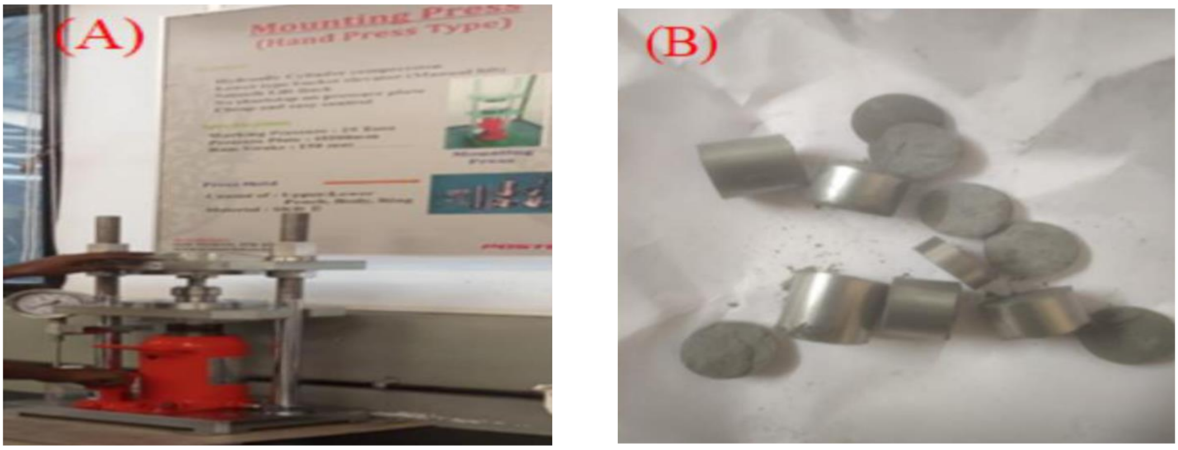

Figure 3.8 Photos of (A) Mounting Press set up and (B) Compacted Specimen (Green Part)

The cold die compaction process was used to produce green compacted samples from mixed powders of matrix and composite materials. The mixed powders were weighed for each sample and filled into a die and punch set-up, which was placed on a 25-ton hydraulic press machine. The compaction was performed at three different pressures: 0, 15 and 40 MPa, with a holding time of 60 minutes for each pressure. The resulting green compacted samples had a diameter of 20 mm and varying heights, depending on the applied pressure and the compressibility of the mixed powders.

The compressibility of powders is a measure of how much the mixed powder can be reduced in volume and increased in density by applying a certain pressure. Higher compressibility means that higher pressure is needed to achieve the same degree of compaction for a given mixed powder. After the compaction, the green compacted samples were ejected from the die cavity. The density of the compacted powder was directly proportional to the applied pressure, meaning that higher pressure resulted in higher density. The density of the compacts was also influenced by the homogeneity and uniformity of the powder mixture, as well as the hardness of the matrix powders. A more homogeneous and uniform powder mixture would lead to a more uniform density distribution in the compacts. Softer matrix powders would deform more easily and fill the gaps between the particles, resulting in higher green density. The die and punch tools were made of high carbon chromium steel, which has high strength and wear resistance. The dimensions of the die and punch tools were pre-designed according to the specifications given in table 3.8.

Table 3.9 The die and punch dimensions

S. No	Parameters of die and punch	Dimension, mm
1	Outer diameter of die	50
2	Inner diameter of die	20
3	Length of the die	50
4	Diameter of the punch	20- clearance
5	Length of the punch	50

3.4.1.3 Sintering

Sintering is a heat treatment process that transforms loose powder into a solid piece by applying high temperature and pressure. It is suitable for materials with high melting points, such as metals, ceramics, and plastics. Sintering involves two steps: compaction and fusion. In the first step, the powder is compressed into a desired shape, called a green compact. The green compact is weak and fragile, because the particles are only held together by weak forces and there are gaps between them. In the second step, the green compact is heated to a temperature below the melting point of the main material, but high enough to cause the particles to bond together (**Issa et al., 2023**). This reduces the gaps and increases the strength of the piece. The bonding agent that was used to compact the powder is also removed during this step.

Sintering can be divided into three stages, based on the changes that occur in the microstructure of the piece. In the first stage, the particles start to form necks at the contact points, but they remain distinct. In the second stage, the necks grow larger and the particles merge into each other. The structure becomes denser and recrystallizes. In the third stage, the remaining gaps become round and isolated, and the density increases slowly (**Issa et al., 2023**).

There are different types of sintering, depending on the temperature and the composition of the powder. Solid state sintering is the most common type, where the powder is heated to a temperature between 70% and 90% of the melting point of the main material. The bonding between the particles is achieved by interparticle diffusion, plastic deformation, grain formation, and grain growth. The term solid state means that the material does not melt during the process. Liquid phase sintering is another type, where the powder contains a component that has a lower melting point than the main material. The component melts and forms a liquid phase that fills the gaps and enhances the bonding between the particles. The density of the piece is improved by liquid phase sintering (**Das et al., 2022**).

Sintering requires a controlled atmosphere to prevent oxidation of the surface of the piece. Oxidation can affect the properties and the appearance of the material. Different gases can be used as sintering atmosphere, such as argon, helium, nitrogen, and nitrogen-hydrogen mixture. The choice of gas depends on the type and the composition of the powder.

In this study, sintering was performed in a controlled atmosphere of argon gas to prevent oxidation of the surface of the (Ti-6Al-4V)-CeO2-Cr samples. The samples were prepared by drying at 150 °C for 30 minutes in an oven and compacting the powder into four different shapes (S1, S2, S3, and S4). The samples were then sintered in a high temperature box furnace with a Graphite heater at ASTU material lab. The sintering temperature was 1100 °C and the sintering time was 120 minutes. The heating rate was 10 °C/min and the argon gas flow rate was 10 liters/min. The samples were held at the sintering temperature for 20 minutes before cooling down. The sintering process was based on the methods of (**Karabulut et al. 2022**), (**Shamsuddin et al. 2008**), (**Shamsuddin et al. 2014**), and (**Duriagina et al. 2020**).

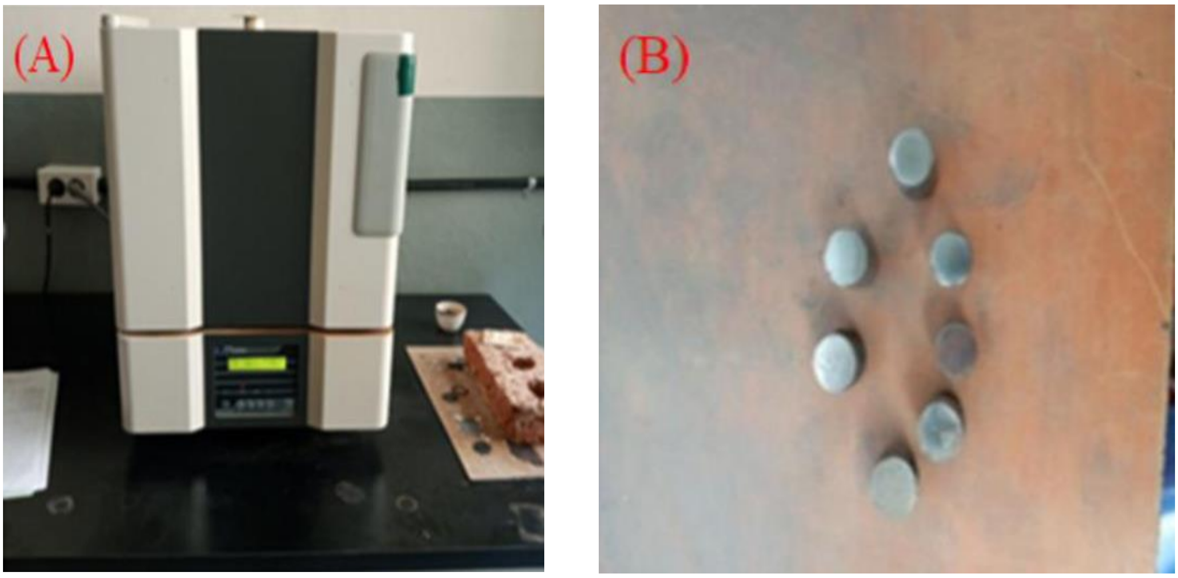

Figure 3.9 (A), The Furnace Set Up and (B) The Sintered Samples

3.5 Specimens Preparation for Microstructural Characterization

The powder metallurgy process was used to fabricate the matrix and composite samples. This process consists of two main steps: compacting and sintering metal powders. The compaction step applies pressure to the metal powders to form a coherent mass, while the sintering step heats the compacted mass to bond the particles together. The resulting products were evaluated by various methods, such as hardness test, compression test, wear test and microstructural characterization. These methods measure the mechanical and physical properties of the samples, such as their resistance to deformation, fracture, abrasion and corrosion. To prepare the samples for these methods, they were cut and shaped according to the ASTM standard by using a hand saw and a file/rasp, as shown in figure 3.10. The hand saw was used to cut the samples into smaller pieces that fit the testing equipment, while the file/rasp was used to smoothen the edges and surfaces of the samples to remove any burrs or irregularities.

3.5.1 Specimen Preparation for Microstructure Studies

The main steps of specimen preparation for light microscopy include; sectioning, mounting, grinding (course grinding and fine grinding), polishing and etching and then microscopic examination.

3.5.1.1 Sectioning

Sectioning is a process of preparing thin slices of a specimen for light microscopy. This process has two main benefits: it reveals the internal structure of the specimen that is otherwise hidden; and it makes the specimen thin enough to fit on the microscope stage and allow light to pass through. Different types of specimens require different methods of sectioning, such as the paraffin technique for soft tissues, frozen sections for urgent diagnosis, and semithin sections for electron microscopy. In this study, we applied a simple method of sectioning for large and hard samples, such as bones, teeth, and shells. This method consisted of cutting the samples with a hand-saw and then smoothing the cut surfaces with a file or a rasp, as illustrated in figure 3.10. This method enabled us to obtain thin and flat sections of the samples without using any chemicals or special equipment.

Figure 3.10 specimen preparation for different tests

3.5.1.2 Mounting

Mounting is a technique that involves embedding specimens in mounting materials, usually thermosetting polymers, to provide them with a regular shape and protect them from damage during further processing. Mounting is not essential for this study, as the specimens were large and regular enough to be handled without difficulty. However, mounting is necessary for specimens that are too small, sharp, or irregularly shaped to be manipulated safely and conveniently. Mounting also helps to preserve the edge retention and surface layers of the specimens, as well as to orient them properly for analysis. There are two main methods of mounting: hot compression mounting and cold mounting, depending on the type of specimen and the resin used.

3.5.1.3 Grinding and Polishing Processes

The sintered samples of the mixed powder composite of (Ti-6Al-4V)-CeO_2-Cr-Graphite were subjected to grinding and polishing for hardness testing and microstructural analysis. The aim of this process was to achieve a flat and smooth surface without excessive deformation or damage. The process consisted of three steps: rough grinding, fine grinding, and polishing. In the rough grinding step, the samples were abraded with emery paper of different grit sizes (120, 400, 800, 1200, and 2000) to remove the scratches and irregularities from the surface, as illustrated in figure 3.8. In the fine grinding step, the samples were further smoothed with finer abrasive materials to reduce the surface roughness. In the polishing step, the samples were rubbed with a diamond suspension on a polishing machine

(**RB 204 Metpol-II Model**) to obtain a mirror-like finish. The pressure and the rotational speed of the sand wheel were gradually decreased during the polishing step to avoid overheating and cracking of the samples, as shown in figure 3.12.

Figure 3.11 grinding process

figure 3.12 polishing process

3.5.1.4 Etching

To reveal the microstructure of the matrix and composites, the polished samples were subjected to a selective etching process using a mixed etchants solution. The solution consisted of 25 ml of methanol, 25 ml of hydrochloric acid, 25 ml of nitric acid, and 1 drop of hydrofluoric acid. The samples were immersed in the solution for 20 seconds and then rinsed with distilled water. This method was based on the different oxidation rates of the polymer and the fillings by the oxygen atoms in the plasma. The etched samples were then ready for microstructural characterization using various techniques.

Figure 3.13 Sample Preparation

3.6 Experimental Test Procedures

The experimental test procedures were conducted to measure the density and porosity value, to know the mechanical properties (hardness and compression strength), wear performance and microstructural characterization of the TI-6Al-4V matrix and TI-6Al-4V/SiC composite materials.

3.6.1 Mathematical Determination for Density and Porosity Measurement

The Ti-6Al-4v matrix and composite theoretical-density (ρth) is determined with the summation of the constituents in the volume of the sample with matrix and composite powder mixing regulation by equation (3.6) Premnath et al. (2014).

$$\rho_{theo} = (\rho_{mat} \times V_{mat}) + (\rho_{rein1} \times V_{rein1}) \tag{3.6}$$

Where, Vmat and Vrein1 represents fraction of the volume, ρmat is the matrix density, ρrein1 is the reinforcement density, respectively.

A. The actual or experimental density for the Ti-6Al-4v matrix and Ti-6Al-4v/SiC composite can be calculated as stated by Archimedes-principles. First of all, the sintered specimens were weighed in the air (W_{air}), and then weighted in the distilled water (W_{water}) by suspended the sample in it. The actual or experimental density of the sintered composite sample was calculated according to Eq. (3.7) Wang et al. (2004) and Wang et al. (2018).

$$\rho_{ac} = \frac{W_1}{W_1 - W_2} \times \rho_w \tag{3.7}$$

Where ρ_{ac} is actual density of samples, W_{air} is weight of samples in the air, W_2 is weight of samples in the distilled water and ρ_w is the distilled water density (1g/cm^3).

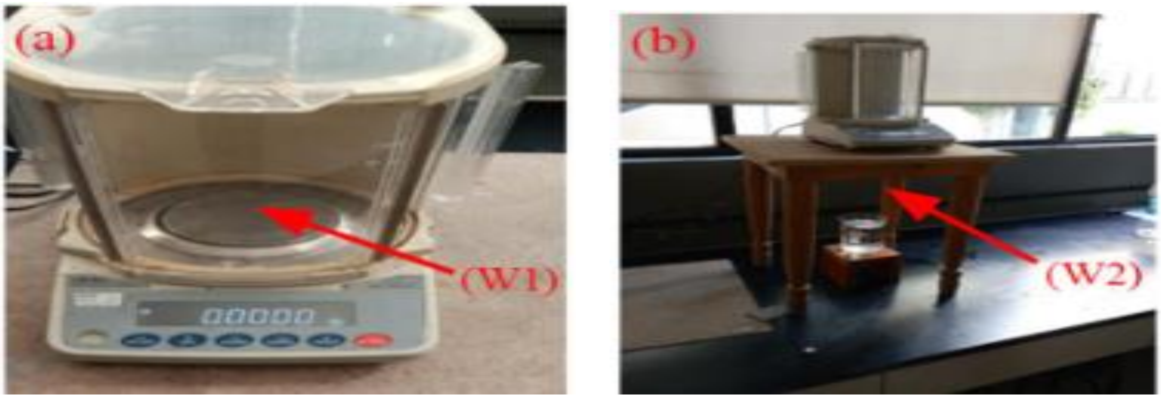

Figure 3.14 Photos of Weighting Balance for Measuring (A) Weight in Air And (B) Suspended Weight in Water

B. Porosity of the all samples were determined by equation (4) Alaneme et al. (2019).

$$\text{Porosity} = 1 - \frac{\rho_{ac}}{\rho_{th}} \tag{3.8}$$

Where, E_s = porosity (%), ρ_{ac} is the actual density (in g/^{cm3}), ρ_{th} is theoretically calculated density (in g/cm^3).

C. The relative-density of the samples were calculated by equation (3)

$$\rho_r = \frac{\rho_{ac}}{\rho_{th}} \times 100 \tag{3.9}$$

Where, ρr is relative density (%) and ρth is theoretically calculated density (in g/cm3)

3.6.2 Hardness test

Hardness test is a method of measuring the resistance of a material to indentation by applying a force on its surface. Hardness is an important property of composite materials, especially for engineering applications that require wear resistance. In this study, the Vickers hardness test was used to evaluate the hardness of Ti-6Al-4v matrix alloy and Ti-6Al-4v/SiC composite. The Vickers hardness test uses a diamond indenter with a square base and a 136° angle between opposite faces. The indenter is pressed into the material with a specified load and the diagonal length of the indentation is measured. The hardness value is calculated from the load and the indentation area.

The specimens for hardness and microstructural tests were cylindrical in shape, with a diameter of 18 mm and a height of 7 mm. They were polished with sand grinding papers of different grit sizes, ranging from 120 to 800, to obtain a smooth surface. The hardness test was performed with a load of 10 kgf and a dwell time of 5 seconds. The indenter was applied at different locations on the specimens to obtain an average hardness value. Figure 3.15 shows the schematic diagram of the Vickers hardness test.

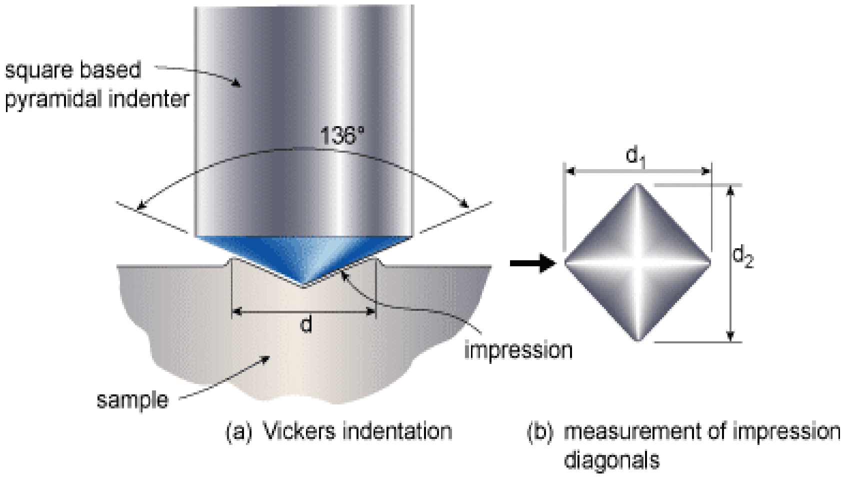

Figure 3.15 The pyramid shape diamond indenter and Vickers hardness machine.

$$HV = P = \frac{Constant\ x\ test\ force}{surface\ area\ of\ indentation} = \frac{0.102x2F(sin\frac{136^2}{2})}{d^2} \quad (3.10)$$

Where, Vickers hardness (HV), P is pressure, F is the force of the indentation(kgf) and d is an average distance between both opposite corners of the indentation (d1 and d2 (mm)).

3.6.3 Microstructure Characterization Test of Sintered Specimen

To investigate the mechanical and microstructural properties of (Ti-6Al-4V)- CeO2- Cr-Graphite composites, experimental tests were conducted to measure the density, porosity, hardness, and compressive strength of the samples. The mechanical properties are influenced by the microstructure of the materials, which includes the following aspects: grain size, segregation, phase distribution, phase composition, and non-metallic inclusions. Therefore, microstructural characterization was performed using X-ray diffraction (XRD), optical microscopy (OM), and scanning electron microscopy (SEM) techniques. These methods can reveal the crystal structure, morphology, and chemical composition of the different phases and inclusions in the composites (**Efeoglu, I 2021**)

3.6.3.1 X-Ray Diffraction (XRD)

A) Phases analysis in sintered composite

The crystalline phases and elements of the Ti-MMC samples were determined by using an X-ray diffractometer (XRD). The XRD instrument was a Shimadzu XRD-7000 Maxima model, which is a high-performance and versatile device for various applications. The samples were prepared and mounted on suitable holders according to the standard procedures for each type of material.

The phase analysis of the sintered samples was carried out by XRD at the ASTU laboratory, using Cu-Kα radiation as the X-ray source. The operating conditions were 40 kV and 30 mA, and the scanning range was 10° to 80° in 2θ with a step size of 3°/min. The data obtained from the XRD measurements were processed by using OriginPro 2022, a powerful software for scientific graphing and data analysis. OriginPro 2022 can perform phase identification and quantitative phase analysis by comparing the experimental data with the reference data from the database. The crystalline phase composition of the matrix and the reinforcement materials in the sintered composite was analyzed by using this method.

B) Determination of crystalline size and lattice strain by XRD peak Analysis

The microstructural parameters of (Ti-6Al-4V)- CeO2- Cr- Graphite composites, such as crystalline sizes, mean squared lattice strain, root mean squared strain, and dislocation density, were calculated by using XRD data and X-RD peak profile analysis by Gauss method (**Venkateswarlu et al., 2014**). This method involves fitting the X-ray diffraction peaks with Gaussian functions and extracting the peak width and position. The peak width is related to the size and strain of the crystallites, while the peak position is affected by the lattice parameter and the elemental composition of the sample. The X-ray peak broadening also depends on the sample preparation conditions, such as temperature, pressure, and annealing time. The X-ray diffraction peaks can be assigned to specific atomic planes using the Bragg's law, and the atomic fine structure of the prepared samples can be analyzed by comparing the experimental and theoretical peak positions and intensities. One of the most widely used formulas to estimate the crystalline size from the peak width is the Scherrer equation, which was first proposed by (**Scherrer in 1918**). The Scherrer equation assumes that the peak broadening is caused only by the finite size of the crystallites and neglects other factors such as strain, defects, and instrumental errors. The Scherrer equation can be written as:

$$D = \frac{K\lambda}{\beta \cos\theta}$$

Where - **D** is the average crystalline size, $\boldsymbol{K}$ is a dimensionless shape factor can be 0.62-2.08, $\boldsymbol{\lambda}$ is the X-ray wavelength, $\boldsymbol{\beta}$ the full width at half maximum (FWHM) of the diffraction peak, and $\boldsymbol{\theta}$ the Bragg angle (**Scherrer, 1918**). By using the Scherrer equation, the crystalline size can be calculated from the FWHM of the diffraction peak for each atomic plane (**Venkateswarlu et al., 2014**). However, the Scherrer equation has some limitations and may not be accurate for nanoscale crystallites or complex microstructures. Therefore, other methods of XRD peak profile analysis, such as the Warren-Averbach method, the Williamson-Hall method, or the Rietveld method, may be more suitable for some applications. Dislocation density is a parameter that quantifies the number of crystallographic defects or irregularities in a crystalline material. It is defined as the total length of dislocation lines per unit volume of the material, and it can be measured by different methods, such as etching, microscopy, or X-ray diffraction (XRD) (**Borbély and Groma, 2001**); (**Rai et al., 2023**). One of the formulas to calculate dislocation density from XRD data is: $\rho = \frac{4\epsilon}{b\cos\theta}$ where- **ρ** is the dislocation density, **ϵ** is the strain, **b** is the magnitude of the Burgers vector, and **θ** is the Bragg angle

Lattice strain refers to the displacement of atoms in a crystal structure from their ideal positions due to various factors. Some of these factors are doping, defects, and external magnetic fields, which can alter the electronic and structural properties of the material (**Augustin and Balu, 2017**). One way to measure lattice strain is by using diffraction techniques, such as X-ray diffraction (XRD), that can detect changes in the distance between parallel planes of atoms in the crystal, known as the d-spacing. When the lattice strain is uniform along a certain direction, the d-spacing along that direction will also change uniformly. However, when the lattice strain is non-uniform, the d-spacing will vary from one region to another, resulting in peak broadening in the diffraction pattern. The degree of peak broadening can be mathematically calculated using equation (3.4) from the XRD data.

$$\varepsilon = \frac{\beta}{4\tan\theta}$$

3.6.3.2 Optical Microscope and Scanning Electron Microscope

The surface structure of a prepared material was observed using an optical microscope (Huvitz HR-300) at the material lab of ASTU. The material was composed of sintered (Ti-6Al-4V)- CeO2- Cr- Graphite composite samples, which were etched with 4% nital solution for 10 seconds to reveal their microstructure. Nital is a mixture of nitric acid and alcohol, which is commonly used for etching carbon steels. After etching, the samples were rinsed with distilled water and dried before testing. Figure 3.16 shows the optical micrographs of the samples, taken with different magnifications. The microstructural characterization was performed to analyze the distribution of composites and the grain size of the samples. Optical microscopy (OM) is a useful technique for studying the morphology and phase contrast of materials.

Figure 3.16 (A) OM Test, and (B) Sample Prepared for Test

The morphology and fractography of the samples were analyzed using scanning electron microscopy (SEM) at the Biology Laboratory of Adama Science and Technology University (ASTU). The samples were cut into shape using a hacksaw and a file, and then polished with emery papers of 800, 1200, and 2000 grit sizes. The final polishing was done with a rotating wheel and a polishing cloth. The chemical bonding and functional groups of the synthesized materials were studied by Fourier-transform infrared (FT-IR) spectroscopy in the range of 4000-400 cm⁻¹ using a FT/IR-6600 type A spectrometer at the Industrial Chemistry Laboratory of Addis Ababa Science and Technology University (AASTU).

3.6.4 Compression Test

Compressive strength is the ability of a material or structure to resist loads that tend to reduce its size. It is measured by the maximum amount of uniaxial compressive stress that a material can withstand before it breaks or deforms. To determine the compressive strength of a material, a compressive test is performed by applying a uniaxial load to a sample until it fails. For this test, cylindrical specimens with a length-to-diameter ratio of 3 (L= 18 mm and D= 6 mm) were prepared according to the ASTM E-9 standard. The specimens were then tested using a universal testing machine (UTM) with a load capacity of 50 kN, as shown in Figure 3.13. The load was increased gradually until the specimens fractured

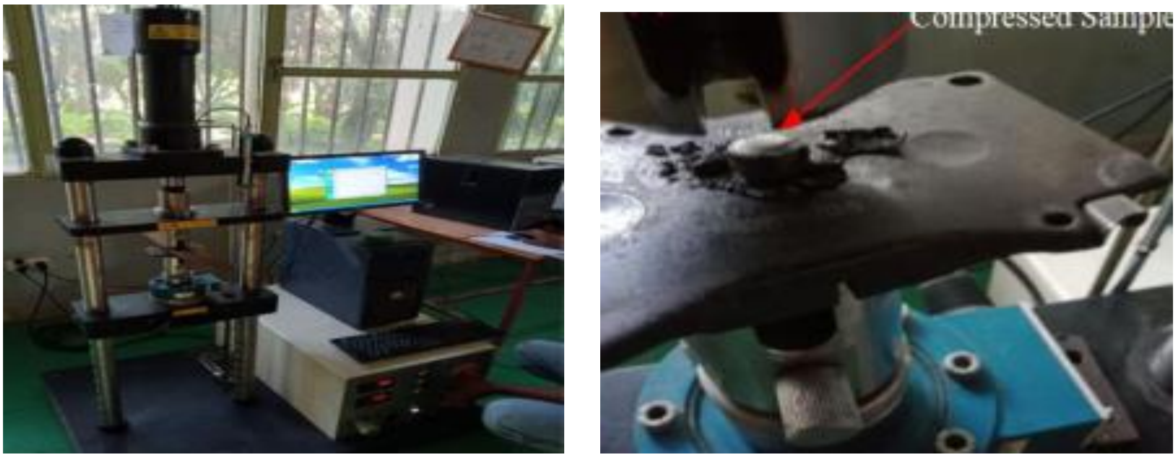

Figure 3.17 (A) UTM (Compression test) set up and (B) the compressed Sample)

The samples of titanium metal matrix composites (Ti-MMCs) were prepared following the ASTM E9-09 standard for axial-load compression testing of metallic materials at room temperature. The samples had a cylindrical shape with a diameter and a height of 10 mm each, resulting in a length-to-diameter ratio of approximately one. The compressive strength of the Ti-MMCs was measured by applying an increasing load to the samples until failure and calculating the ratio of the applied load to the cross-sectional area of the samples. Ti-MMCs are composed of a titanium alloy matrix reinforced with fibers, particles, or whiskers that provide them with superior properties such as high specific modulus, high specific strength, high-temperature and wear resistance, and potential weight reduction. Ti-MMCs have a wide range of applications in aerospace, automotive, and biomedical industries

. $\sigma_c = \frac{F}{A}$ Where, σ_c stand for Ultimate compressive strength, F is Ultimate compressive load and A is Cross-sectional area of samples.

The compression test is performed to evaluate the effect of the reinforcement composition, compaction pressure, and sintering time on the mechanical properties of the composite materials. The test follows the ASTM E9 standard, which specifies the equipment, sample preparation, and testing procedure for axial-load compression testing of metallic materials at room temperature. The test results may include the yield strength, the yield point, Young's modulus, the stress-strain curve, and the compressive strength of the materials. These properties are important for the analysis of structures that are subject to compressive or bending loads, and for the optimization of metal working and fabrication processes that involve large compressive deformation, such as forging and rolling.

3.6.5 Corrosion Test

The corrosion resistance of the specimens was evaluated by immersion testing, which is one of the most common and simplest methods in laboratory tests. The specimens, which had a cylindrical shape with a diameter of 12 mm and a length of 8 mm, were immersed in a 3% NaCl solution for one hour. Before the immersion, the specimens were polished with emery polishing paper of 800 and 1200 grit sizes, and then with 12 m diamond paste on a double disc polishing machine, to achieve a mirror-like surface and remove any surface defects. The electrochemical measurements were carried out in a three-electrode cell using an electrochemical analyzer (SP300 EC-LAB, Biologic Science Instruments, ASTU, Material science laboratory). The three-electrode cell consisted of a working electrode (the specimen), a counter electrode (a platinum wire), and a reference electrode (a saturated calomel electrode). The corrosion potential, corrosion current, and polarization resistance of the specimens were measured using potentiodynamic and potentiostatic techniques. The corrosion rate was calculated from the corrosion current using Faraday's law. The corroded specimens were also examined by optical microscopy and scanning electron microscopy to observe the morphology and extent of corrosion damage.

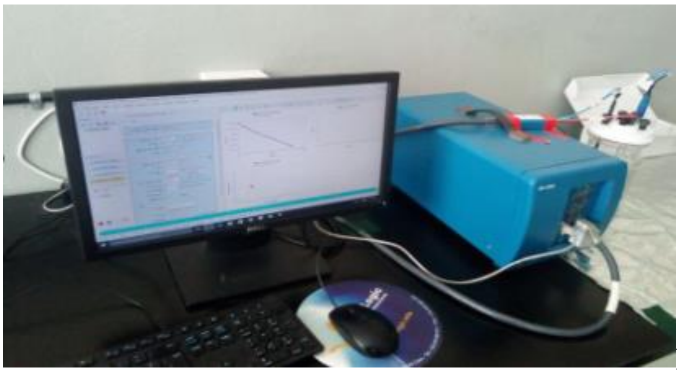

Figure 3.18 Electrochemical Analyzer

The working electrodes were fabricated from titanium-based composite powders with different reinforcement contents using powder metallurgy. The exposed area of each working electrode was 1 cm^2. A Graphite rod served as the auxiliary (counter) electrode, and a standard calomel electrode (SCE) or a mercury electrode was used as the reference electrode. The corrosion behavior of the composites was evaluated by recording the Tafel polarization curves in a three-electrode cell. The electrode potential was scanned from -250 to +250 mV relative to the corrosion potential (Ecorr) at a rate of 1 mV s^{-1}. The effect of reinforcement content on the corrosion resistance of the composites was investigated by comparing the corrosion current density (icorr), corrosion potential (Ecorr), and polarization resistance (Rp) obtained from the Tafel curves.

Tafel polarization curves are graphical representations of the relationship between the potential and the logarithm of the current density of an electrochemical reaction. They can be used to determine important electrochemical parameters such as corrosion potential (Ecorr), corrosion current density (Icorr), corrosion rate (CR), and corrosion protection efficiency (μp%). The corrosion potential (Ecorr) is the potential at which the net current is zero, meaning that the anodic and cathodic reactions are balanced. The corrosion current density (Icorr) is the current at the corrosion potential, which indicates the rate of the corrosion reaction. The corrosion rate (CR) is a measure of how fast the metal degrades in a specific environment, usually expressed in terms of penetration or weight loss. The corrosion protection efficiency (μp%) is a measure of how effective a coating or inhibitor is in reducing the corrosion rate of the metal. To calculate these parameters from the Tafel polarization curves, the following steps are usually followed:

- Plot the potential (E) versus the logarithm of the current density (log i) for both the anodic and cathodic reactions.
- Draw a straight line that best fits the linear region of each curve, and extend the lines until they intersect at a point. This point is the corrosion potential (Ecorr).
- Read the value of the current density (i) at the corrosion potential (Ecorr) from either curve. This value is the corrosion current density (Icorr).
- Use the following formula to calculate the corrosion rate (CR) in terms of penetration (mmy $^{-1}$):

$$CR = \frac{0.00327 \times I_{corr} \times EW}{\rho \times A}$$

Where Icorr is the corrosion current density in µA/cm ^{2}. EW is the equivalent weight of the metal in g, ρ is the density of the metal in g/cm^3, and A is the area of the metal in cm^2.

- Use the following formula to calculate the corrosion rate (CR) in terms of weight loss (mdd):

$$CR = \frac{I_{corr} \times EW \times 8.76}{A \times 10^4}$$

where Icorr is the corrosion current density in µA/cm^2, EW is the equivalent weight of the metal in g, and A is the area of the metal in cm^2.

- Use the following formula to calculate the corrosion protection efficiency (μp%) of a coating or inhibitor:

$$\mu_{p\%} = \frac{I_{corr,unprotected} - I_{corr,protected}}{I_{corr,unprotected}} \times 100$$

where Icorr,unprotected is the corrosion current density of the uncoated or uninhibited metal, and Icorr,protected is the corrosion current density of the coated or inhibited metal.

CHAPTER FOUR

RESULTS AND DISCUSSIONS

4.1 Introduction

This chapter discusses the experimental results of various characterizations and tests performed on synthesizes Titanium matrix composites (Ti-MMCs) with Cerium oxide and Chromium as reinforcements. Ti-MMCs are lightweight and high-temperature materials that have improved hardness and wear resistance due to the incorporation of ceramic particles with micro/Nano-scale sizes into titanium alloys. The characterizations and various tests included the analysis of density, hardness, X-ray diffraction (XRD), optical microscopy, scanning electron microscopy (SEM), compression, and corrosion of the TMCs and summarizes the main conclusions and implications of the study.

4.2 Analysis of Density and porosity of sintered sample

Composite materials are made of high-strength, high-modulus fibers embedded in a matrix (polymer, metal, or ceramic). The mechanical properties of composite materials, such as hardness and compression, are influenced by the density and porosity of the matrix and the fibers. Density is the mass per unit volume of a material, and porosity is the fraction of void space in a material. Both density and porosity affect the stiffness, strength, and durability of composite materials.

Therefore, it is important to measure these parameters in composite materials using various techniques, such as density gradient column, mercury intrusion porosimetry, and micro-CT scanning. Generally, lower porosity indicates higher quality of composite materials, as they result in higher specific strength and modulus, and lower moisture absorption and corrosion. On the other hand, higher hardness and compressive strength indicate better performance of composite materials, as they reflect the resistance to deformation and fracture under applied loads. Hardness and compressive strength can be measured by indentation, compression, or bending tests. (**Bayu et al., 2021**).

4.2.1 Density of Composites

Table 4.1 presents the compositions and labels of four samples that were fabricated by powder metallurgy using a Ti-6Al-4V alloy as the matrix material and CeO2 and Cr particles as the reinforcements. The fabrication process involved compaction at a constant pressure of 60 MPa, followed by sintering at a temperature of 1100°C for 2 hours.

Table 4.1 composition and samples design

SAMPLE CODE	SAMPLE COMPOSITION IN Wt%
S_1	**Ti-6Al-4V** - 81%, **$Ce0_2$**- 5%, **Cr**- 10%, **Graphene**- 4%
S_2	**Ti-6Al-4V** - 81%, **$Ce0_2$**- 10%, **Cr**- 5%, **Graphene**- 4%
S_3	**Ti-6Al-4V** - 81%, **$Ce0_2$**- 7.5%, **Cr**- 7.5%, **Graphene**- 4%
S_4	**Ti-6Al-4V** - 100%, **$Ce0_2$**- 0%, **Cr**- 0%, **Graphene**- 0%, (pure)

The theoretical density (ρth) of the composite material is calculated by applying the mixing rule for matrix and reinforcement powders, as shown in equation (3.5) in chapter 3. The sintered density (ρs) is determined experimentally by using the Archimedes principle, as shown in equation (3.6) in the same chapter. The relative density (ρr) is then obtained by dividing the sintered density by the theoretical density, as shown in equation (3.7). The densities of the matrix (Ti-6Al-4V) and the reinforcements (CeO_2, Cr, and Graphene) are given as (4.5, 7.65, 7.19, and 2.2) g/cm, respectively. Since the reinforcements have higher densities than the matrix, adding them to the composite increases the overall density of the material. The theoretical density also increases slightly as the weight fraction of the reinforcements increases, due to the different volume fractions of the components.

Sample two (**Ti-6Al-4V** - 81%, **$Ce0_2$**- 10%, **Cr**- 5%, **Graphene**- 4%) has a higher CeO_2 content than Cr, and CeO_2 is denser than Cr, which results in a higher theoretical density than the other samples. Sample three (S3) shows the second highest theoretical density value (4.8461 g/cm^3), followed by sample one (4.8345 g/cm3). Figure 4.1 illustrates the discrepancy between the theoretical and sintered densities of the composites, which can be attributed to the downward segregation of voids and heavy particles (**Olani et al., 2023**). Despite the higher density of CeO_2 and Cr compared to Ti-6Al-4V, their addition to the composite leads to a reduction in its total density and an increase in its porosity percentage.

After the mixing process, the blended particles tended to form clusters or aggregates, which resulted in agglomeration during the mixing stage. This was the main factor that increased the number of pores and reduced the density of the metal matrix composites (MMCs) (**Shamsuddin, 2014**). The sintered densities of the samples (S1, S2, S3 and S4) were 4.619 g/cm3, 4.396 g/cm3, 4.351 g/cm3 and 4.291 g/cm3, respectively. The addition of lower density Titanium metal matrix to higher density Cerium Oxide and Chromium reinforcements decreased the theoretical density, experimental density and relative density of the MMCs, as reported by (**Jha et al. 2022**).

4.2.2 Porosity of Composite

Porosity was calculated from the actual and theoretical densities by measuring the total void space within the composite. Equation (3.8) can be used to compute the porosity of the generated composites. Particles addition in the base matrix, trapping air between them, and interconnected in nature the main reason for generation of voids, therefore the percentage of porosity increases with the number of particles added (**Li et al., 2020**) and the porosity increases as the reinforcement content increases according to (**Arif et al., 2017**); (**Lin et al., 2018**). The porosity of all samples was determined using theoretical and experimental densities as shown in the table below.

The porosity of the composites was determined by measuring the total void space within the material and using equation (3.8) to calculate the ratio of the pore volume to the total volume. The main cause of void formation was the addition of particles in the base matrix, which trapped air between them and created interconnected pores. As a result, the porosity increased with the number of particles added, as reported by (**Li et al., 2020**). Moreover, the porosity also increased as the reinforcement content increased, as observed by (**Arif et al., 2017**) and (**Lin et al., 2018**). The theoretical and experimental densities of all samples are shown in the table below. The theoretical density was computed by using the rule of mixtures, while the experimental density was obtained by dividing the mass by the volume of the samples.

Table 4.2 Experimental Density, Relative Density and Porosity

SAMPLE NO	THEORETICAL DENSITY	SINTERED DENSITY	RELATIVE DENSITY (%)	POROSITY (%)
S_1	4.8345 g/cm^3	4.619 g/cm^3	95.56	4.44
S_2	4.8575 g/cm^3	4.396 g/cm^3	90.5	9.5
S_3	4.8461 g/cm^3	4.351 g/cm^3	89.8	10.2
S_4	4.5125 g/cm^3	4.291 g/cm^3	95.09	4.91

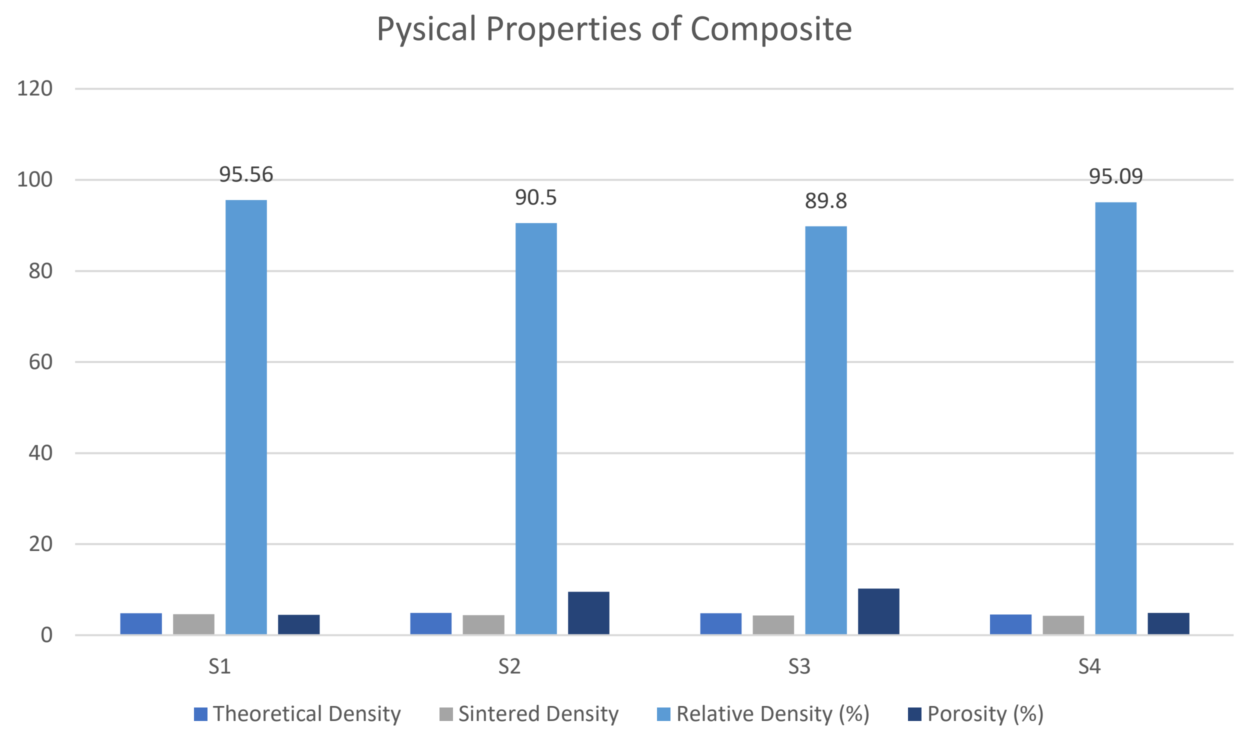

Figure 4.1 Physical Properties of Sintered Samples

The weight percentage of the reinforcing materials, Cerium Oxide and chromium, affects the porosity values of the composite material. The sample (S3) has equal weight percentages of both reinforcing materials, and it shows higher porosity values than the other samples. This is because the powder particles of Cerium Oxide and chromium tend to agglomerate and create larger voids in the composite matrix. According to (**Chawla and Deng, 2005**) and (**Bautista et al., 2008**), when the porosity fraction exceeds 5%, the pores become more interconnected and irregular in shape. This phenomenon was also observed by (**Ali Dad Chandio et al., 2019**) in their study of composite materials.

The pore size and shape have an impact on the mechanical properties of the composite material. The elastic properties and the failure mode of the material can vary depending on the shape and size of the pores. The sample with the lowest porosity, S1, has a porosity of 4.44% and a higher relative density. It also has more chromium, which has a similar density to the base metal titanium. This makes the matrix and the reinforcement more compatible in terms of density, resulting in a more consistent and compact composite material. The lower porosity and the higher relative density enhance the compressive strength and the energy absorption of the sample. (**Chawla and Deng, 2005**); (**Meignanamoorthy and Ravichandran, 2018**); (**Ashebir, 2022**).

4.3 Hardness Test

Hardness is an important property of materials that reflects their ability to resist deformation, penetration, scratching, or indentation. Hardness testing is a method of measuring the hardness of a material by applying a controlled force on a specified area of the material and observing the resulting indentation or impression. There are different types of hardness tests, such as Brinell, Rockwell, Vickers, Knoop, Mohs, and others, each with their own advantages, disadvantages, and applications. The selection of the appropriate hardness test depends on various factors, such as the type, size, shape, and condition of the material, the required accuracy and precision, the available equipment, and the relevant standards and specifications. In this report, we will focus on the analysis of hardness test results using different methods and compare their performance and suitability for different materials.

4.3.1 Analysis Hardness Test

The Vickers hardness test was used to measure the resistance of Ti-6Al-4V-Ce02-Cr-Graphite composites to permanent deformation. The test involved applying a known force to a diamond-shaped indenter that penetrated the surface of the specimen, as illustrated in figure 3.10 of Chapter Three. The Vickers hardness value was calculated from the size of the indentation using equation (3.9). The results of the test for sintered specimens Ti-6Al-4V-Ce02-Cr-Graphite composites with different reinforcement contents are presented in (appendix 2). The mean hardness values for S1, S2, S3, and S4 are (682, 650, 616, and 390) respectively. Sample 1 (S1) exhibited the highest hardness value of 585 HV, which was higher than the hardness of grade V Titanium (390 HV) and consistent with previous studies (**Chauhan et al., 2017**); (**Olani et al., 2023**). The hardness values of the samples varied with the volume percent of the reinforcement due to the effect of smart particles, namely Cerium oxide and chromium.

As shown in table 4.6, (**Kesarwani et al., 2015**), adding 10 weight percent of hard chromium particles and 5 weight percent of Cerium oxide to the matrix metal (Ti-6Al-4V) enhances the hardness of the sample by 75%, which is equivalent to 1.75 times increase. The hardness values of the samples range from S1 to S4, depending on the number of hard-smart particles added. The highest hardness value is obtained for the S1 Ti-MMC sample, which is 682, and it is 1.75 times higher than the typical hardness value of the matrix metal Ti-6Al-4V. This is consistent with the minimum dislocation density and lattice strain analyzed in section

(4.3.1.3), (**Venkateswarlu et al., 2014**). The hard-smart particles improve the resistance to plastic deformation and increase the strength of the sample.

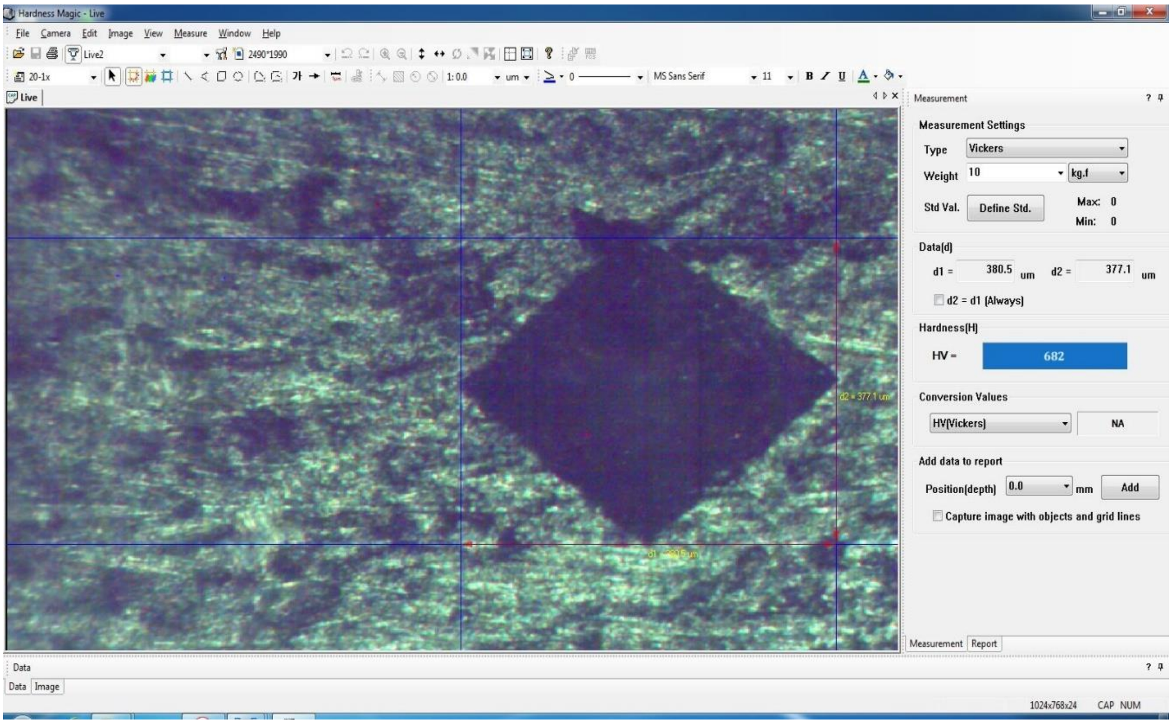

Figure 4.2 Vickers Hardness value trial for (Ti-6Al-4v)- CeO2/ Cr Composite

The hardness of the composite samples was enhanced by adding chromium and cerium oxide as reinforcements. The highest hardness value was obtained for sample two, which contained 10 wt% of chromium and 5 wt% of cerium oxide. The hardness of this sample was 1.67 times higher than that of the unreinforced sample, with an improvement of 67%. Sample three, which had 7.5 wt% of both chromium and cerium oxide, also showed a significant increase in hardness, reaching 1.58 times the base value, with an improvement of 58.46%. The results indicate that chromium has a more pronounced effect on the hardness than cerium oxide in this work, as the hardness increased proportionally with the chromium content up to 10 wt%. However, the cerium oxide content also influenced the hardness, as it increased the porosity of the composite, which reduced the strength and resistance to deformation. These findings are consistent with previous studies that reported the positive effects of chromium and cerium oxide reinforcements on the hardness of metal matrix composites (**Chauhan et al., 2017**); (**Li et al., 2020**); (**Han et al., 2019**). The weight fractions of the reinforcements were found to be the most important factor affecting the hardness (**Veličković et al., 2018**); (**Fanani et al., 2021**).

Table 4.3 Experimental Results of Hardness Values

Samples	Experimental Results of Hardness Value (HV)				
	Trial 1	Trial 2	Trial 3	Average (HV)	Improvement (%)
S1	675.4	680.3	690.3	682	75
S2	636.2	646.5	667.3	650	67
S3	604.2	619.2	624.6	616	58.46
S4	389.2	389.3	391.5	390	0

The percentage of improvement in material properties was calculated using the following equation:

$$improvement\ (\%) = \frac{NEW\ (Yi) - Original\ (Yo)}{Original\ (Yo)} * 100 \qquad (4.1)$$

New (Yi) is the average value of the Ti-MMC samples and Original (Yo)is the average value of base metal (Ti-6Al-4V).

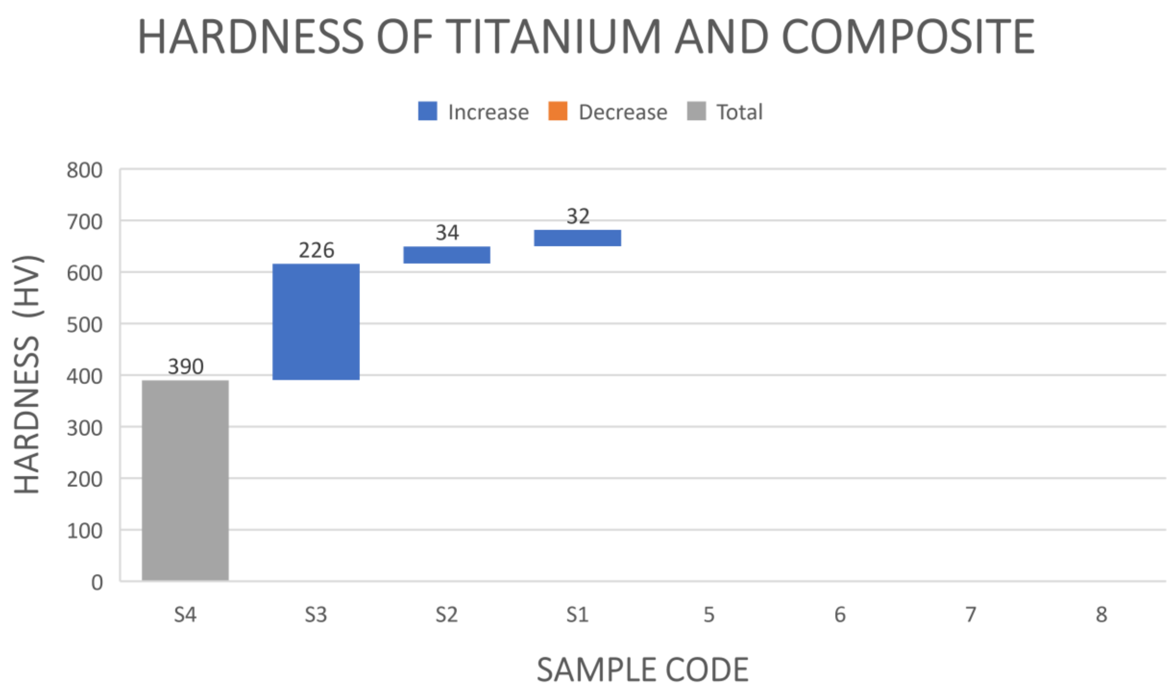

4.5 Compression Test

A compression test is a method of measuring the mechanical properties of materials, such as strength, stiffness, and ductility, under compressive loading. Compression tests are commonly used to evaluate the behavior of materials such as metals, ceramics, polymers, composites, concrete, and wood. The results of compression tests can provide useful information for design, quality control, and failure analysis of various engineering applications.

4.5.1 Analysis of Compression Test

The analysis of compression test involves determining the stress-strain relationship of the material, which can be obtained by measuring the applied load and the deformation of the specimen during the test. The stress-strain curve can reveal important characteristics of the material, such as the elastic modulus, the yield strength, the ultimate strength, the strain hardening, and the fracture strain. Additionally, the analysis of compression test can also include examining the failure mode and the microstructure of the material after the test.

Four samples of different compositions were subjected to compression tests using the universal testing device. The stress-strain curves of the samples were plotted based on the data collected during the tests, as shown in Figure (4.9). The samples had the following compositions: (Ti-6Al-4V - 81%, Ce02- 5%, Cr- 10%, Graphene- 4%), (Ti-6Al-4V - 81%, Ce02- 10%, Cr- 5%, Graphene- 4%), (Ti-6Al-4V - 81%, Ce02- 7.5%, Cr- 7.5%, Graphene- 4%) and (Ti-6Al-4V - 100%, Ce02- 0%, Cr- 0%, Graphene- 0%, (pure)). The ultimate stresses of these samples were 914, 889, 842, and 791 MPa, respectively. The results indicate that the addition of Chromium enhanced it up to 17% to the Titanium matrix increased the yield strength of the samples compared to the pure Titanium sample. The CeO_2 and Cr particles were incorporated into the Ti matrix to enhance the mechanical properties of the composite, as reported by previous studies. The use of hard and smart particle powder resulted in a high compressive strength. The second sample, which had 10% Cr and 10% CeO_2, showed the highest ultimate stress and compressive strength among the four samples, as evident from the stress-strain curves in Figure (4.9).

The presence of pores in composites due to agglomeration can reduce the uniformity of the compressive strength. The composites also show signs of fracture and lower ductility when they contain harder chromium and cerium oxide particles, which make the matrix less stable under compression. The elastic modulus of the Ti-MMCs varies depending on the amount and distribution of the reinforcement, while the cerium oxide particles have a damping effect that reduces the vibration of the matrix (**Chauhan et al., 2020**). The young modulus, which measures the stiffness of the material, is not affected by the reinforcement, as reported by previous studies (**Nguyen and Gupta, 2010**; **Shamsuddin et al., 2013**).

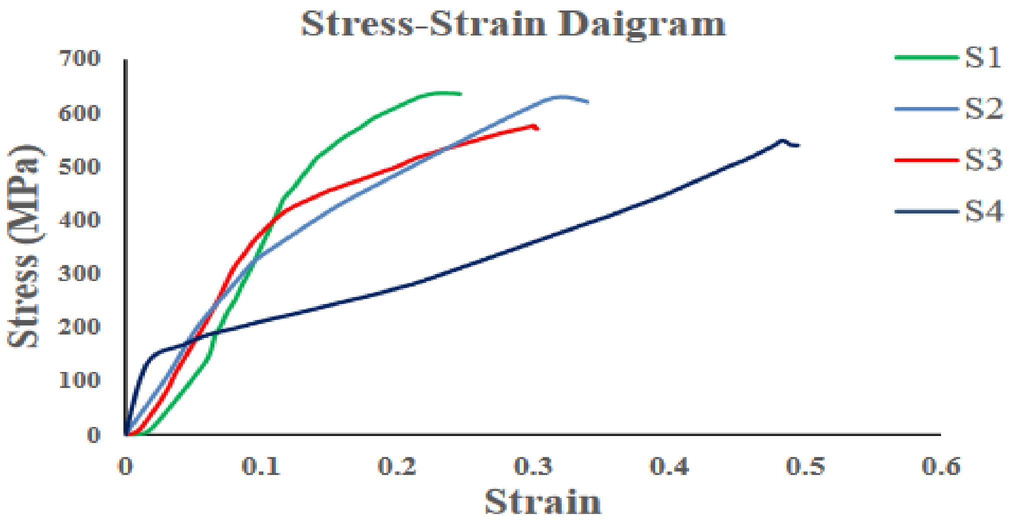

Figure 4.3 Stress- Strain Diagram of (S1, S2, S3 and S4)

The sample with the highest chromium content and the lowest Cerium Oxide content (S1) (Ti-6Al-4V - 81%, Ce02- 5%, Cr- 10%, Graphene- 4%) exhibited the best performance in the compression test, achieving the highest compressive strength among the four samples. This result can be attributed to the increased hardness and reduced porosity of the sample, which enhanced its resistance to deformation and fracture. Therefore, the compressive strength of the samples is more dependent on the chromium addition than the Cerium oxide addition.

A) Average Vickers Hardness and Compressive Strength (Mpa)

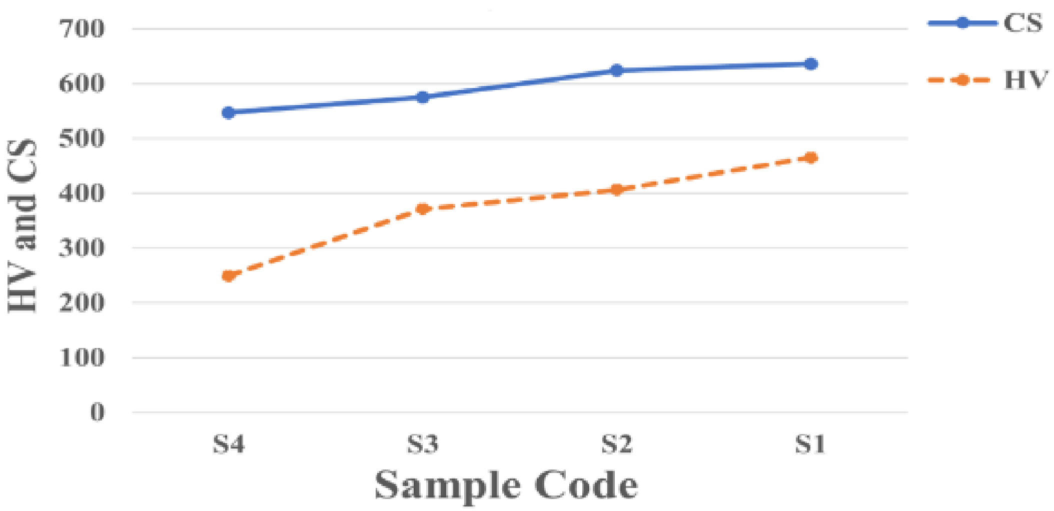

B) Hv and CS Improvement (%) of Titanium and Ti- MMCs

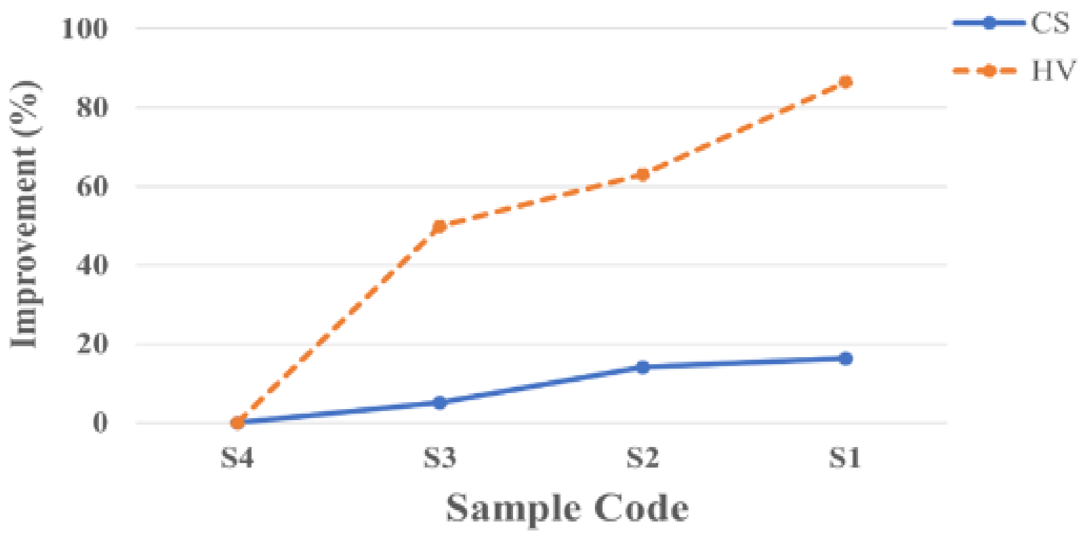

Figure 4.4 (A) Average Vickers Hardness and Compressive Strength, and (B) Improvement Recorded

4.6 Fracture Analysis

Fracture analysis is a method in failure analysis for studying the fracture surface of materials. Studying the characteristics of the fractured surface can help to determine the cause of failure in an engineered product. Fracture analysis using scanning electron microscopy (SEM) is a technique that uses a beam of electrons to scan the surface of a material and produce a magnified image of its features. SEM can reveal details of the fracture mode, crack initiation, crack propagation, and fracture mechanisms that are not visible with other methods. SEM can also be combined with other techniques, such as Energy Dispersive Spectroscopy (EDS), to analyze the chemical composition of the fracture surface and identify possible contaminants or corrosion products. SEM is a powerful tool for fracture analysis because it can provide high resolution, direct observation, and quantitative measurements of the fracture surface.

4.6.1 Fracture Analysis Using SEM

The surface morphology of the samples was mapped by fractography at different magnifications, as shown in Figure 4.11. The fracture mechanisms of the composites were investigated by SEM analysis to reveal the microstructural features of the micrographs. Figures 4.11 (a) and (b) show the fractures and cross-sections of the Ti-MMCs, which exhibit brittle failure modes. The presence of pores in the composites, which resulted from agglomeration during powder mixing, affected the mechanical properties and the fracture behavior of the samples. The pores varied in size, with some being larger and some being smaller, depending on the degree of compaction and sintering. The micrographs also show many indentations on the surface, which indicate the occurrence of plastic deformation. The samples were subjected to a force that was applied normal to the surface, which caused the initiation and propagation of cracks in several locations. The composites were brittle in nature, and some regions showed cleavage fracture, which increased the fracture susceptibility of the samples.

S2 A) 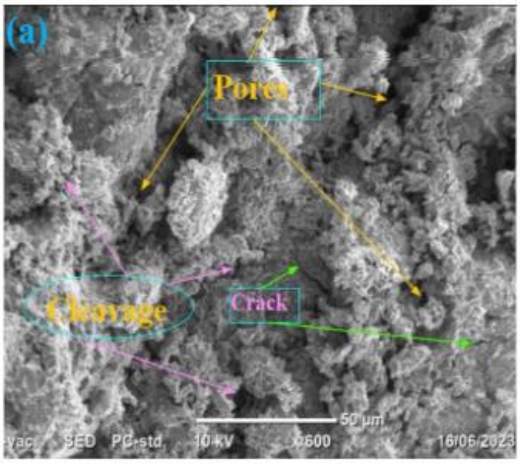

B) 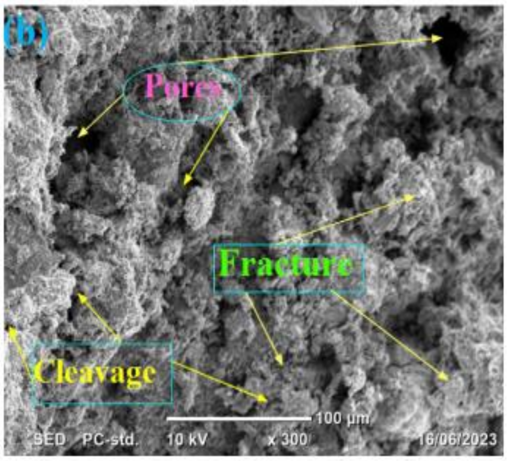

S3 A) 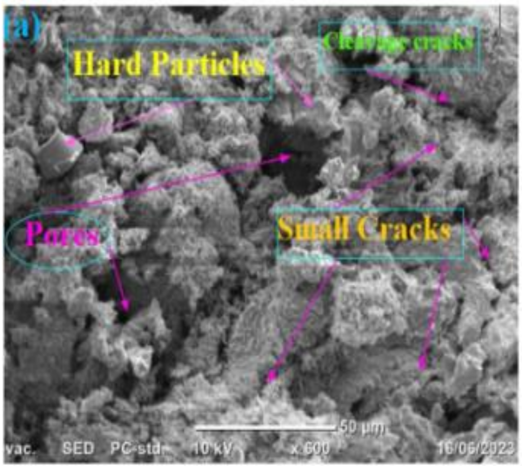

B) 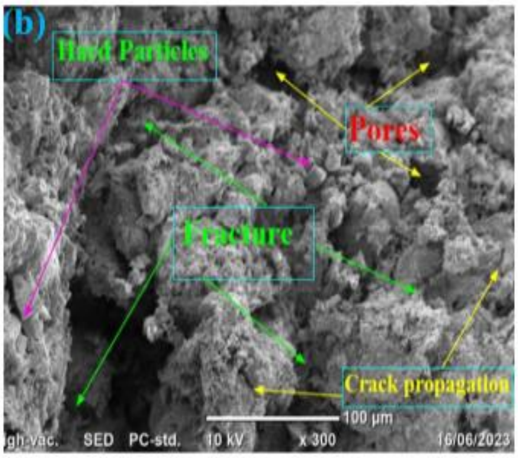

Figure 4.5 Fractography Analysis Using SEM for (S2) and (S3) at 50 and 100 um

The effect of reinforcement content on the fracture morphology of the composites was also studied by SEM. Figures 4.11 © and (d) show the micrographs of the composites with 5 wt% and 10 wt% of reinforcement, respectively. It can be seen that the reinforcement particles were well distributed in the matrix, and no obvious interfacial debonding was observed. The reinforcement particles acted as crack arresters, preventing the cracks from propagating through the matrix. The composites with higher reinforcement content showed more ductile fracture modes, such as dimples and tear ridges, which indicate the occurrence of plastic deformation and energy dissipation during fracture. The composites with lower reinforcement content showed more brittle fracture modes, such as trans-granular and inter-granular fracture, which indicate the occurrence of grain boundary weakening and stress concentration during fracture.

The composite with 10 wt% of chromium (Cr) reinforcement showed a significant improvement in its mechanical properties, which were about 1.5 times higher than those of the unreinforced matrix. Cr reinforcement is a type of particle reinforcement that enhances the strength and stiffness of the composite by preventing crack propagation and dislocation movement and The enhancement of fracture toughness can be attributed to the following factors:

- The reinforcement particles increased the hardness and strength of the composites, which increased the resistance to crack initiation and propagation;
- The reinforcement particles acted as crack arresters, which reduced the crack length and crack opening displacement;
- The reinforcement particles induced plastic deformation and energy dissipation in the matrix, which increased the fracture energy and the work of fracture.

4.7 Corrosion Science

Corrosion is the degradation of metals in different environments. It causes economic, environments, and safety problems in many applications. To prevent or reduce corrosion, we need to understand how it happens and what factors affect it. Corrosion science is a field that studies the interactions between metals and their environments using chemistry, physics, materials science, and engineering. This thesis explores the corrosion behavior of some metals and alloys in various corrosive media, using different methods. The goals are to analyze the corrosion products, measure the corrosion rates, and find out the corrosion mechanisms. The results will help us improve the corrosion resistance and protection of these materials.

4.7.1 Corrosion Study

The corrosion behavior of different Titanium-based composite materials in a saltwater environment was investigated in the ASTU material lab. The experiment was conducted in a three-electrode bio-electrochemical cell connected to a bio-instrument Potentiostat. The cell contained a 3.5 wt% NaCl solution as the electrolyte, which was prepared by dissolving 35 g of NaCl in 1000 mL of distilled water. For each run, 150 mL of the electrolyte solution was used. The electrodes were immersed in the solution for about an hour before the test to reach a stable open circuit potential (OCP), which was recorded and shown in appendix-4 (A). The corrosion potential and current of the electrodes were measured by applying a Linear Sweep Voltammetry (LSV) technique in the range of -250 to 250 mV from the OCP at a scan rate of 1 mV/sec.

The resulting potentiodynamic polarization curves, also known as Tafel plots, were plotted on a logarithmic scale with the corrosion current on the x-axis and the corrosion potential on the y-axis. The Electrochemical Impedance Spectroscopy (EIS) technique was also used to measure the impedance and resistance of the electrodes by applying a small sinusoidal voltage over a range of frequencies. The EIS data were plotted as Nyquist plots, which show the real part of the impedance on the x-axis and the imaginary part of the impedance on the y-axis. The polarization and EIS curves were processed and plotted using the EC-LAB software. After the test was completed, the data from the different runs were extracted and analyzed using the Origin Pro software.

4.7.2 Potentiodynamic Polarization Measurements

To investigate the corrosion behavior of the fabricated samples, the Tafel extrapolation method was applied to measure the potentiodynamic polarization curves. This method can estimate the corrosion current density, which is related to the rate of corrosion reactions, by analyzing the shape of the polarization curve. Tafel plots are another electrochemical technique that has the advantages of being fast and relatively simple **Olani et al. (2023)**. The figure below shows the Tafel plots for four samples obtained from the potentiodynamic polarization test using the experimental

The corrosion current density (Icorr) and corrosion potential (Ecorr) are the parameters that indicate the rate and extent of corrosion, respectively. They can be obtained from the Tafel plot, which is a graph of the current density versus the potential for a corroding metal. The Tafel plot consists of two linear regions: the cathodic region and the anodic region. The intersection point of these two regions corresponds to the Icorr and Ecorr values. To find this point, the Origin Graphs Analysis Method was used, which is a software tool that can project the linear segments of the Tafel plot to their intersection point. The method and the results are shown in appendix 4, (C). After finding the Icorr and Ecorr values, the anodic and cathodic slopes of polarization were also calculated using the linear fitting dialog box in the Origin Graphs Analysis Method. The slopes of polarization represent the resistance of the metal to corrosion. The method and the results are shown in appendix 4 as well.

The polarization resistance, which is the slope of the current-voltage plot near the corrosion potential, was calculated using the Stern-Geary equation (4.2), as described by **Andrade** and **Martínez, (2010)** in their book on concrete corrosion rate measurement and analysis. This equation relates the polarization resistance to the corrosion current and the anodic and cathodic Tafel slopes, which are the slopes of the logarithmic current-voltage plot in the anodic and cathodic regions.

$$\boldsymbol{Rp} = \frac{\boldsymbol{\beta a \beta c}}{\mathbf{2.303}\boldsymbol{Icorr}(\boldsymbol{\beta a} + \boldsymbol{\beta c})} \qquad \textbf{\textit{(4.2)}}$$

Where, $\boldsymbol{\beta a}$ and $\boldsymbol{\beta c}$ are anodic and cathodic slopes of polarization curves, and **I** is corrosion current density in (mA/cm^2).

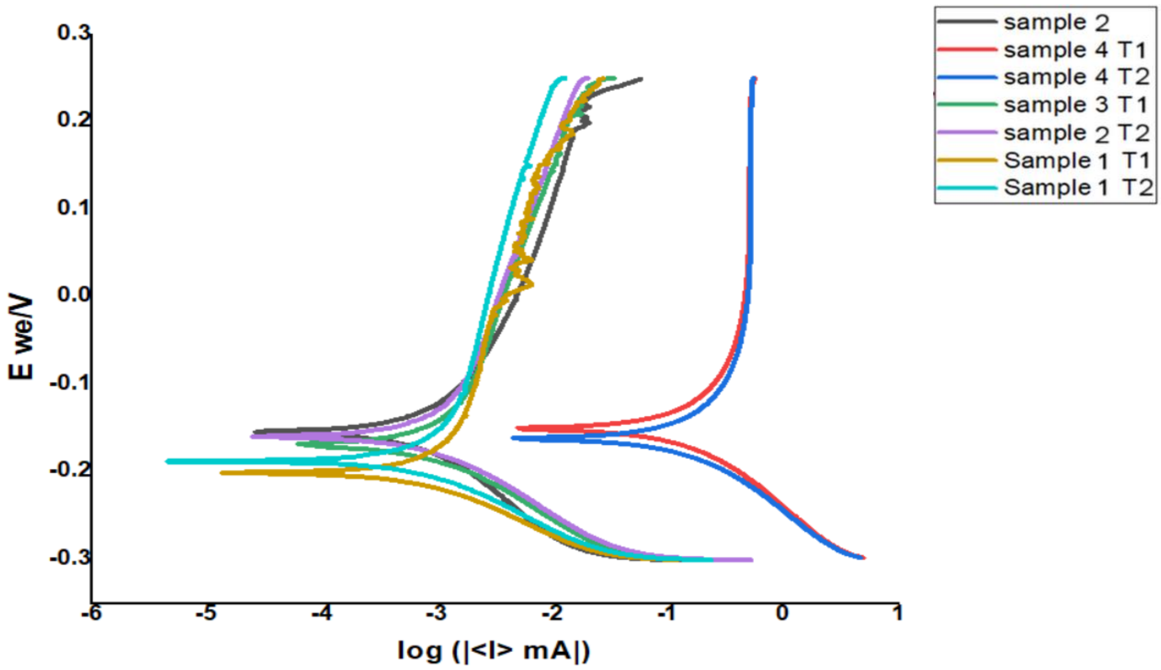

Figure 4.6 The Tafel Polarization Plot of Titanium and Ti-MMC's

To evaluate the performance of the manufactured samples in terms of corrosion resistance and protection efficiency, two equations from Chapter 3 were applied. Equation (3.12) calculates the corrosion rate (CR) based on the polarization resistance (Rp) and the Stern-Geary constant (B). Equation (3.13) estimates the protection efficiency (PE) by comparing the corrosion current densities (Icorr) of the bare and coated samples. The table below summarizes the values of Icorr, corrosion potential (Ecorr), anodic and cathodic Tafel slopes (**βa** and **βc**), Rp, CR, and PE obtained from the experiments.

Table 4.4 Tafel Polarization Experimental Parameters Values

Samples	**Icorr** (mA/cm^2)	**Ecorr** (mV)	**βa** (mV)	**βc** (mV)	**RP** (Ω)	**CR** (mm/yr)	μ_p (%)
S1	2.51	-157.91	11.06	21.48	16.45	0.34	76.55
S2	3.57	-161.85	17.07	23.34	15.6	0.51	66.5
S3	3.68	-160.2	14.24	39.01	16.05	0.54	65.1
S4	7.245	-182.04	12.6	39.94	7.53	1.090	32.5
Pure Ti-6Al-4V	10.5	-246.94	7.21	45.68	3.34	1.34	0.00

The corrosion resistance of titanium alloys depends on the oxide film that forms on their surface. This film protects the metal from the corrosive environments., but it can be damaged by various factors. The corrosion current density and the corrosion potential are two parameters that measure how well the film resists corrosion. A lower corrosion current density and a higher corrosion potential mean better corrosion resistance.

According to Figure (4.12) and Table (4.6), the base metal and three composites with different particles added to the metal. By using a test in a salt solution (3.5% NaCl) to measure the corrosion current density and the corrosion potential of each sample. The results showed that the base metal had the highest corrosion current density and the lowest corrosion potential, meaning that it was the most prone to corrosion. This was because the metal ions dissolved into the solution, weakening the film and exposing the metal surface to more corrosion. This caused rust to form on the surface of the base metal. (**Kimura et al., 2005**); (**Konishi et al., 2005**); (**Szewczyk-Nykiel** and **Kazior, 2017**).

Since CeO_2 and Cr are resistant to severe corrosion attack. The composites had better corrosion resistance than the base metal. The corrosion potential values increased, and the corrosion current density values decreased. This meant that the film on the composites was stronger and less damaged. It is because of the particles that were added to the metal, which were very resistant to corrosion in salt environments. The particles blocked the metal ions from dissolving and helped the film to protect the metal surface. The composite with both types of particles had the best corrosion resistance among the composites. It had the lowest corrosion current density and the highest corrosion potential.

The corrosion resistance of a material can be enhanced by adding chromium and cerium oxide (CeO2) to its composition. Chromium increases the passivation of the surface, which means that it forms a thin and protective oxide film that prevents further oxidation (**Santos et al., 2021**). CeO_2 also contributes to the formation of a dense and stable inner oxide layer that acts as a barrier against corrosive agents (**Konishi et al., 2005**). In particular, CeO_2 can resist the attack of chloride ions (Cl-), which are known to cause pitting corrosion in many metals. This is because CeO_2 can form alloy phases with titanium (Ti), such as Ti-CeO_2, that have higher resistance to chloride-induced damage (**Singh et al., 2018**). However, corrosion can still occur in environments with high salinity, such as seawater. This is because sodium ions (Na+) can migrate from the middle and outer rust layers, where they are separated from the chloride ions, to the inner rust layer and the metal-oxide interface. There, they can increase the chloride activity, which is the effective concentration of chloride ions in the solution. When the chloride activity exceeds the hydroxyl activity, which is the effective concentration of hydroxide ions (OH-), the passivation of the surface is disrupted and corrosion accelerates (**Usami et al., 2003**); (**Konishi et al., 2005**).

The table above Table (4.6) shows the corrosion potential (Ecorr) and the polarization resistance (Rp) of different metal samples, including pure Titanium and four composites (S1-S4) with varying amounts of chromium (Cr). The corrosion potential is a measure of how easily a metal can be oxidized, and the polarization resistance is a measure of how well a metal can resist the electrochemical reactions that cause corrosion. The lower the corrosion potential (more negative), the more prone the metal is to corrosion. The lower the polarization resistance, the faster the corrosion rate. The table shows that pure Titanium has the lowest corrosion potential and the lowest polarization resistance, meaning that it has the highest corrosion rate and the lowest corrosion resistance. The composites have higher corrosion potentials and higher polarization resistances than pure Titanium, meaning that they have lower corrosion rates and higher corrosion resistance. The composites also have different corrosion potentials and polarization resistances depending on the amount of Cr in their composition.

Cr is an alloying element that can improve the corrosion resistance of metals by forming a protective oxide layer on the surface. The table shows that the composite with the highest amount of Cr (S1) has the highest corrosion potential and the highest polarization resistance, meaning that it has the lowest corrosion rate and the highest corrosion resistance. The composites with lower amounts of Cr (S2-S4) have lower corrosion potentials and lower polarization resistances, meaning that they have higher corrosion rates and lower corrosion resistance. The table also shows that the corrosion potential and the corrosion rate of the composites are slightly affected by the Cr percentage. The corrosion potential decreases slightly (becomes more negative) and the corrosion rate increases slightly as the Cr percentage decreases from S1 to S3. This means that the composites become more susceptible to corrosion as the Cr content decreases. However, the corrosion potential and the corrosion rate of the composites are still much higher than those of pure Titanium, indicating that the composites are still much more resistant to corrosion than pure Titanium (**Bharat and Bose, 2021**).

The corrosion rate of a smart material can be reduced by adding 15 wt% of (Cr and CeO2), which also enhances its efficiency from 65% to 76%. This material has more corrosion resistance than Titanium and Ti-MMCs, which have different levels of protective efficiency according to the order of (S1 >S2 > S3>S4), as shown in Table 4.7. Sample One (S1) has the best performance among the Ti-MMCs, as it exhibits high hardness, high compressive strength, uniform distribution of hybrid reinforcements and minimum porosity. It also has the highest protective efficiency and the lowest corrosion rate. This is consistent with the fact that materials with higher positive corrosion potential (Ecorr) and lower corrosion current density (Icorr) on the Tafel curves have better corrosion resistance (low corrosion rate), as confirmed by many studies (**Gupta et al., 2013**); (**Lei et al., 2012**); (**Singh et al., 2018**); (**Karabulut et al., 2022**).

4.7.3 Electrochemical Impedance Spectroscopy (EIS) Analysis

The Nyquist plots shown in (Figure 4.12) were obtained by performing electrochemical impedance spectroscopy (EIS) on four types of sample electrodes: Titanium and titanium metal matrix composite (Ti-MMC). The electrodes were immersed in a 3.5% sodium chloride (NaCl) solution for one hour to simulate the seawater corrosion environment. The

EIS measurements were carried out at the open-circuit potential (OCP) of the electrodes, which is the equilibrium potential between the electrode and the electrolyte. A saturated calomel electrode (SCE) was used as the reference electrode to measure the potential difference, and a platinum electrode was used as the counter electrode to complete the circuit. The EIS spectra were recorded with a sinusoidal voltage signal of 10 mV amplitude and a frequency range from 100 kHz to 10 MHz

The corrosion resistance of the electrodes can be evaluated by the diameter of the semicircle in the Nyquist plot, which represents the charge transfer resistance (Rct) at the electrode/electrolyte interface. The larger the Rct, the higher the corrosion resistance of the electrode (**Balaraju et al., 2010**); (**Zhang et al., 2015**); (**Singh et al., 2018**). The Nyquist plot in (Figure 4.12) showed that the Rct values increased from the base metal Titanium (S4) to the Ti-MMC samples (S3, S2, S1). This indicates that the Ti-MMC samples had better corrosion resistance than the base metal Titanium in the 3.5% NaCl solution. Moreover, the Rct values increased with the increase of chromium reinforcement content from 5 wt% to 10% (from S1 to S3), while keeping the CeO_2 content constant. This suggests that the chromium particles had a more significant effect on enhancing the corrosion resistance of the Ti-MMC samples than the CeO_2 particles (**Zhang et al., 2015**). However, the addition of CeO_2 up to 10 wt% also improved the corrosion resistance of the Ti-MMC samples to some extent, by forming a protective oxide layer on the surface of the electrodes (Deepan Bharathi Kannan et al., 2016).

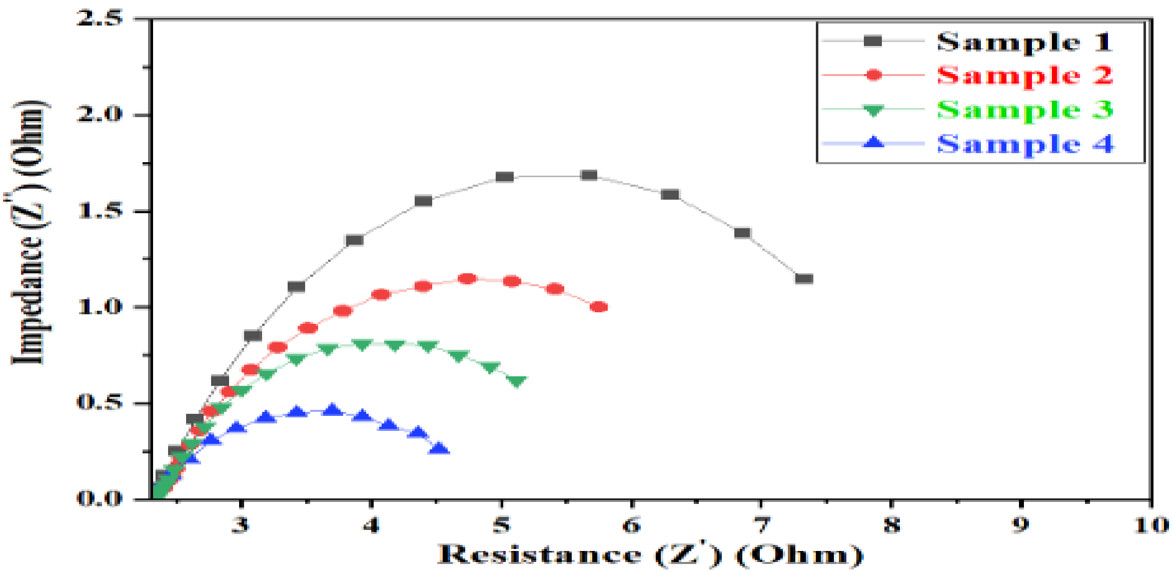

Figure 4.7 Electrochemical Impedance Nyquist Plots of Pure Titanium and Ti-MMC in 3.5 Wt% NaCl Solution.

The corrosion resistance of pure titanium and titanium metal matrix composites (Ti-MMCs) with different compositions was investigated using electrochemical impedance spectroscopy (EIS) and potentiodynamic polarization measurements. The EIS results showed that the Nyquist plots of pure titanium had a depressed semicircle with a smaller diameter, indicating a lower corrosion resistance and a non-ideal capacitive behavior. On the other hand, the (**Ti-6Al-4V** - 81%, **Ce0$_2$**- 5%, **Cr**- 10%, **Graphene**- 4%) (S1) had a larger diameter of the semicircle, suggesting a higher corrosion resistance and a more ideal capacitive behavior. The other Ti-MMCs with different weight percentages of chromium and Cerium oxide (S2, S3, and S4) had intermediate values of the semicircle diameter, indicating a moderate corrosion resistance.

The EIS data were consistent with the potentiodynamic polarization measurements, which showed that the corrosion current density and the corrosion potential of S1 were the lowest and the highest, respectively, among all the samples. The corrosion resistance of the samples increased with the increase in the weight percentage of chromium reinforcements, as chromium formed a protective oxide film and corrosion products on the surface of the Ti and Ti-MMCs, which hindered the penetration of chloride ions from the 3.5% NaCl solution. The base material (pure Ti) had the highest corrosion current and the lowest corrosion potential, indicating that it was the most susceptible to corrosion among all the samples. The addition of Graphite also improved the corrosion resistance of the Ti-MMCs, as Cerium oxide enhanced the mechanical properties and the electrical conductivity of the matrix. All the experimental data supported the conclusion that the corrosion resistance of the Ti and Ti-MMCs depended on the composition and the microstructure of the samples.

4.7.3 Surface Investigation After Corrosion

To evaluate the corrosion behavior of the samples, potentiodynamic polarization tests were performed. This technique measures the current and potential of the electrode in a solution, and can provide information about the corrosion rate and mechanism. After the tests, the samples were examined by optical microscopy (OM) and scanning electron microscopy (SEM) to observe the surface morphology and features of the corroded areas. OM uses visible light to produce images, while SEM uses a focused beam of electrons to scan the surface and generate high-resolution images. These methods can reveal the shape, size, texture, and composition of the materials.

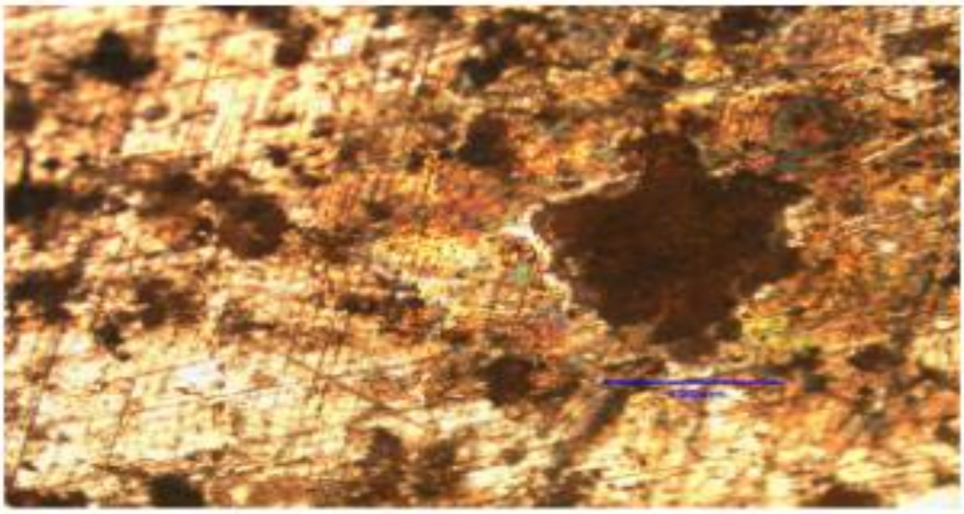

S1

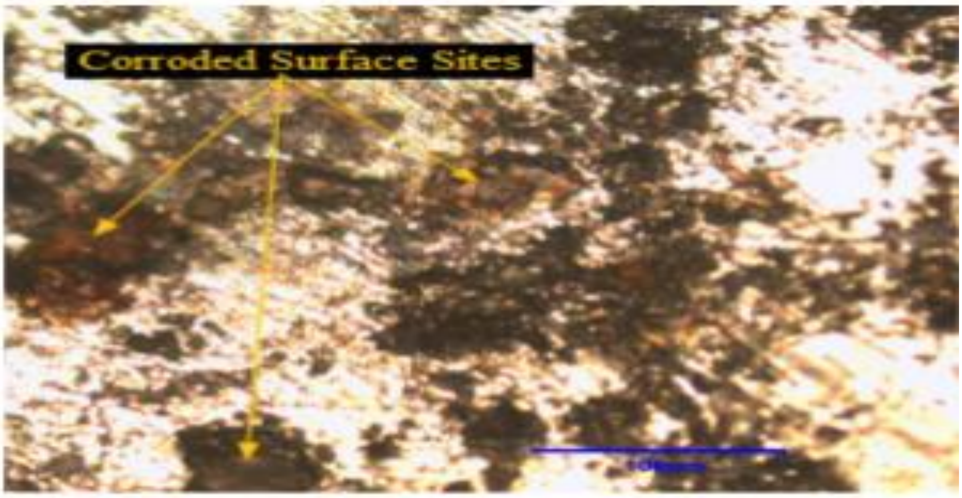

S2

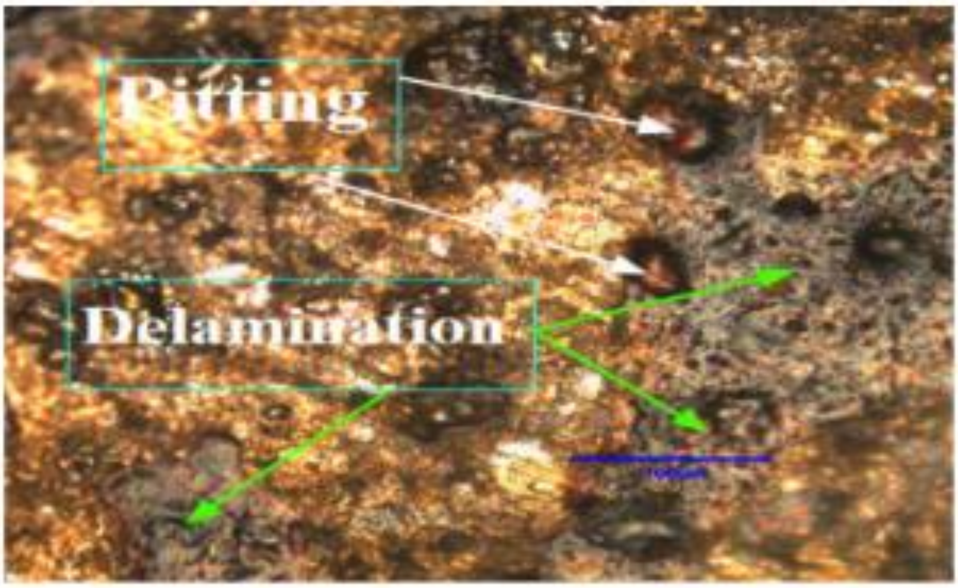

S3

Figure 4. 8 OM Micrographs of Corroded for (S1, S2, and S3) at 100μm

The SEM micrographs of the (Ti-6Al-4V)- CeO_2- Cr composite also reveal the effect of CeO_2 and Cr on the corrosion behavior of the composite. The micrographs show that the composite has a dense and uniform surface layer, which is composed of CeO_2 and Cr oxides. These oxides form a protective film that prevents the penetration of corrosive agents into the matrix. The micrographs also show that the composite has a lower porosity than the pure Ti-6Al-4V alloy, which reduces the possibility of crevice corrosion and pitting corrosion. The micrographs also indicate that the composite has a finer and more homogeneous grain structure than the pure Ti-6Al-4V alloy, which improves the resistance to intergranular corrosion and stress corrosion cracking. Therefore, the SEM micrographs demonstrate that the addition of CeO_2 and Cr enhances the corrosion performance of the (Ti-6Al-4V)- CeO_2-Cr composite.

Sample 1

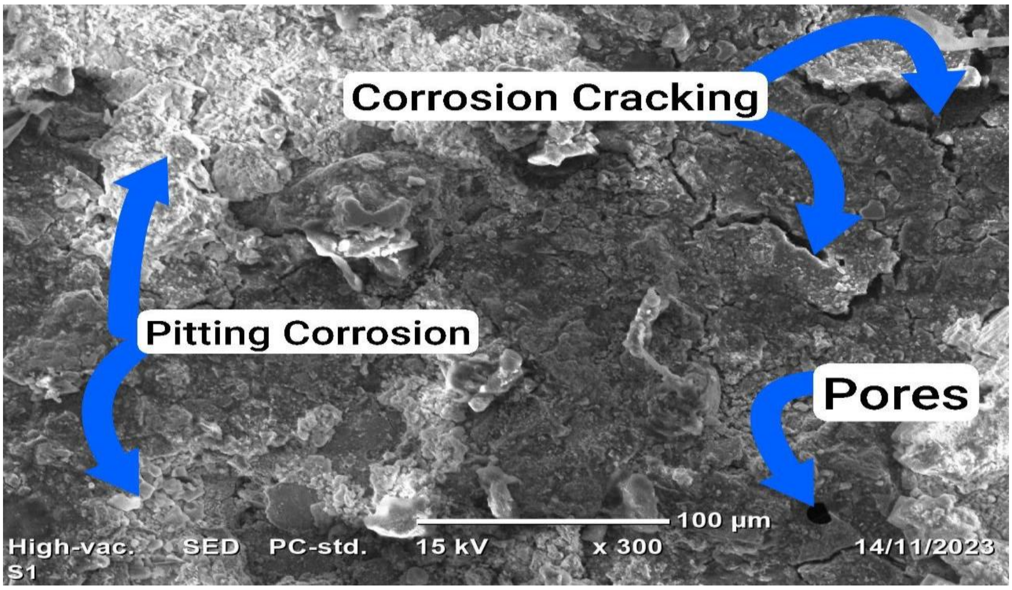

Figure 4. 15 SEM Micrographs After Corrosion

4.3 Microstructural Characterization

Microstructural characterization is the process of examining the structure and composition of materials at different scales, from the atomic to the macroscopic level. Microstructural characterization techniques can reveal information such as the phase, crystallography, morphology, defects, and chemical composition of materials. These techniques are essential for understanding the relationship between the microstructure and the properties of materials, as well as for designing and optimizing materials for various applications. Some of the common microstructural characterization techniques are optical microscopy, Scanning electron microscopy and X-ray diffraction.

4.3.1 XRD Analysis

X-ray analysis is a method of studying the structure and composition of materials using X-rays. X-rays are electromagnetic radiation with wavelengths shorter than visible light, which can penetrate through matter and interact with the atoms and molecules inside. By measuring the scattering, absorption, reflection, or emission of X-rays from a material, one can obtain information such as the crystal structure, phase, texture, stress, strain, defects, chemical elements, and bonds of the material. X-ray analysis can be used for various purposes, such as identifying unknown substances, determining the quality and purity of materials, investigating the properties and behavior of materials under different conditions, and solving structural problems.

4.3.1.1 Phase Analysis of sintered samples

The X-ray diffraction (XRD) patterns of three samples, namely Ti- 5% CeO_2- 10%Cr (S1), Ti-7.5% CeO_2 - 7.5%Cr (S2) and Ti- 10 % CeO_2- 5%Cr (S3), were obtained in the range of (10°-2θ-80°) with a scan speed of 3° min. The diffraction peaks of the samples were matched with the XRD-JCPDS files of various phases, as shown in Figure 4.10. The addition of small amounts of CeO_2 and Cr as smart materials in the Ti matrix resulted in separate small peaks in the XRD spectra, indicating the formation of Ti-CeO_2-Cr composites. The XRD analysis revealed the presence of Ti (high intensity peak) and reinforcements (CeO_2 and Cr), which were marked by different symbols and XRD-JCPDS numbers, in the composite matrix (**Wang et al., 2021**). According to the literature, the CeO_2 and Cr phases can improve the microstructure, hardness, wear resistance and corrosion resistance of the Ti-based coatings.

As the percentage of reinforcements increased, the intensity of the corresponding peaks in the X-ray diffraction (XRD) patterns also increased, as reported by (**Bahari et al. 2012**) and (**N. Singh et al. 2018**). The highest peak, located at 2θ=44.79° and (110) plane, was assigned to the Ti phase (JCPDS card number: 037-0474), which indicated a high concentration of titanium in the composite. Another peak, observed at 2θ=33.8° and (111) plane, corresponded to the Ti- CeO_2 (**Kamacite**) phase (JCPDS card number: 035-1375), which was consistent with the findings of (**Singh et al. 2018**). The Ti-Cr phase (200) was identified by three peaks with JCPDS card numbers 054-0331, 034-0396, and 041-1224, respectively, at an angle of 2θ=64.4829° This agreed with the results of (**Bautista et al. 2008**) and (**Li et al. 2020**). Additionally, small peaks at 2θ=24.64°, (101) plane and JCPDS code 004-0850 for CeO_2 and at 2θ=55.42°, (220) plane and JCPDS code 006-0694 for Cr were detected, indicating the presence of these phases in the composite.

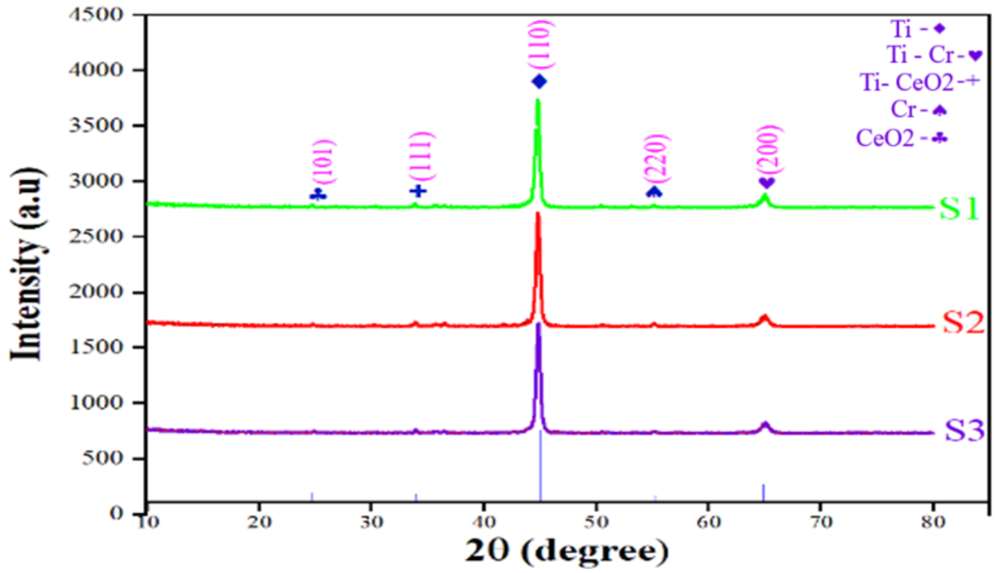

Figure 4.10 XRD Spectrum of Ti-MMC at Different Reinforcement Content

The reinforcements have a low weight percentage in the composite, which results in a lower peak intensity than the matrix in the XRD pattern. The peak intensity of the reinforcements may be too low to be detected by the XRD technique, as suggested by (**Olani et al. 2023**). Titanium, which is expected to be present in the composite due to the addition of Graphite , has not been identified by XRD. This could be because titanium reacts with nickel and the matrix phase, forming new phases that are not easily distinguishable by XRD. The small size of the reinforcements also makes it difficult to verify their phase composition by XRD. The matrix phase of the composite shows very weak peaks in the XRD pattern, indicating a low degree of crystallinity or a high level of disorder.

4.3.1.2 Crystalline Sizes of Sintered Samples

We used equation (3.3) to calculate the crystalline size from the XRD data, which is based on the Scherrer equation. This equation is commonly used to estimate the size of spherical crystallites from the broadening of their X-ray diffraction peaks. We chose K = 0.94, which is the recommended value for Ti-CeO2-Cr according to a recent study by (Lee et al., 2022). This value represents the most extreme acceptable run for the Scherrer condition, which assumes that the crystallites are spherical and have a uniform size distribution. We used the average value of the diffraction peak width, which was 1.54056 (°), as the input for the equation.

Table 4.5 Crystalline Sizes of Samples Using XRD Data

Parameters		**Data from XRD peak analysis**			
K	**λ (Å)**	**Peak Position 2θ (°)**	**FWHM β (°)**	**D(μm)** $D=\frac{K\lambda}{\beta\cos\theta}$	**Average (D) (μm)**
0.94	1.54056	43.8314	0.3	25.66	27.87
		44.7982	0.4102	18.7	
		45.4705	0.24	31.89	
		64.4829	0.28	25.06	
		64.9977	0.65	10.77	

The X-ray diffraction wavelength was varied as much as possible to obtain different values of the crystalline size. The average crystalline size was 27.87 μm, which was consistent with the average grain size obtained from the optical microscopy (OM) measurements. This indicates a good correlation between the XRD and OM data, and suggests that the grains are composed of single crystals.

4.3.1.3 Dislocation Density and Lattice Strain of Composited Material

During the fabrication of Titanium based composite materials, mixing, blending, compaction, and sintering processes were applied. These processes enabled the particles to interact and disperse in the matrix (**Saberi et al., 2009**). As the milling time increased, the lattice strain of metal matrix composites also increased, while the particle size decreased (**Bahari et al., 2012**). Ideally, these particles should be distributed uniformly in the matrix, but there was a risk of creating defects such as dislocations and lattice strain due to the irregularities in mixing, compaction, and the temperature fluctuations in the furnace. These defects could affect the mechanical properties and performance of the composite materials.

To address these problems, the Scherrer formula was applied to the XRD peak analysis using the Gauss method to estimate the parameters of microstructure. The Gauss method for peak variance analysis enables a more accurate assessment of the microstructural properties of materials, such as lattice strain and dislocation density, as reported by previous studies (**Venkateswarl et al., 2014**); (**Altuntaş et al., 2022**); (**Zhu et al., 2023**). The dislocation density of the sintered composite samples was calculated numerically using equation (3.3) from chapter 3, which relates the dislocation density to the full width at half maximum

(FWHM) of the XRD peaks. The lattice strain of the composite was determined using equation (3.4) from chapter 3, which expresses the lattice strain as a function of the FWHM and the Bragg angles of the XRD peaks (**Venkateswarlu et al., 2014**).

Table 4.6 Crystalline Sizes, Dislocation Density and Lattice Strain Experimental Calculation

Sample Code	**Parameters Obtained from XRD Data**		**Experimental Calculation using Scherrer equation, (**Venkateswarlu et al., 2014**)**		
	2θ (°)	**FWHM β (°)**	**D(μm)** $D = \frac{K\lambda}{\beta\cos\theta}$	**δ*10^{-3} μm^{-2}** δ= 1/ D^2	**ε*10^{-3}** $\varepsilon = \frac{\beta}{4\tan\theta}$
Sample 1	43.8314	0.3	29.81	1.13	3.25
	44.7982	0.4102	21.88	2.09	4.34
	45.4705	0.24	37.48	0.71	2.49
	64.4829	0.28	35.034	0.81	1.94
	64.997	0.65	15.13	4.37	4.45
Average	**-**	**-**	**27.87**	**1.73**	**3.3**
Sample 2	43.9313	0.32	27.96	1.28	3.46
	44.864	0.4008	22.39	1.99	4.24
	45.4905	0.28	32.13	0.97	2.91
	64.5229	0.2534	38.72	0.67	1.75
	65.026	0.78	12.61	6.28	5.34
Average	**-**	**-**	**26.76**	**2.24**	**3.54**
Sample 3	33.9389	0.2534	34.23	0.85	3.62
	43.9913	0.44	20.34	2.42	4.75
	44.8379	0.4088	21.96	2.07	4.32

	64.9877	0.79	12.45	6.45	5.41
Average	**-**	**-**	**22.4**	**2.95**	**4.53**

The table (4.4) shows the calculated values of dislocation density and lattice strain for different compositions of chromium and Cerium oxide. Dislocation density is the measure of the total length of dislocations per unit volume of a material, while lattice strain is the deviation of the atomic positions from their ideal locations in a perfect crystal. As the table indicates, increasing the chromium content from 5 wt% to 10 wt% and decreasing the Cerium oxide content from 10 wt% to 5 wt% resulted in a reduction of crystalline size, an enhancement of lattice strain, and an increment of dislocation density. This implies that the chromium reinforcement has a significant effect on the microstructure and deformation behavior of the material.

As shown in the table above, the crystalline size decreases from 27.87 nm to 22.4 nm when the sample number increases from one to three. However, the dislocation density and the lattice strain increase correspondingly from 1.73μm^{-2} to 2.95 μm^{-2} and from 3.3% to 4.53%, respectively. This indicates that the smaller the crystalline size, the higher the strain gradient and the accumulation of geometrically necessary dislocations (GNDs). In contrast, the addition of chromium (up to 10%) to Titanium metal matrix composites (MMCs) results in a reduction of both lattice strain and dislocation density, as reported in this study (**Khitouni et al.,2010**). This could be attributed to the enhanced work hardening and grain refinement due to the presence of chromium particles, which hinder the dislocation motion and increase the activation volume. Therefore, based on these results and the literature review, I conclude that there is an inverse relationship between the crystalline size and the dislocation density and lattice strain of composite materials, which is consistent with the findings of, (**Bahari et al. 2012**), (**Madhavi, 2019**) and (**Rai et al. 2023**)

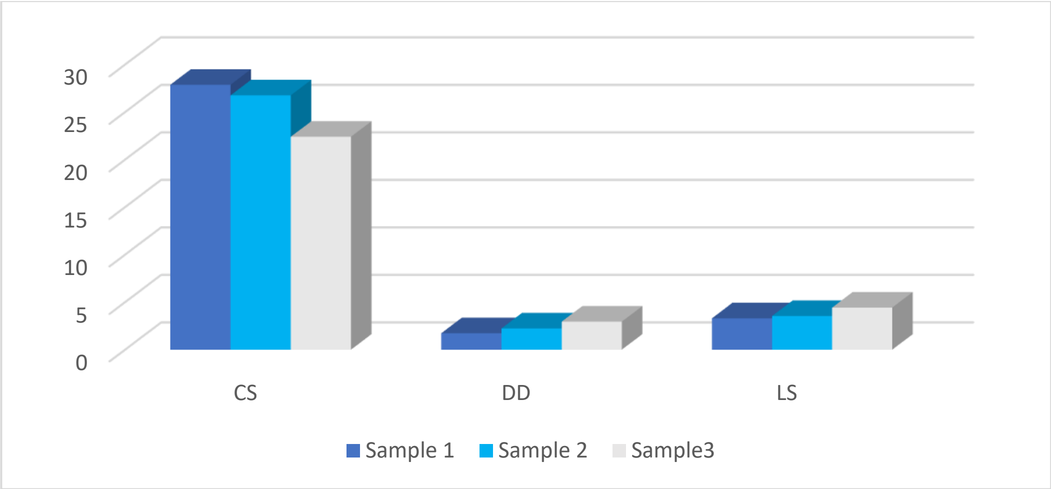

Figure 4.11 Comparison Between Crystalline Size (CS), Dislocation Density (DD) And Lattice Strain (LS) Using Bar Chart

4.3.2 Optical Microscopy

An optical microscope for metallurgy is a type of microscope that uses reflected light to examine the microstructure and properties of metals and alloys. Unlike a biological microscope that illuminates the specimen from below, a metallurgical microscope illuminates the specimen from above by a high-intensity light source. Metallurgical microscopes can be upright or inverted, depending on the orientation of the objective lens and the stage. Metallurgical microscopes are widely used in various fields of material science, such as metallurgy, mineralogy, gemology, and engineering. They can reveal the grain size, shape, distribution, phase, defects, and other features of metallic materials.

4.3.2.1 Distribution of Reinforcing Particles

Figure (4.4) shows the distribution of the reinforcing particles in the Titanium matrix, which was observed using optical microscopy (OM). The image below compares the microstructure of the Titanium matrix before and after etching. The etching process involved immersing the sample in 4% nital (a solution of nitric acid and distilled water) for 10 seconds. The grain boundary is highlighted in the third column of the image. Etching enhances the visibility of the grain boundary by creating contrast between the grains and the matrix. This allows for better analysis of the microstructure and the particle distribution.

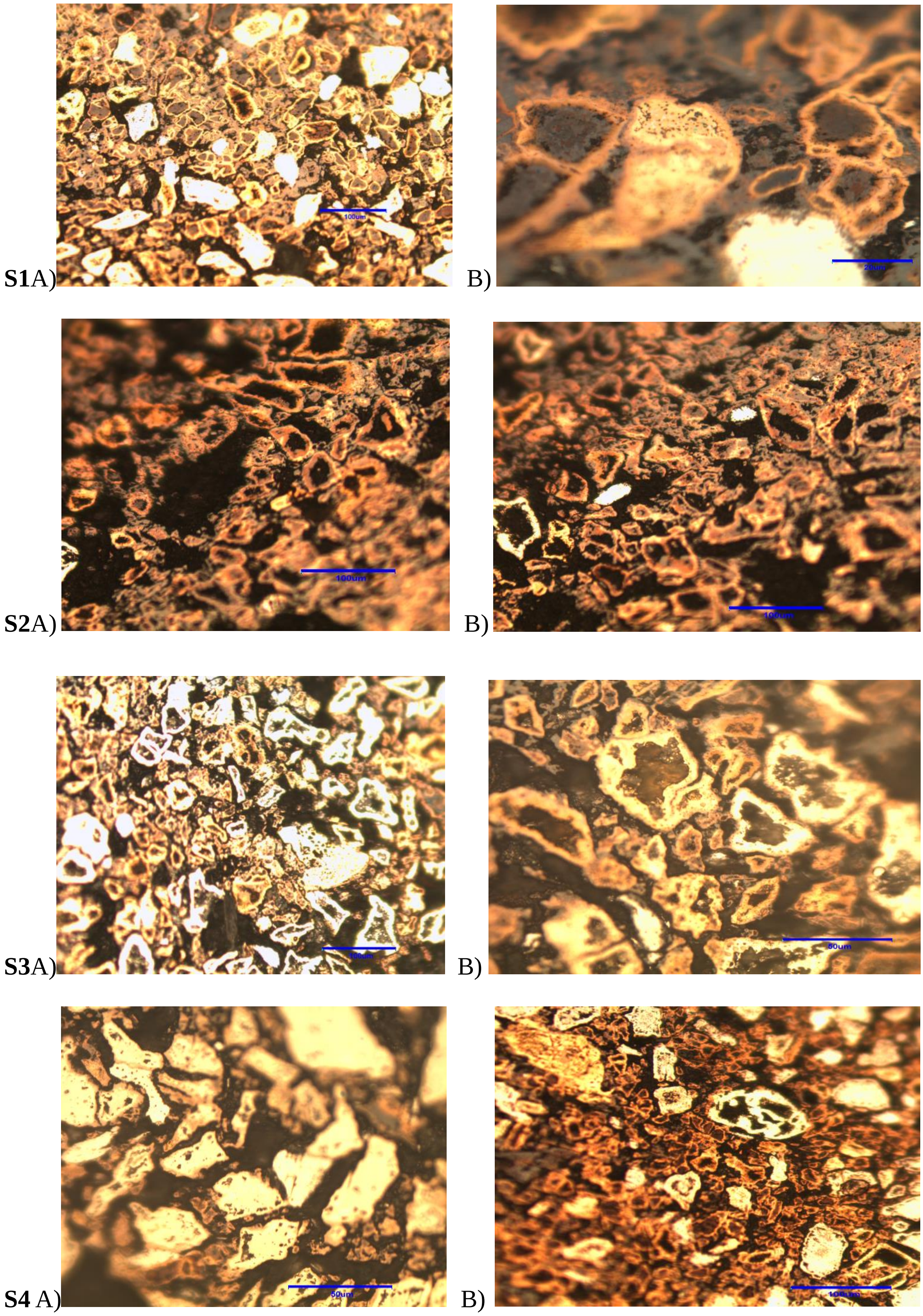

Figure 4.12 Optical Micrographs of S1, S2, S3, And S4 A) Before and B) After Etchant at Different Magnification

4.3.2.2 Grain Size of Sintered Samples

The pore size distribution (PSD) of the sintered sample was calculated using ImageJ software, which is a tool for image analysis and processing. ImageJ can measure the pore radii of a pore structure based on the distance transform method. The PSD can be calculated in either 2D or 3D depending on the image stack.

The grain size of the sample was also determined using ImageJ software, but with a different method. The line intersect method was applied to estimate the grain size from the optical microscope (OM) image. This method involves counting the number of grains or grain boundaries intercepted by a line or a circle, and then calculating the mean lineal intercept length. The grain size varied from 20.138 μm to 156.47 μm, and the average grain size was 63.35 μm, based on the data collected from several random locations on the specimen image. The porosity of the sample was obtained by analyzing the image through ImageJ software and measuring the percentage of the pore area. The porosity values for the four specimens (S1, S2, S3, and S4) were 4.44%, 9.5%, 10.2%, and 4.91%, respectively.

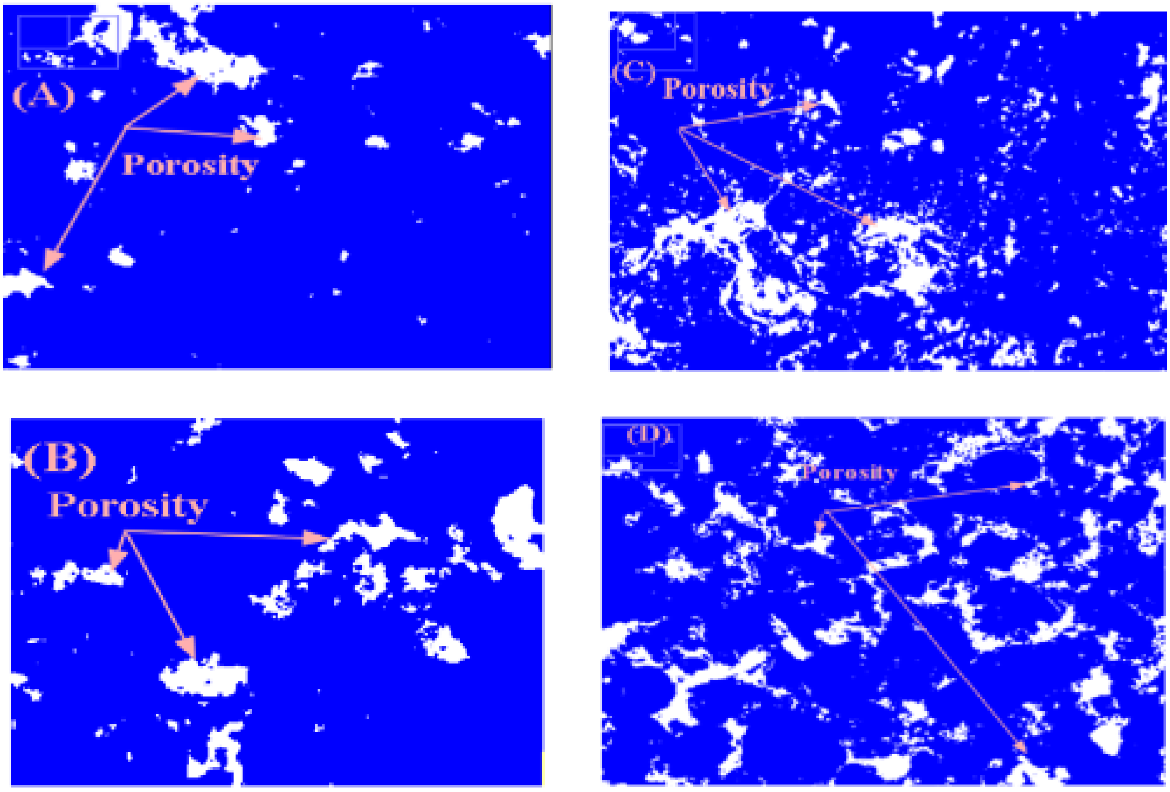

Figure 4.13 Porosity Analysis of Using ImageJ Software from OM Image

4.3.3 Scanning Electron Microscope (SEM)

The distribution of reinforcements in composites is a crucial factor that affects the mechanical, chemical, and physical properties of powder metallurgy composites. Therefore, it is essential to conduct research on how to optimize the reinforcement dispersion and achieve a homogeneous microstructure. Scanning electron microscopy (SEM) is a powerful technique that can provide high-resolution images of the surface morphology and composition of composites. By using SEM, (**Ali Dad Chandio et al.2019**) observed that the sintering process resulted in a uniform distribution of particles and a significant reduction of porosity in the composites. This improved the density, hardness, and wear resistance of the materials.

Figure (4.6) illustrates the microstructure of the hybrid titanium composite, which consists of a titanium matrix reinforced by cerium oxide and chromium particles. The pore spaces in the composite are formed by the uniform distribution of the reinforcements in the matrix. The reinforcements exhibit minimal or no clustering and are well dispersed in the Ti-6Al-4V alloy. In contrast, sintered pure titanium shows a high degree of porosity and aggregation of titanium particles, which may be attributed to the poor mixing or blending of the powder during the high-energy ball milling process and the inherent interconnectivity of the particles

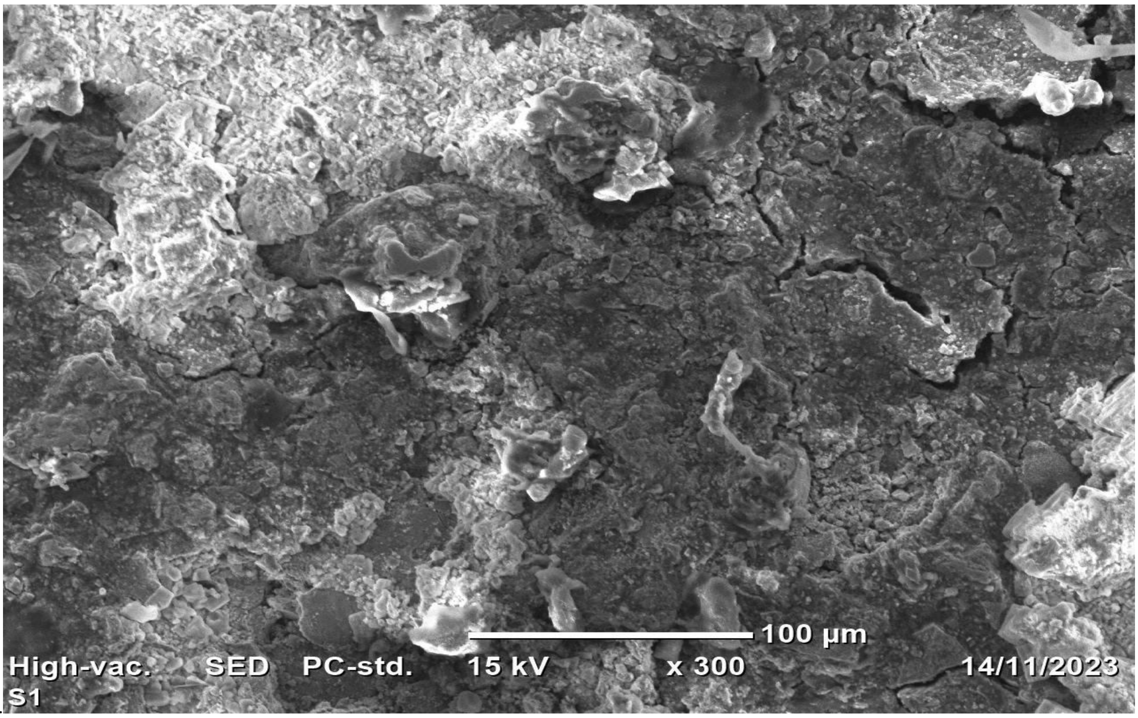

S1

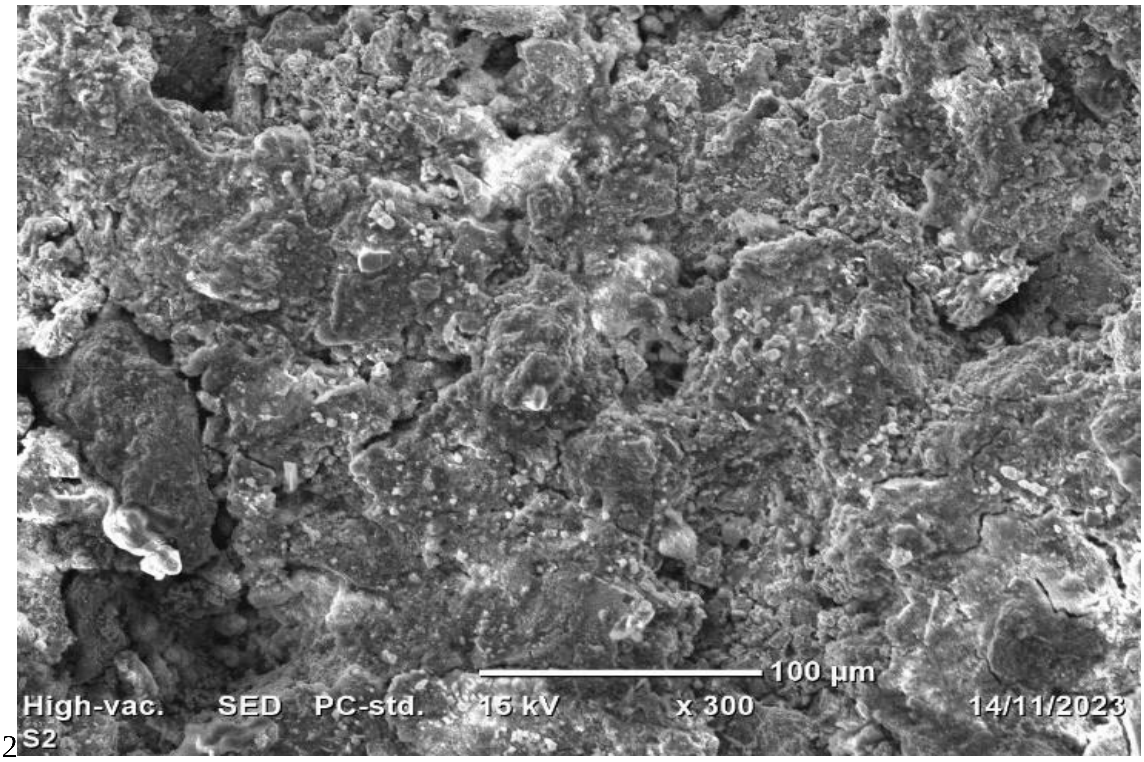
100 µm
High-vac. SED PC-std. 15 kV x 300 14/11/2023
S2
S2

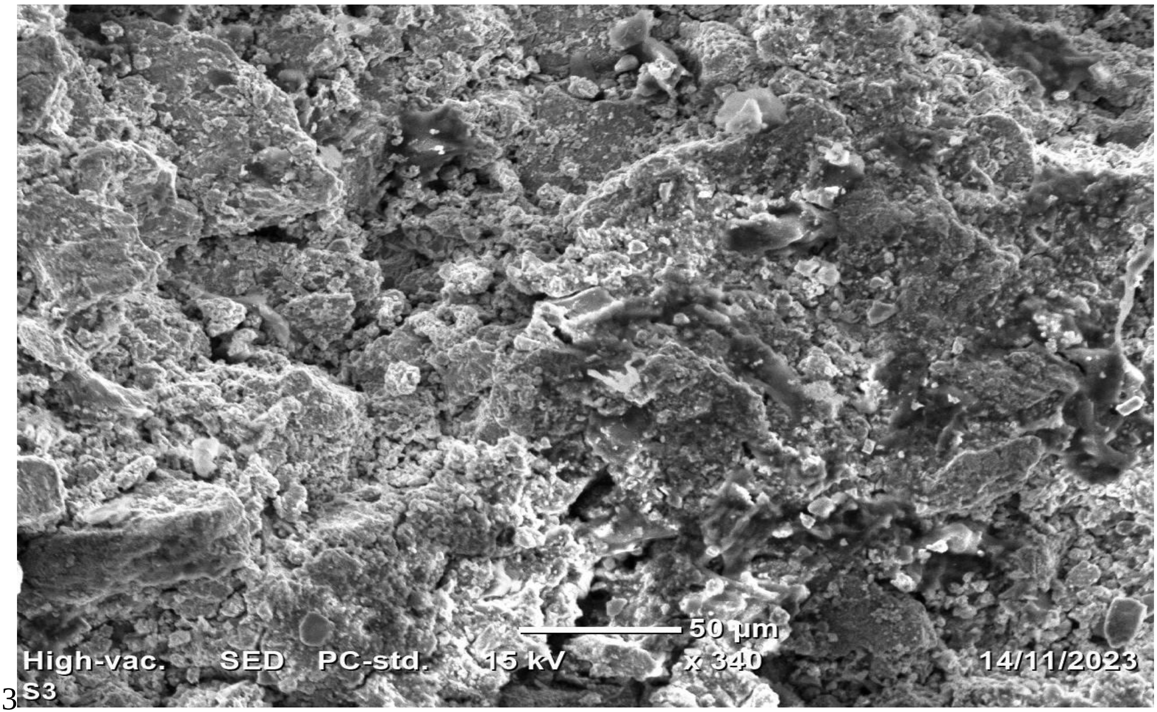
50 µm
High-vac. SED PC-std. 15 kV x 340 14/11/2023
S3
S3

S4 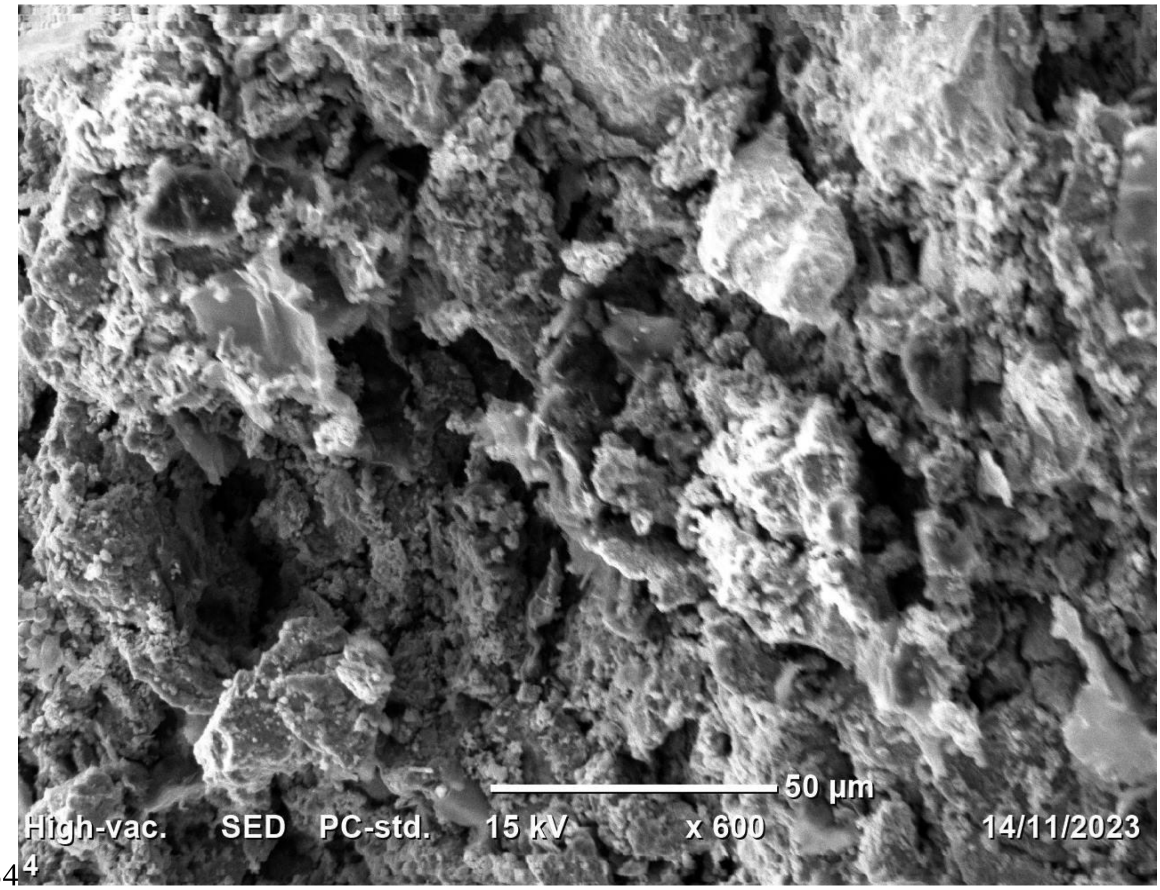

Figure 4.14 SEM Micrographs of (S1, S2, S3 And S4) at Different Magnification

CHAPTER 5

CONCLUSION AND RECOMMENDATION

This study aimed to develop and characterize a titanium-based metal matrix composite (MMC) reinforced with ceramic particles of chromium and cerium oxide. These particles were chosen for their potential to enhance the metallurgical and mechanical properties of the Titanium matrix. The MMCs were fabricated by the powder metallurgy process, which involves producing metal powders, mixing them with additives, compacting them in a die, and sintering them at high temperatures. Different samples with varying weight percentages of the ceramic reinforcement were prepared and analyzed to investigate the effect of reinforcement content on the microstructure, corrosion resistance, and mechanical performance of the MMCs. The results showed that the addition of chromium and cerium oxide particles improved the hardness, wear resistance, and corrosion resistance of the MMCs, but also increased the porosity and reduced the ductility. The optimal weight percentage of the reinforcement was found to be 10%, which provided a good balance between the desired properties.

5.1 Conclusions

Based on the results and discussion, the following conclusions have been drawn:

- The addition of Cerium Oxide and Chromium to the Titanium metal matrix resulted in a slight decrease in the density of the sintered specimen compared to the base metal. The specimen with the composition of (Ti-6Al-4v)- 5%CeO_2- 10%Cr- 4%Graphite exhibited a low porosity of 4.44% and a high relative density of 95.56%, which indicated a high degree of densification. Moreover, the specimen showed minimal dislocation density and lattice strain, which suggested a low level of residual stress and defect formation. These properties were superior to those of other specimens manufactured by different methods.
- The addition of chromium and cerium oxide to the titanium alloy (Ti-6Al-4V) matrix enhances the hardness and compressive strength of titanium metal matrix composites (Ti-MMCs) by forming a reaction layer between the matrix and the reinforcements. The hardness and compressive strength of Ti-MMCs increase with the reinforcing fraction up to 17%. Moreover, substituting cerium oxide with chromium up to 10% content further improves the hardness and compressive strength of Ti-MMCs. Therefore, the Ti-MMC with the composition of (Ti-6Al-4v)- 5%CeO_2- 10%Cr- 4% Graphite has the

highest hardness of 682 HV and compressive strength of 914 MPa among all the fabricated samples.

- The corrosion resistance of titanium alloys depends on the formation of a stable oxide film on their surface. However, some environments can degrade this film and cause corrosion. One way to enhance the corrosion resistance of titanium alloys is to add ceramic particles such as CeO_2 and Cr to the metal matrix. These particles can improve the stability and thickness of the oxide film, as well as reduce the galvanic coupling between the alloy and the environment. In this study, we investigated the corrosion behavior of (Ti-6Al-4v)-CeO2-Cr-Graphite composites in different electrolytes. We used optical microscopy (OM) and scanning electron microscopy (SEM) to examine the surface morphology and microstructure of the composites before and after corrosion. We also measured the corrosion current and the protection efficiency of the composites using electrochemical techniques. We found that the composite with 5% CeO_2, 10% Cr and 4% Graphite had the best corrosion resistance among the tested samples. It achieved a protection efficiency of 76% and a corrosion current of 19.27 mA cm^{-2}, which were significantly lower than those of the pure Ti-6Al-4v alloy. The OM and SEM images showed that this composite had a uniform and compact oxide film that protected the metal matrix from corrosion. The results of this study suggest that adding CeO_2 and Cr particles to the titanium alloy can effectively improve its corrosion resistance in various environments.
- The fabricated samples were characterized by optical microscopy (OM) and scanning electron microscopy (SEM) to observe the distribution of base metal and particulates. OM and SEM are techniques that use light and electrons, respectively, to produce magnified images of a sample. The sample composition was (Ti-6Al-4v)- 5%CeO2-10%Cr- 4%Graphite, which is a titanium alloy with cerium oxide, chromium, and Graphite additions. Ti-6Al-4v is an alpha-beta titanium alloy with high strength and corrosion resistance. The SEM image showed a fine and uniform distribution of titanium and particles, with low porosity and agglomeration, indicating good hardness. The sample was also analyzed by Fourier-transform infrared spectroscopy (FT-IR), which is a technique that measures the absorption or emission of infrared light by a sample. The FT-IR spectrum revealed the presence of (Ti-6Al-4v)-O bond stretching and bending modes, with a small peak in the range of (500-670) cm-1, and the absence of OH-absorption band, which confirmed the material’s ability to resist corrosion.

5.2 Recommendation

Powder metallurgy techniques are increasingly used to prepare the components for Titanium-based metal matrix composites (Ti-MMCs) with all the required factors, especially during the compaction and sintering process. These techniques produce Ti-MMC components with remarkable improvement in hardness and corrosion resistance performances. These outstanding results are of the greatest importance for the applications of Ti-MMCs in various fields such as aerospace, biomedical, and automotive industries. Therefore, the use of powder metallurgy to produce alloy and particle reinforced Ti-MMCs could enhance their popularity and demand in the market.

One of the challenges in producing titanium metal matrix composites (Ti-MMCs) is to reduce the porosity level, which affects the mechanical and physical properties of the composites. Ti-MMCs have interconnected pores that tend to agglomerate after milling and compaction processes. Therefore, it is recommended to develop a method that can reduce the porosity level effectively and uniformly. Additionally, every process parameter in powder metallurgy, such as milling time, compaction pressure, sintering time, and sintering temperature, should be optimized to minimize their impact on the composites. For instance, longer milling time can increase the surface area and reactivity of the powders, but also cause more oxidation and contamination. Higher compaction pressure can increase the density and strength of the composites, but also cause more residual stress and deformation. Sintering time and temperature should be carefully controlled to achieve good bonding between the matrix and the reinforcement, but avoid excessive grain growth and diffusion. Furthermore, it is strongly suggested that secondary operations, such as thermal stability and extrusion, should be performed in the future, depending on the application requirements of the composites. These operations can enhance the microstructure, mechanical properties, and dimensional accuracy of the composites.

REFERENCES

Ali Dad Chandio, A. D. C., Muhammad Basit Ansari, M. B. A., Shahid Hussain, S. H., & Muhammad Ali Siddiqui, M. A. S. (2019). Silicon Carbide Effect as Reinforcement on Aluminium Metal Matrix Composite. Journal of the Chemical Society of Pakistan, 41(4), 650–650. https://doi.org/10.52568/000776/jcsp/41.04.2019.

Altuntaş, G., Altuntaş, O., Öztürk, M. K., & Bostan, B. (2022). Metallurgical and Crystallographic Analysis of Different Amounts of Deformation Applied to Hadfield Steel. International Journal of Metalcasting, 17(2), 1340–1349.https://doi.org/10.1007/s40962-022-00860-3.

An, H., Liu, L., Song, N. et al. (2022) Rational design and synthesis of cerium dioxide-based nanocomposites. Nano Res. 16, 3622–3640 (2023).https://doi.org/10.1007/s12274-022-4941-y

Anand, A., & Tiwari, S. K. (2022). Recent advancements in the production of hybrid metal matrix composites (HMMC): A Review. IOP Conference Series: Materials Science and Engineering, 1248(1), 012087. https://doi.org/10.1088/1757-899x/1248/1/012087.

Anandajothi, M., Ramanathan, S., Ananthi, V. et al (2017). Fabrication and characterization of Ti6Al4V/TiB2–TiC composites by powder metallurgy method. Rare Met. 36, 806–811 (2017). https://doi.org/10.1007/s12598-016-0732-5

Andrade, C., & Martínez, I. (2010). Techniques for measuring the corrosion rate (polarization resistance) and the corrosion potential of reinforced concrete structures. Non-Destructive Evaluation of Reinforced Concrete Structures: Non-Destructive Testing Methods, 284–316. https://doi.org/10.1533/9781845699604.2.284.

Ankur, N., & Singh, N. (2021). Performance of cement mortars and concretes containing coal bottom ash: A comprehensive review. Renewable and Sustainable Energy Reviews, 149(January), 111361. https://doi.org/10.1016/j.rser.2021.111361.

Arif, S., Alam, M. T., Ansari, A. H., Siddiqui, M. A., & Mohsin, M. (2017). Study of mechanical and tribological behaviour of Al/SiC/ZrO2 hybrid composites fabricated through powder metallurgy technique. Materials Research Express, 4(7). https://doi.org/10.1088/2053-1591/aa7b5f.

Ashebir, D. A. (2022). Synthesis , Characterization , and Testing of Self-Lubricating Tetra Hybrid Reinforced Al Matrix Composites via Powder Metallurgy Processing Synthesis , Characterization , and Testing of Self-Lubricating Tetra Hybrid Reinforced Al Matrix Composites via Po.

Ashwath, P., Xavior, M.A (2016). Processing methods and property evaluation of Al2O3 and SiC reinforced metal matrix composites based on aluminium 2xxx alloys. Journal of Materials Research 31, 1201–1219 (2016). https://doi.org/10.1557/jmr.2016.131

Augustin, M., & Balu, T. (2017). Estimation of Lattice Stress and Strain in Zinc and Manganese Ferrite Nanoparticles by Williamson-Hall and Size-Strain Plot Methods., 16(3), 1–7. https://doi.org/10.1142/S0219581X16500356

Aydogmus, T. (2015). Processing of interpenetrating Mg-TiNi composites by spark plasma sintering. Materials Science Engineering and Proceedings in Engineering Science 62(4), 261– 270. https://doi.org/10.1016/j.msea.2014.11.092.

Bahari, A., Sadeghi Nik, A., Roodbari, M., & Mirnia, N. (2012). Investigation the Al-Fe-Cr-Ti nano composites structures with using XRD and AFM techniques. Sadhana – Academy Proceedings in Engineering Sciences, 37(6), 657–664. https://doi.org/10.1007/s12046-012- 0103-3.

Balaraju, J. N., Selvi, V. E., & Rajam, K. S. (2010). Electrochemical behavior of low phosphorus electroless Ni – P – Si 3 N 4 composite coatings. (2– 3), 546–551. https://doi.org/10.1016/j.matchemphys.2009.11.047.

Barrado, M., López, G. A., Nó, M. L., & San Juan, J. (2009). Composites with ultra high damping capacity based on powder metallurgy shape memory alloys., 521–522, 363–367. https://doi.org/10.1016/j.msea.2008.10.075.

Bautista, A., González-Centeno, A., Blanco, G., & Guzmán, S. (2008). Application of EIS to the study of corrosion behaviour of sintered ferritic stainless steels before and after high- temperature exposure. International Journal of Engineering, Science and Technology 59(1), 32–39. https://doi.org/10.1016/j.matchar.2006.10.008.

Bayu, D., Kumar, D., Venkatesh, C., Kumar, A., & Jha, P. (2021). Materials Today : Proceedings Mathematical modeling and mechanical characterization through process parameters optimization of AlMg-matrix SiC p reinforced composites produced by powder metallurgy route. Materials Today: Proceedings, 2021 03 078 xxxx https://doi.org/10.1016/j.matpr.2021.03.078.

Chu, C., Chen, W., Chen, Z., Jiang, Z., Wang, H., & Fu, Z. (2021). Microstructure and Mechanical Behavior of FeNiCoCr and FeNiCoCrMn High - Entropy Alloys Fabricated by Powder Metallurgy. Acta Metallurgica Sinica (English Letters), 34(4), 445–454. https://doi.org/10.1007/s40195-020-01150-9.

Cicek, H., Akar, O.C. & Efeoglu, I (2021). Tribological Properties of TiNi/MoS2 Functional Coatings. J. of Materi Eng and Perform 30, 3632–3641 (2021). https://doi.org/10.1007/s11665-021-05703-6

Das, R., Mondal, M. K., & Pramanik, S. (2022). Strengthening Behaviour and Microstructural Properties during the Compaction of Reduced Blast Furnace Flue Dust—Fly Ash—Iron Metal Matrix Composite Fines using Powder Metallurgy Route. Transactions of the Indian Institute of Metals, 75(9), 2255–2263. https://doi.org/10.1007/s12666-022-02592-8

Deepan Bharathi Kannan, T., Ramesh, T., & Sathiya, P. (2016). A Review of Similar and Dissimilar Micro-joining of Nitinol. 1227–1245. https://doi.org/10.1007/s11837-016- 1836-y.

Delavari, M., Salarvand, A., Rahi, A., & Shahri, F. (1970). The effect of powder metallurgy process parameters on mechanical properties of micro and nano-iron powder. International Journal of Engineering, Science and Technology, 86–94. https://doi.org/10.4314/ijest.v3i9.7

Dhanunjay Kumar Ammisetti and S S Harish Kruthiventi (2020). Recent trends on titanium metal matrix composites:.2020. 08732 https://doi.org/10.1016/j.matpr.2020.08.732

Di Wang and Song- Sheng Lin (2022). Research on high temperature wear resistance mechanism of CrN/CrAlN multilayer coatings - ScienceDirect108184. https://doi.org/10.1016/j.triboint.2022.108184

Duriagina, Z. A., Romanyshyn, M. R., Kulyk, V. V, Kovbasiuk, T. M., Trostianchyn, A. M., & Lemishka, I. A. (2020). The character of the structure formation of model alloys of the Fe- Cr-(Zr, Zr-B) system synthesized by powder metallurgy. 100(2), 49–57. https://doi.org/10.5604/01.3001.0014.3344.

Fatemeh Nemati and Maryam Rezaie (2021). Cerium functionalized Graphite Nano-structures and their applications; A review - ScienceDirect. https://doi.org/10.1016/j.envres.2022.112685

Gao et al. (2019), "Tool Wear Behavior in Turning of Titanium Matrix Composites Reinforced with In Situ Synthesized TiC Particles", Materials, 2019.

Ghasemi, F., Moazami-Goudarzi, M. & Najafi, H (2021). Microstructures, hardening and tribological behaviors of tin matrix composites reinforced with SiC and Zn particles. Rare Met. 40, 2584–2592 (2021). https://doi.org/10.1007/s12598-020-01535-w

Gupta et al (2022). Synergetic Effect of CeO2 Doping on Structural and Tribological Behavior of Fe-Al2O3 Metal Matrix Nanocomposites. https://doi.org/10.1149/2162-8777/ac9c92

Gupta, P., Kumar, D., Parkash, O., & Jha, A. K. (2013). Effect of sintering on wear characteristics of Fe-Al2O3 metal matrix composites. Proceedings of the Institution of Mechanical Engineers, Part J: Journal of Engineering Tribology, 228(3), 362–368. https://doi.org/10.1177/1350650113508934.

Han, T., Xiao, M., Zhang, Y., & Shen, Y. (2019). Laser cladding Ni-Ti-Cr alloy coatings with different process parameters. Materials and Manufacturing Processes, 34(15), 1710–1718. https://doi.org/10.1080/10426914.2019.1686521.

Hanieh Ghodrati and Reza Ghomashchi (2019). Effect of Graphite dispersion and interfacial bonding on the mechanical properties of metal matrix composites: An overview - ScienceDirect. https://doi.org/10.1016/j.flatc.2019.100113

Hao, S., Cui, L., Jiang, D., Han, X., Ren, Y., Jiang, J., Liu, Y., Liu, Z., Mao, S., Wang, Y., Li, Y., Ren, X., Ding, X., Li, J. (2013). A transforming metal nanocomposite with large elastic strain, low modulus, and high strength. Science, 339(6124), 1191–1194.https://doi.org/10.1126/science.1228602.

Hao, S., Cui, L., Shao, Y., Jiang, J., Jiang, D., Wang, S., Du, M., Wang, Y., Brown, D. E., & Ren, Y. (2012). In situ X-ray diffraction study of deformation behavior in a Fe/NiTi composite. 101(22), 2010–2014. https://doi.org/10.1063/1.4767993.

Hill, H., Weber, S., Siebert, S., & Theisen, W. (2011). Investigation of corrosion and wear properties of fe based metal matrix composites consolidated by sintering and hot isostatic pressing. 455–462. https://doi.org/10.1179/003258910X12678035166656.

Himyan Mohammed et al (2018). Structural and mechanical properties of CeO2 reinforced Al matrix nanocomposites. https://doi.org/10.5185/amlett.2018.2030

Honnaiah, C., Srinath, M. S., & Shashank Lingappa, M. (2023). Metallographical characterization of Al-SiCP metal matrix composites processed through microwave sintering technique. https://doi.org/https://doi.org/10.1016/j.matpr.2023.03.077.

Hui Jiang and Li Li (2021) Effects of Chromium on the Microstructures and Mechanical Properties of $AlCoCr_xFeNi_{2.1}$ Eutectic High Entropy Alloys. volume 34, pages1565–1573 (2021)

Imataka, H., Tanaka, K., Maeda, S., Yuya, M., & Kobayashi, A. (2017). Development of High- strength Nitriding Steel for Gear. Nippon Steel & Sumitomo Emtal Technical

Imataka, H., Tanaka, K., Maeda, S., Yuya, M., & Kobayashi, A. (2017). Development of High- strength Nitriding Steel for Gear. Nippon Steel & Sumitomo Emtal Technical

Issa, S. A. M., Almutairi, A. M., Albalawi, K., Dakhilallah, O. K., Zakaly, H. M. H., Ene, A., Abulyazied, D. E., Ahmed, S. M., Youness, R. A., & Taha, M. A. (2023). Production of Hybrid Nanocomposites Based on Iron Waste Reinforced with Niobium Carbide/Granite Nanoparticles with Outstanding Strength and Wear Resistance for Use in Industrial Applications. Nanomaterials, 13(3). https://doi.org/10.3390/nano1303053.

Ivannikov, A. Y., Grebennikov, I. K., Klychevskikh, Y. A., Mikhailova, A. V., Sergienko, K. V., & Kaplan, M. A. (2022). Elemental Powders. Jabur, A. S. (2013). Effect of powder metallurgy conditions on the properties of porous bronze. Powder Technology, 237, 477–483. https://doi.org/10.1016/j.powtec.2012.12.027..

Jacob, J., & Khadar, M. A. (2010). Investigation of mixed spinel structure of nanostructured nickel ferrite. Journal of Applied Physics, 107(11). https://doi.org/10.1063/1.3429202.

Jha, P., Kumar, D., & Mishra, V. K. (2022). Development of mathematical models to predict the density and hardness of Fe-ZrO2 composites. 8(3), 3042–3056. https://doi.org/10.1080/2374068X.2021.1945298.

JianHui Yan and Maojian Li (2020) Effects of Cr Content on Microstructure and Mechanical Properties of WMoNbTiCr High-Entropy Alloys Journal of Materials Engineering and Performance volume 29, pages2125–2133 (2020)

klaus Reinhardt and Herwig Winkler (2000). Cerium Mischmetal, Cerium Alloys, and Cerium Compounds. Ullmann's Encyclopedia of Industrial Chemistry - Reinhardt . https://doi.org/10.1002/14356007.a06_139

Li, J., Zhu, Z., Peng, Y., & Shen, G. (2020). Microstructure and wear characteristics of novel fe-ni matrix wear-resistant composites on the middle chute of the scraper conveyor. Journal of Materials Research Technology, 935–947. https://doi.org/10.1016/j.jmrt.2019.11.033.

Li, Y., Li, C., Tang, S., Zheng, Q., Wang, J., Zhang, Z., & Wang, Z. (2019). Interfacial Bondingand Abrasive Wear Behavior of Iron Matrix Composite Reinforced by Ceramic Particles.

Liaoyuan Chen and Yu Zhao (2021) Effects of CeO2 addition on microstructure and properties of ceramics reinforced Fe-based coatings by laser cladding. The International Journal of Advanced Manufacturing Technology volume 115, pages2581–2593 (2021)

Lingyue Hu and Xuefeng Song (2020). A robust, hydrophobic CeO2/NiCoCrAlY composite coating with excellent thermal stability and corrosion resistance prepared by air plasma spray - ScienceDirect. https://doi.org/10.1016/j.jallcom.2021.158623

López, G. A., Barrado, M., San Juan, J., & Nó, M. L. (2009). Mechanical spectroscopy measurements on SMA high-damping composites. Materials Science and Engineering A, 521–522, 359–362. https://doi.org/10.1016/j.msea.2008.09.121.

Manjunath, R., Kumar, (2021) A Review on the Significance of Hybrid Particulate Reinforcements on the Mechanical and Tribological Properties of Stir-Casted Aluminum Metal Matrix Composites. *J Bio Tribo Corros* 7, 122 (2021). https://doi.org/10.1007/s40735-021-00558-9

Manjunatha, C.J., Venkata Narayana, B., Bino Prince Raja, D. et al (2022). Tribological, Thermal and Corrosive Behaviour of Aluminium Alloy 2219 Reinforced by Si3N4 Nanosized Powder. Silicon (2022). https://doi.org/10.1007/s12633-021-01214-0

Manohar, G., Pandey, K. M., & Ranjan Maity, S. (2020). Effect of compaction pressure on mechanical properties of AA7075/B4C/Graphite hybrid composite fabricated by powder metallurgy techniques. Materials Today: Proceedings, 38(xxxx), 2157–2161. https://doi.org/10.1016/j.matpr.2020.05.194.

Mavhungu, S. T., Akinlabi, E. T., Onitiri, M. A., & Varachia, F. M. (2017). Aluminum MatrixComposites for Industrial Use: Advances and Trends. Procedia Manufacturing, 7, 178–182. https://doi.org/10.1016/j.promfg.2016.12.045.

McCall, J. L. (1986). Systematic analysis of gear failures. Metallography, 19(2), 249. https://doi.org/10.1016/0026-0800(86)90042-x.

Mendez, J.A., Vong, Y.M. & Bueno, J.d (2022). Cerium and Other Rare Earth Salts as Corrosion Inhibitors. (2022). https://doi.org/10.1134/S2070205122040141

Milani, A. S., Shanian, A., Madoliat, R., & Nemes, J. A. (2005). The effect of normalization norms in multiple attribute decision making models: A case study in gear material selection. Structural Multidisciplinary Optimization, 29(4), 312–318. https://doi.org/10.1007/s00158-004-0473-1.

Mohammad Fallah Barzoki and Shohreh Faremi (2022). Fabrication and comparison of composites of cerium metal-organic framework/reduced Graphite oxide as the electrode in supercapacitor application -. https://doi.org/10.1016/j.est.2022.105545

Mohammed Ali and Tun Nyo (2020) Influence of Chromium Content on the Microstructure and Mechanical Properties of Thermomechanical Hot-Rolled Low-Carbon Bainitic Steels Containing Niobium. https://doi.org/10.3390/app10010344

Monowar Wadud Hridoy et al (2019). Effect of Chromium Reinforcement on Mechanical Behavior of Aluminum Matrix Composites. ICMERE2019-PI-188

Naghmeh Abavi Torghabeh and Rasoul Pouriamanesh (2022). A review on Ti-based metal matrix composite. journal of composites and compounds 4 (2022) 209-219

Nguyen, B., & Gupta, M. (2010). Enhancing compressive response of AZ31B using nano-Al 2O3 and copper additions. Journal of Alloys and Compounds Alloys Compounds, 490, 382–387. https://doi.org/10.1016/j.jallcom.2009.09.188.

Obadele, B. A., Ramabulana, K., Alaneme, K. K., & Durowoju, M. O. (2015). composite coatingson AISI 316 stainless steel. June.

Öksüz, K. E., Çevik, M., Bozdağ, A. E., Özer, A., & Şimşir, M. (2014). Production of (V-B) Reinforced Fe Matrix Composites. 8(8), 800–804.

Olani, M., Kumar, D., & Asrat, G. (2023). Mechanical and corrosion properties of Fe–SiC–ZrO2 hybrid composite fabricated through powder metallurgy process. Results in Engineering, 17 100866. https://doi.org/10.1016/j.rineng.2022.100866.

P. F. Jiang and C. H. Zhang (2020). Microstructure and Properties of CeO2-Modified FeCoCrAlNiTi High-Entropy Alloy Coatings by Laser Surface Alloying. Journal of materials engineering and performance volume 29, pages1346–1355 (2020)

Pan, S., Jin, K., Wang, T. et al (2022). Metal matrix nanocomposites in tribology: Manufacturing, performance, and mechanisms. Friction 10, 1596–1634 (2022). https://doi.org/10.1007/s40544-021-0572-7

Panda, D. (2016). Development of Al-Fe 3 Al Composites by Powder Metallurgy Route National Institute of Technology Rourkela Supervisors' Certificate. Parande, G., Manakari, V., Wakeel, S., Kujur, M. S., & Gupta, M. (2018). Enhancing mechanical response of monolithic magnesium using nano-NiTi (Nitinol) particles. Metals, 8(12), 1–13. https://doi.org/10.3390/met8121014.

Paswan, S. K., Kumari, S., Kar, M., Singh, A., Pathak, H., Borah, J. P., & Kumar, L. (2021). Optimization of structure-property relationships in nickel ferrite nanoparticles annealed at different temperature. Journal of Physics and Chemistry of Solids, 151(January), 109928. https://doi.org/10.1016/j.jpcs.2020.109928.

Patange, S. M., Shirsath, S. E., Jadhav, S. P., Hogade, V. S., Kamble, S. R., & Jadhav, K. M. (2013). Elastic properties of nanocrystalline aluminum substituted nickel ferrites prepared by co-precipitation method. Journal of Molecular Structure, 1038, 40–44. https://doi.org/10.1016/j.molstruc.2012.12.053.

Praveena, B. A., Santhosh, N., Buradi, A., Srikanth, H. V., Shankar, G., Ramesha, K., Manjunath, N., Karthik, S. N., Rudra Naik, M., & Praveen Kumar, S. (2022). Experimental Investigation on Density and Volume Fraction of Void, and Mechanical Characteristics of Areca Nut Leaf Sheath Fiber-Reinforced Polymer Composites. International Journal of Polymer Science, 2022. https://doi.org/10.1155/2022/6445022.

R. Sivakumar, B. R. Senthil Kumar, G. Gopalarama Subramaniyan (2022) microstructure and mechanical behavior of Ti-6Al-4v matrix reinforced with WCp Developed by Squeeze casting. https://doi.org/10.1155/2022/6381265

Rai, A., Rai, P., Kumar, A., Chaturvedi, R. K., & Singh, V. K. (2023). Study of Mechanical Characteristics of Silicon Carbide Reinforced Zn-Mg Based Metal-Ceramic Composite. Silicon, 0123456789. https://doi.org/10.1007/s12633-023-02474-8.

Rajak, D. K., Pagar, D. D., Kumar, R., & Pruncu, C. I. (2019). Recent progress of reinforcement materials: A comprehensive overview of composite materials. Journal of Materials Research and Technology, 8(6), 6354–6374. https://doi.org/10.1016/j.jmrt.2019.09.068.

Rajesh Kumar, L., Saravanakumar, A., Bhuvaneswari, V., Gokul, G., Dinesh Kumar, D., & Jithin Karunan, M. P. (2019). Optimization of wear behaviour for AA2219-MoS2 metal matrix composites in dry and lubricated condition. Materials Today: Proceedings, 27(xxxx), 2645–2649. https://doi.org/10.1016/j.matpr.2019.11.087.

Raturi, A. (2019). Analysis Of Mechanical And Micro Structural Behaviour Of Al Based Metal Matrix Composite Reinforced With Ball Milled Nano Particles :.

Raviraj Shetty and Aditihya Hegde (2022). Processing and Mechanical Characterization of Titanium Metal Matrix Composites: A Literature Review *J. Compos. Sci.* 2022, *6*(12), 388; https://doi.org/10.3390/jcs6120388

Sajan, S., & Philip Selvaraj, D. (2021). A review on polymer matrix composite materials and their applications. Materials Today: 5493–5498. https://doi.org/10.1016/j.matpr.2021.08.034.

Samira Bagheri and Ibrahim Khalil (2019) Cerium (IV) oxide nanocomposites: Catalytic properties and industrial application - ScienceDirect.2020. 02022 https://doi.org/10.1016/j.jre.2020.02.022

Shetty et al. (2022), “Processing and Mechanical Characterizations of Titanium Metal Matrix Composites: A Literature Review”, Journal of Composites Science, 2022.

Singh, N., Banerjee, S., Parkash, O., & Kumar, D. (2018). Tribological and corrosion behavior of (100-x)(Fe70Ni30)-(x)ZrO2 composites synthesized by powder metallurgy. Materials chemistry and Physics, 205, 261–268. https://doi.org/10.1016/j.matchemphys.2017.11.031.

Singh, P., Abhash, A., Yadav, B. N., Shafeeq, M., Singh, I. B., & Mondal, D. P. (2019). Effect of milling time on powder characteristics and mechanical performance of Ti4wt%Al alloy. 275–287. https://doi.org/10.1016/j.powtec.2018.09.075.

Skotnicova, K., Kirillova, V. M., Ermishkin, V. A., Cegan, T., Jurica, J., Kraus, M., & Burkhanov, G. S. (2015). Influence of alloying and testing conditions on mechanical properties and deformation behavior of <100> tungsten-based single crystals. 636, 536–542. https://doi.org/10.1016/j.msea.2015.03.126.

Song, G. Q., & Sun, Q. P. (2000). Effect of microstructure on the mechanical behavior of NiTi shape memory alloy reinforced aluminum matrix composite. Smart Materials and Structures, 9(5), 693–700. https://doi.org/10.1088/0964-1726/9/5/314.

Szewczyk-Nykiel, A., & Kazior, J. (2017). Effect of Aging Temperature on Corrosion Behavior of Sintered 17-4 PH Stainless Steel in Dilute Sulfuric Acid Solution. Journal of Materials Engineering and Performance, 3450–3456. https://doi.org/10.1007/s11665-017-2778-4.

T.Somasekhar, & P Niteesh kumar. (2018). Review Paper on Processing of Metal Matrix Composites & Its Properties. 284–287. www.ijcrt.org.

Usami, A., Kihira, H., & Kusunoki, T. (2003). 3%-Ni weathering steel plate for uncoated bridges at high airborne salt environment. Nippon Steel Technical Report, 87,

Varadaraj, K. R., Kumar, S., Vitala, H. R., Ravishankar, M. K., & Dileep, B. P. (2023). Effect of Chromium on Mechanical and Corrosion Behaviour of Ferrous Metal Matrix Composites by Using Powder Metallurgy Route BT - Recent Developments in Mechanics and Design (S.Hegde, A. Mishra, & D. K. Singh (eds.); pp. 225–234). Springer Nature Singapore.

Wang et al. (2018), “Tool wear characterization in high-speed milling of titanium metal matrix composites”, The International Journal of Advanced Manufacturing Technology, 2018.

Wang, Hd (2013). Graphite Solid Lubrication Materials. In: Wang, Q.J., Chung, YW. (eds) Encyclopedia of Tribology. Springer, Boston, MA. https://doi.org/10.1007/978-0-387-92897-5_1261

Wang, Li, Zhang, Liu, and Li (2019) Diffusion bonding characteristics of CeO2-Cr particle reinforced titanium matrix composite using Ni-based interlayer", journal Materials Science and Engineering

Wu, M. W., & Hwang, K. S. (2010). Formation mechanism of weak ferrite areas in Ni-containing powder metal steels and methods of strengthening them. https://doi.org/https://doi.org/10.1016/j.msea.2010.05.089.

Xie, C. L., Hailat, M., Wu, X., Newaz, G., Taya, M., & Raju, B. (2007). Development of short fiber-reinforced NiTi/Al6061 composite. Journal of Engineering Materials and Technology, 129(1), 69–76. https://doi.org/10.1115/1.2400271.

Xie, L., Xu, Z., Qi, Y., Liang, J., He, P., Shen, Q., & Wang, C. (2023). Effect of ball milling time on the microstructure and compressive properties of the Fe-Mn-Al porous steel. International ournal of Minerals, Metallurgy and Materials, 30(5), 917–929. https://doi.org/10.1007/s12613-022-2568-3.

Ying Zhou and Guoyou Gan (2020) Microstructure and thermophysical properties of CeO_2-doped $SmTaO_4$ ceramics for thermal barrier coatings. Journal of Materials Research volume 35, pages242–251 (2020)

Yu, Y., Guo, Y (2019). Cerium oxide-modified lithium chromium titanite as high-performance anode material for lithium-ion battery. 367–371 (2019). https://doi.org/10.1007/s11581-018-2758-1

Yutao Zhai. Ajit Pal Singh, Leandro Bolzoni (2022). Fabrication and Characterization of In Situ Ti-6Al-4V/TiB Composites by the Hot-Pressing Method using Recycled Metal Chips. Metals 2022, 12(12), 2038; https://doi.org/10.3390/met12122038

Zhang, H., Zou, Y., Zou, Z., & Shi, C. (2014). Effects of chromium addition on microstructure and properties of TiC-VC reinforced Fe-based laser cladding coatings. Journal of Alloys and Compounds, 614, 107–112. https://doi.org/10.1016/j.jallcom.2014.06.073.

Zhang, H., Zou, Y., Zou, Z., & Wu, D. (2015). Microstructure and properties of Fe-based composite coating by laser cladding Fe-Ti-V-Cr-C-CeO2 powder. Optics and Laser

APPENDIX

Appendix – 1

Vickers Hardness Measurements for (S4, S3, S2, and S1) at trial 1, 2, 3

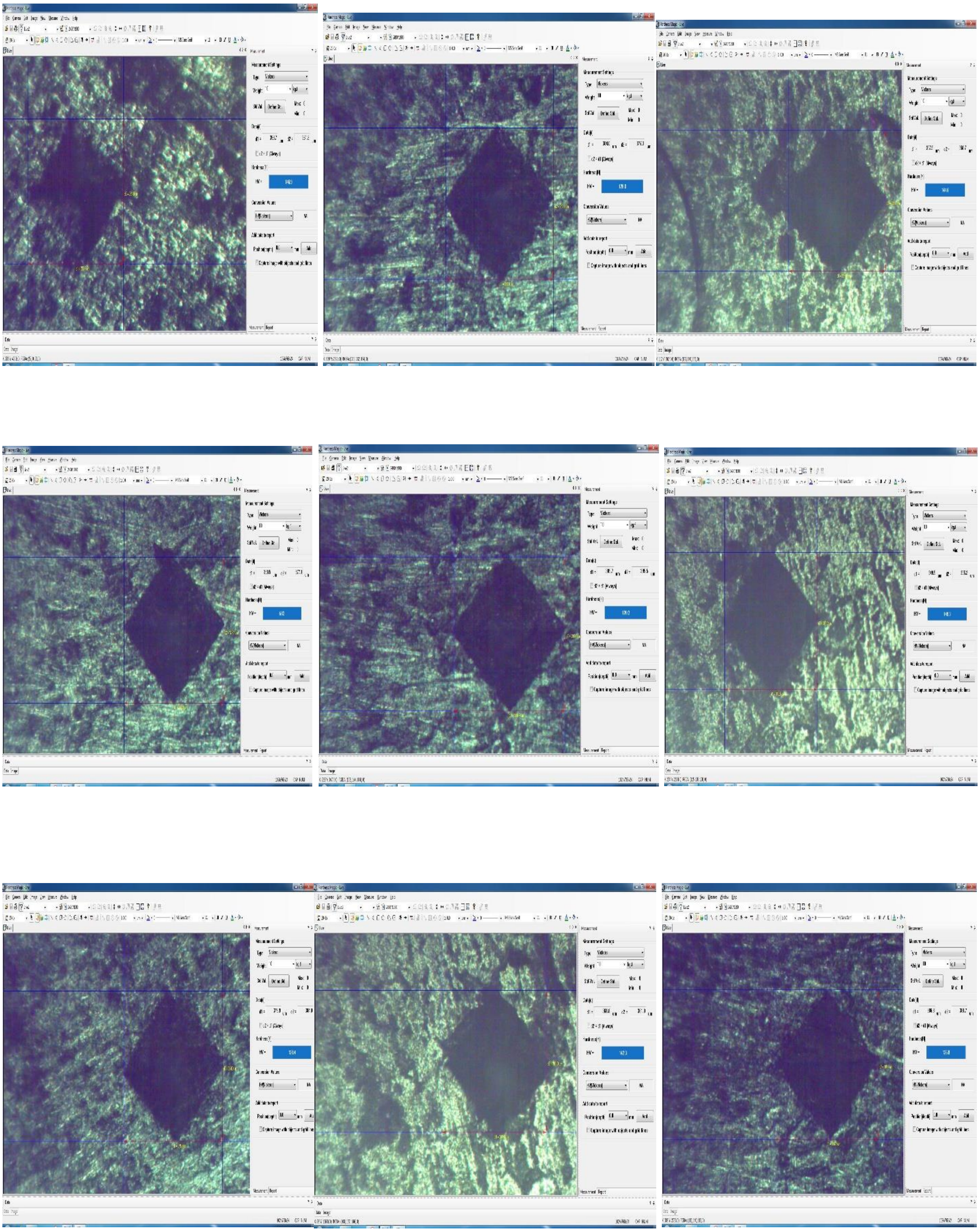

Appendix – 2

Compression Test (Stress-Elongation Curve for (S1) And Test Report For (S1)

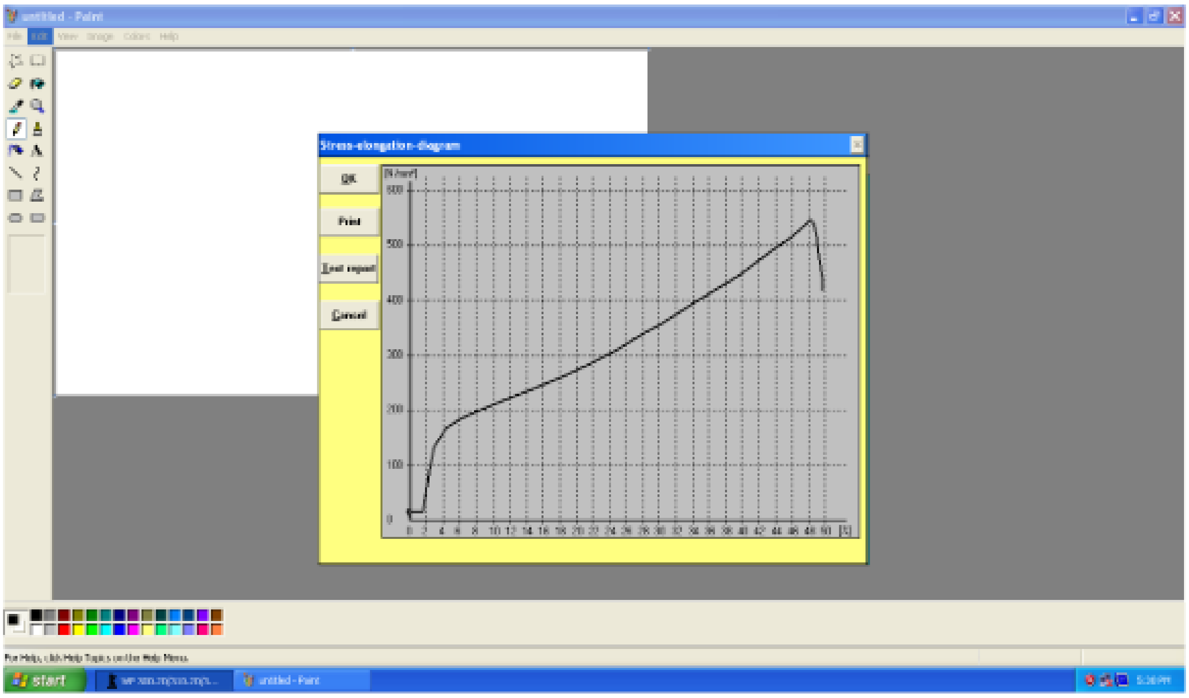

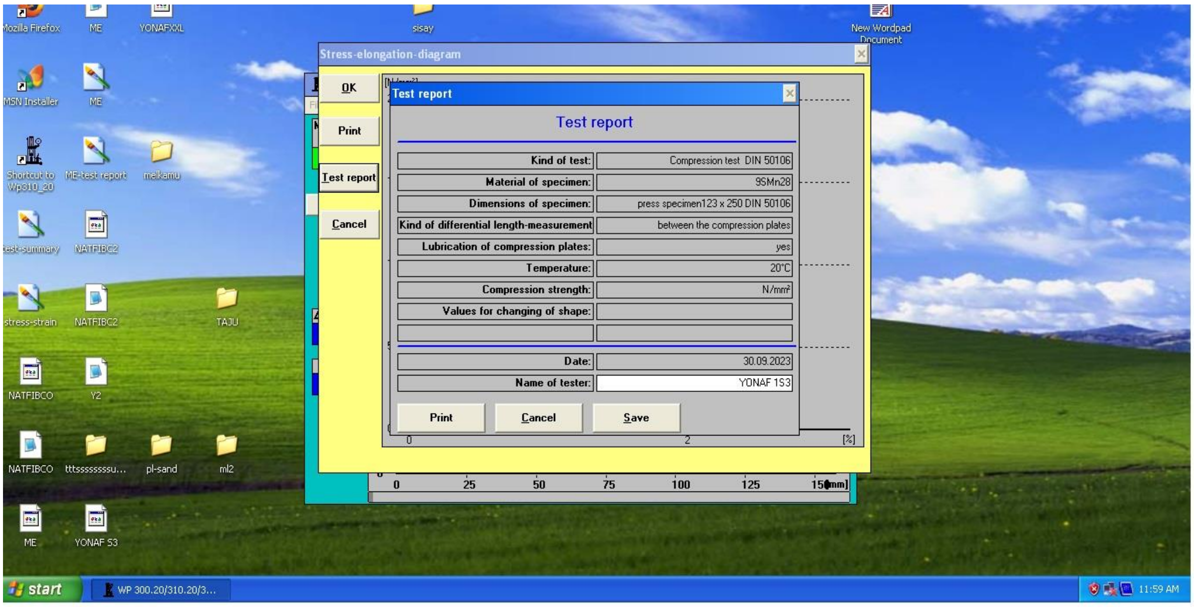

Appendix – 3

Crystalline size (CS), Dislocation density (DD), and Lattice Strain (LS) measurment in origin software using Gausses curve fit analysis from XRD data

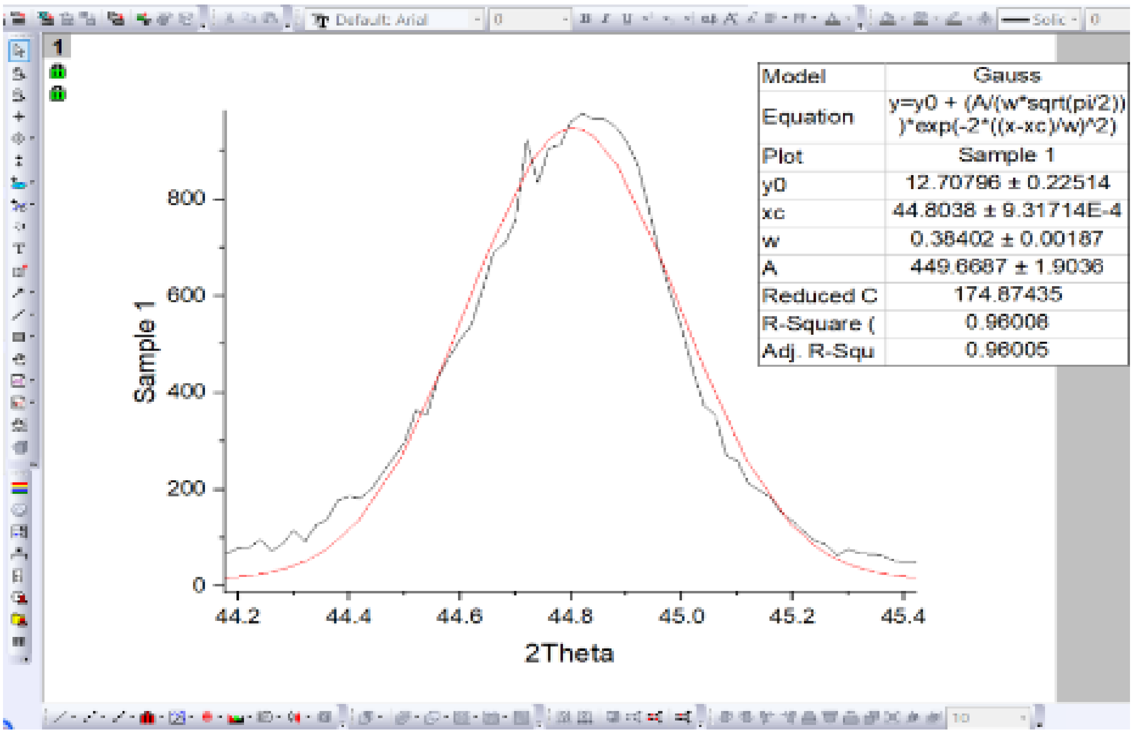

Appendix – 4

(A) Open circuit potential (OCP) (Potential with Time)

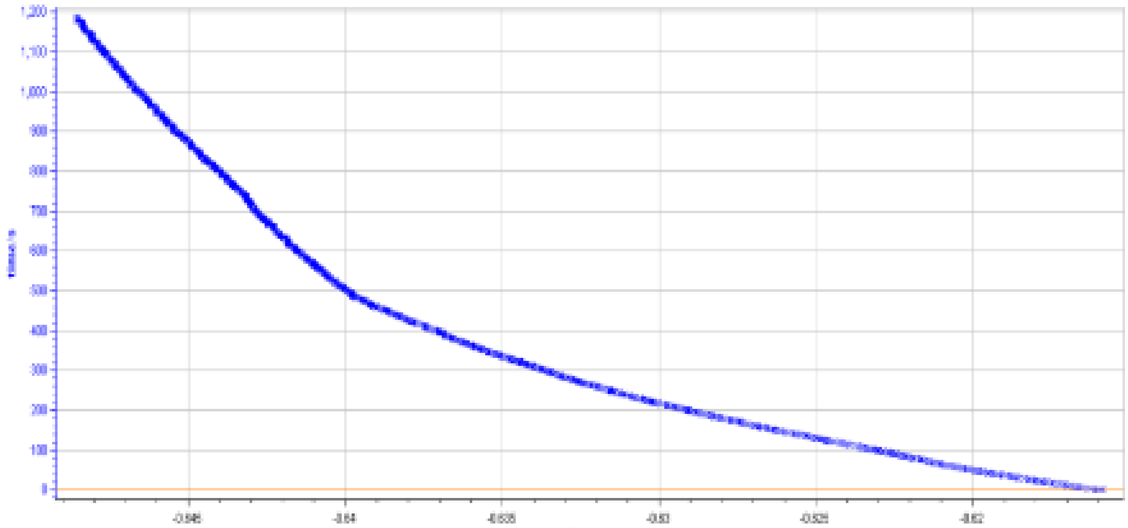

(B) Nyquist Impedance Plot, During Corrosion Test (Resistance Versus Impedance)